Supporting Information

Harnessing the Substrate Promiscuity of Dioxygenase AsqJ and Developing Efficient Chemo-enzymatic Synthesis for Quinolones

Haoyu Tang,[a] Yijie Tang,[b] Igor V. Kurnikov,[b] Hsuan-Jen Liao,[c] Nei-Li Chan,*[c] Maria G. Kurnikova,*[b] Yisong Guo,*[b] and Wei-chen Chang*[a]

a. Department of Chemistry, North Carolina State University, Raleigh, NC, 27695

b. Department of Chemistry, Carnegie Mellon University, Pittsburgh, PA, 15213

c. Institute of Biochemistry and Molecular Biology, College of Medicine, National Taiwan University, Taipei, 100 Taiwan

wchang6@ncsu.edu, ysguo@andrew.cmu.edu, kurnikova@cmu.edu, nlchan@ntu.edu.tw

Contents:

General procedure

The chemical shift values are recorded on Bruker Ascend™ 500 (500 MHz) and reported in δ values (parts per million, ppm) relative to the standard chemical shift for the hydrogen residue peak and carbon-13 peak in the deuterated solvent, $CDCl_3$, or DMSO-d_6. The coupling constant (*J*) values are expressed in hertz (Hz). The numbers of protons directly attached to the individual carbons were determined by ^{13}C NMR and DEPT135 experiments. High performance liquid chromatography with detection by mass spectrometry (LC-MS) was conducted on an Agilent Technologies (Santa Clara, CA) 1200 system coupled to an Agilent Technologies 6120 quadrupole mass spectrometer. Separation was conducted on an agilent SB-C18 column (2.1*50 mm, 1.8 um). Detection was performed using electrospray ionization in positive mode (ESI+). Thin-layer-chromatography (TLC) was performed on silica gel plates. Compounds on TLC were visualized by illumination under UV light (254 nm). Solvent systems are expressed as a ratio of the components with respect to volume (*v/v*). Silica gel (230-400 mesh) was used for flash column chromatography. Evaporations were carried out under reduced pressure (water aspirator or vacuum pump) with the bath temperature below 50 °C unless specified otherwise. Materials obtained from commercial suppliers were used without further purification.

Preparation of Compounds 5a-5d

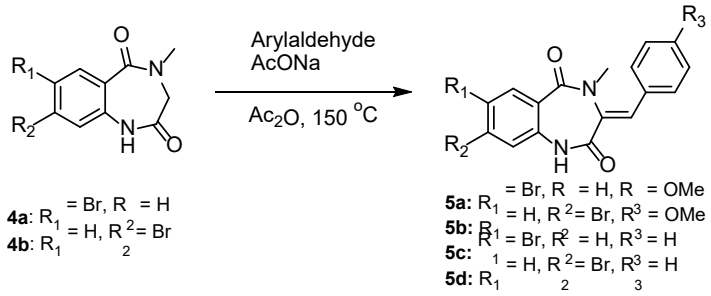

A reaction mixture contains the substrate (**4a** or **4b**)[1] (5.38 g, 20 mmol), benzaldehyde (3.2 g, 30 mmol) or *p*-anisaldehyde (4.0 g, 30 mmol), sodium acetate (1.8 g, 22 mmol), and acetic anhydride (5.6 mL) was stirred under reflux condition. After 15 hrs., water was added to the reaction and the mixture was stirred at room temperature for another 1 h. The reaction was extracted using ethyl acetate. The resulting organic layer was washed with brine and then dried over anhydrous $MgSO_4$. After evaporating the organic solvent, the crude product was purified by silica gel column chromatography (hexanes/ethyl acetate (3:1)) to give the desired product **5a** (2.3 g, 29%), **5b** (0.85 g, 11%), **5c** (3.5 g, 49%), **5d** (1.8 g, 25%), respectively.

7-Br-(4'-methoxy)dehydrocyclopeptin (**5a**), amorphous solid, ^1H NMR ($CDCl_3$, 500 MHz) δ 8.87 (1H, br. s, NH), 8.12 (1H, d, 2.3), 7.56 (1H, dd, 8.5, 2.2), 7.33 (2H, d, 8.7), 6.94 (4H, m), 3.84 (3H, s), 3.22 (3H, s); ^{13}C NMR ($CDCl_3$, 125 MHz) δ 171.9, 165.6, 161.0, 135.5, 135.0, 134.0, 131.8, 131.4, 130.3, 127.2, 124.2, 122.2, 117.9, 114.6, 55.4, 36.0 (Figure S1).

8-Br-(4'-methoxy)dehydrocyclopeptin (**5b**), amorphous solid, ^1H NMR (DMSO-d_6, 500 MHz) δ 10.60 (s, 1 H, NH), 7.72 (1H, d, 8.4), 7.39 (1H, dd, 8.4, 1.8), 7.36 (1H, d, 1.8), 7.33 (2H, d, 8.8), 7.00 (2H, d, 8.8), 6.86 (1H, s), 3.77 (3H, s), 3.05 (3H, s); ^{13}C NMR (DMSO-d_6, 125 MHz) δ 170.0, 165.3, 160.3, 138.1, 132.6, 131.2, 131.0, 129.7, 126.9, 125.4, 124.3, 124.3, 123.0, 114.6, 55.3, 35.1 (Figure S2).

7-Br-dehydrocyclopeptin (**5c**), amorphous solid, ^1H NMR (DMSO-d_6, 500 MHz) δ 10.72 (s, 1 H, NH), 7.93 (1H, d, 2.4), 7.72 (1H, dd, 8.5, 2.4), 7.45 (2H, m), 7.40 (3H, m), 7.13 (1H, d, 8.7), 6.95 (1H, s), 3.03 (3H, s); ^{13}C NMR (DMSO-d_6, 125 MHz) δ 169.3, 164.5, 135.9, 135.3, 133.7, 132.8, 131.9, 129.9, 129.7, 129.1, 129.1, 126.9, 123.1, 116.0, 35.3 (Figure S3).

8-Br-dehydrocyclopeptin (**5d**), amorphous solid, 1H NMR (DMSO-d_6, 500 MHz) δ 10.68 (s, 1 H, NH), 7.75 (1H, d, 8.4), 7.39-7.46 (4H, m), 7.36 (3H, m), 6.93 (1H, s), 3.01 (3H, s); ^{13}C NMR (DMSO-d_6, 125 MHz) δ 169.5, 165.2, 137.9, 133.7, 132.8, 132.0, 130.0, 129.8, 129.1, 129.1, 127.1, 125.5, 124.4, 123.2, 35.3 (Figure S4).

Overexpression and Purification of AsqJ

A plasmid encoding AsqJ gene was transformed into E. coli BL21 (DE3) cells (New England Biolabs, MA). A seed culture was prepared by inoculating a single colony into Luria broth (LB) broth (10 mL) containing 50 μg/mL kanamycin. The seed culture was grew overnight in a shaking incubator (37 °C, 220 rpm). For large-scale growth, a seed culture was added into Terric-Broth (TB) broth with 50 ug/mL kanamycin in a ratio of 1:80. The culture was grown in a shaking incubator (37 °C, 220 rpm). After culture has reached OD_{600} 0.5-0.6, isopropyl β-D-1-thiogalactopyranoside (IPTG) was added with a final concentration of 0.25 mM. After lowering temperature to 18 °C and the culture was grown for 20 hrs. The cells were harvested by centrifugation at 4 °C and the cell pellets were stored at -20 °C. The protein purification was carried out following the reported procedure.[2]

Analytic assay of AsqJ with 1a, 1b, 5a-5d

Reconstituted AsqJ (by adding ferrous ion into enzyme solution) and 2-oxoglutarate (2OG) were added to a buffer solution (100mM TRIS, pH 7.5) containing substrate (**1a**, **1b**, **5a**, **5b**, **5c** or 5**d**) with a final concentration of 0.5 mM substrate, 2.5 mM 2OG and 0.1mM reconstituted AsqJ. The reactions were carried out on ice and quenched with an equal volume of acetonitrile at 4 hrs. and 20 hrs. An aliquot of 1uL was analyzed by LCMS equipped with Agilent SB-C18 (2.1*50 mm, 1.8 um) column. The LCMS was conducted under isocratic solvent condition (Acetonitrile/H_2O (50mM ammonia formate) = 1/1).

Enzymatic synthesis and structural determination of 2a, 2b, 6a-6d

Preparative scale AsqJ reaction and product isolation:

Substrate dissolved in DMSO was added dropwisely to a buffer solution (100 mM TRIS, pH 7.5) containing reconstituted AsqJ and 2OG. The reaction mixture contains 1 μM reconstituted AsqJ, 3 mM 2OG and 1 mM substrates (**1a**, 0.29 mg, 0.90 mmol; **1b**, 0.21 g, 0.72 mmol; **5a**, 1.35 g, 3.49 mmol; **5c**, 1.14 g, 3.20 mmol; **5d**, 1.50 g, 4.20 mmol). For **5b**, a reaction contains 3 uM reconstituted AsqJ, 3mM 2OG and 0.7 mM of **5b** (1.29 g, 3.33 mmol). All reactions were conducted at 4 ˚C with stirring (50 rpm) for 24 hrs. The reactions were halted by adding ethyl acetate to the reaction mixture. After two times extraction using ethyl acetate, the combined organic layers were washed with brine three times and dried over $MgSO_4$. A portion of the crude product (~ 100mg) was subjected to either a silica column chromatography (chloroform/methanol = 100:1) to give **2a** and **2b**, a preparative TLC to give afford **6a** and **6b**, or re-crystallization (acetone/methanol) to obtain **6c** and **6d**. The structures were elucidated by NMR. In addition, the structure and the absolute configuration of oxirane moiety of **6c** was determined using X-ray analysis.

Structural characterization

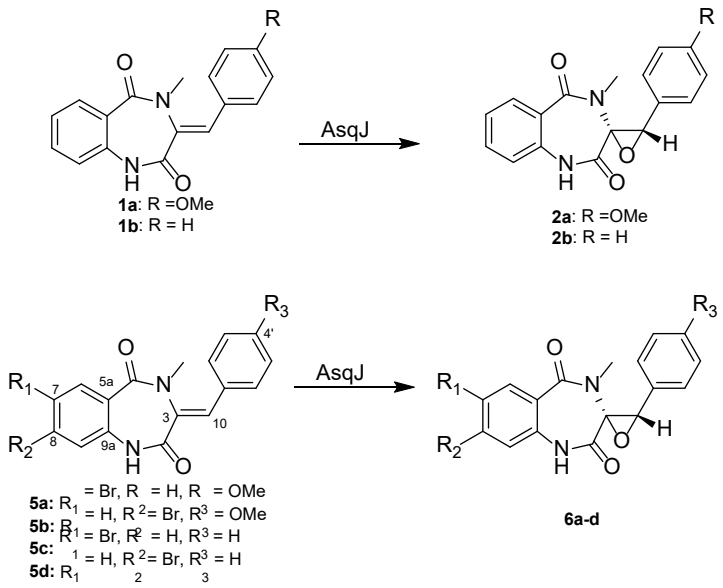

(4'-methoxy)cyclopenin (**2a**), amorphous solid.[3] ^{1}H NMR (500 MHz, DMSO-d_6) δ 10.80 (1H, s), 7.53 (1H, ddd, 8.1, 7.1, 1.5), 7.14 (1H, d, 8.2), 7.09 (1H, ddd, 7.9, 7.3, 1.5), 6.98 (1H, dd, 7.8, 1.5), 6.78 (2H, d, 8.8), 6.57 (2H, d, 8.8), 4.26 (1H, s), 3.72 (3H, s), 3.07 (3H, s); ^{13}C NMR (125 MHz, DMSO-d_6) δ 166.2, 165.4, 159.5, 135.2, 132.3, 130.4, 127.5, 126.5, 124.2, 122.8, 121.1, 113.4, 70.2, 63.7, 55.1, 30.7 (Figure S5).

Cyclopenin (**2b**), amorphous solid.[3] ^{1}H NMR (500 MHz, DMSO-d_6) δ 10.83 (1H, s), 7.54 (1H, ddd, 8.1, 7.2, 1.5), 7.29 (1H, m), 7.22 (2H, m), 7.15 (1H, dd, 8.1, 1.0), 7.08 (1H, ddd, 7.8, 7.0, 1.1), 6.92 (1H, dd, 7.9, 1.4), 6.63 (2H, d, 7.2), 4.36 (1H, s), 3.07 (3H, s); ^{13}C NMR (125 MHz, DMSO-d_6) δ 165.9, 165.3, 135.1, 132.4, 131.0, 130.5, 128.7, 127.9, 126.4, 126.1, 124.2, 121.1, 70.1, 63.7, 30.8 (Figure S6).

7-Br-(4'-methoxy)cyclopenin (**6a**), colorless oil. The ^{1}H and ^{13}C NMR spectrums showed similar resonances to those of 7-Br-cyclopenin (**6c**) except an additional resonance of a methoxy group (δ_H 3.82 (3H, s), δ_C 55.3, 160.5). The substituted carbon (C-7, δ 113.8) was determined using HMBC correlations (H-6/C-5, H-6/C-7, H-6/C-8, H-6/C-9a). In addition, the HMBC correlations from H-1 to C-9, C-5a, C-3 and from N-CH_3 to C5, C3 suggested a benzo-diazepine core. The spin coupling system of H-2'/H-3' and the HMBC correlations of H-3'/C-1', H-2'/C-4', H-10/C-2', OMe/C-4' indicates a *p*-anisic moiety. Furthermore, The HMBC correlations of H-10/C-3, H-10/C-1', H-10/C-2' connected *p*-anisic moiety to the benzodiazepine core via the oxirane. Based on the similar correlations as of **6c**, the stereochemistry of C3 and C10 are assigned as *R* and *S*, respectively. ^{1}H NMR (500 MHz, $CDCl_3$) δ 9.23 (1H, s), 7.60 (1H, dd, 8.5, 2.3), 7.34 (1H, d, 2.3), 7.01 (1H, d, 8.5), 6.80 (2H, d, 8.7), 6.60 (2H, d, 8.7), 3.98 (1H, s), 3.82 (3H, s), 3.23 (3H, s); ^{13}C NMR (125 MHz, $CDCl_3$) δ 167.7, 164.6, 160.5, 135.3, 134.2, 133.0, 128.8, 127.3, 122.5, 121.6, 118.6, 113.8, 70.0, 64.8, 55.3, 31.4 (Figure S7-10).

8-Br-(4'-methoxy)cyclopenin (**6b**), colorless oil. The substituted carbon (C-8, δ 113.6) is determined through the HMBC correlations of H-6/C-5, H-6/C-8, H-6/C-9a and spin coupling of H-6/H-7 shown in the ^{1}H-^{1}H COSY. ^{1}H NMR (500 MHz, DMSO-d_6) δ 7.34 (1H, d, 1.8), 7.30 (1H, dd, 8.4, 1.8), 6.91 (1H, d, 8.4), 6.82 (2H, d, 8.7), 6.64 (2H, d, 8.7), 4.36 (1H, s), 3.72 (3H, s), 3.06 (3H, s); ^{13}C NMR (125 MHz, DMSO-d_6) δ 166.0, 164.7, 159.6, 136.6, 132.4, 127.6, 127.1, 125.5, 125.1, 123.5, 122.7, 113.6, 70.0, 63.6, 55.1, 30.8 (Figure S11-14).

7-Br-cyclopenin (**6c**), colorless cube. The ^{1}H and ^{13}C NMR spectra of **6c** are very similar to cyclopenin (**2b**) with the corresponding benzoic moiety (δ_H 7.35 (1H, m), 7.26 (2H, m), 6.67 (2H, m); δ_C 130.8, 126.1, 127.9,

128.9), the oxirane (δ_H 3.98 (1H, s), δ_C 69.9, 63.7), and N-methyl group (δ_H 3.08 (3H, s), δ_C 30.9). The substituted carbon (C-7, δ 116.3) is determined by HMBC correlations (H-6/C-5, H-6/C-7, H-6/C-8, H-6/C-9a) and the up-shifted the resonance resulted from the bromide substitution. In addition, the HMBC correlations from H-1 to C-9, C-5a, C-3, and from N-CH_3 to C5, C3 suggest a fused bicyclic structure of a benzodiazepine core. Based on the HMBC correlations of H-10/C-3, H-10/C-1' and H-10/C-2', a benzene moiety is connected to the benzodiazepine via the oxirane. Furthermore, X-ray analysis of **6c** reveals the absolute configuration of the oxirane. Thus, the stereochemistry of C3 and C10 can be assigned as *R* and *S*, respectively. Therefore, the structure was determined as (3*R*, 10*S*)-7-Br-cyclopenin as shown. ^{1}H NMR (500 MHz, DMSO-d_6) δ 10.94 (1H, s), 7.75 (1H, dd, 8.7, 2.4), 7.35 (1H, m), 7.26 (2H, m), 7.13 (1H, d, 8.5), 6.89 (1H, d, 2.4), 6.67 (2H, m), 4.42 (1H, s), 3.08 (3H, s); ^{13}C NMR (125 MHz, DMSO-d_6) δ 165.7, 164.0, 135.0, 134.6, 132.5, 130.8, 128.9, 128.2, 127.9, 126.1, 123.6, 116.3, 69.9, 63.7, 30.9 (Figure S15-18 (NMR), S19 (X-ray) and Table S1).

8-Br-cyclopenin (**6d**), colorless crystal. The substituted carbon (C-8, δ 125.1) is determined through a detailed HMBC correlations (H-6/C-5, H-6/C-8, H-6/C-9a) and ^{1}H-^{1}H COSY relation (H-6/H-7). ^{1}H NMR (500 MHz, DMSO-d_6) δ 10.94 (1H, s), 7.36 (1H, d, 2.0), 7.31 (1H, m), 7.29 (1H, m), 7.25 (2H, m), 6.85 (1H, d, 8.4), 6.70 (2H, m), 4.46 (1H, s), 3.06 (3H, s); ^{13}C NMR (125 MHz, DMSO-d_6) δ 165.7, 164.6, 136.6, 132.4, 130.9, 128.8, 128.0, 127.1, 126.1, 125.4, 125.1, 123.5, 70.0, 63.7, 30.9 (Figure S 20-23).

Kinetics of the AsqJ reaction using 1a, 1b, 5a-5d

Substrate (**1a**) and 2OG were added to a buffer solution (TRIS 100mM pH 7.5) containing reconstituted AsqJ with the final concentration of 0.5 μM reconstituted AsqJ, **1a** (ranging from 0.025-0.200 mM) and 5 eq. of 2OG to the substrate. The reaction was carried out at the ambient temperature and atmosphere. An aliquot of 80 μL was removed at 30, 50, 70, 90 seconds and quenched with an equal volume of acetonitrile. After spin down the precipitate by centrifugation at 12,000 rpm for 30 mins, an aliquot of 1 μL was analyzed by LCMS. Under the similar conditions, reactions using **2a** (0.1-0.4 mM), **5a** (0.2-0.8 mM) and **5c** (0.2-0.8 mM) were conducted in the presence of 1 μM reconstituted AsqJ. Due to the lower reactivity of **5b** and **5d**, reaction using **5b** (0.2-0.8 mM) and **5d** (0.3-0.8 mM) were conducted using 2 uM and 5 uM reconstituted AsqJ, respectively. The reaction products are quantified using the purified product standards obtained through scale-up reactions. The Michaelis-Menten plots are shown in Figure S24 and the corresponding kinetics parameters are listed in Table S2.

Assess rearrangement reactions

To a D_2O solution (450 μL) in NMR tube was added **2a** and **2b** ((100 mM, dissolved in 50 μL DMSO-d_6)) with the final concentration of 10 mM. For assessment under pH 7.60 and pH 8.50 conditions, TRIS buffer were applied (100mM). For the experiment under pH 5.00 condition, acetate buffer was used (100mM). The ^{1}H-NMR spectra were collected at different time points (T = 10 min, 20 min, 60 min, and 120 min) (Figure S25a-c and S26). Neither substrate consumption nor product formation can be detected.

BF_3 Et_2O (0.1 mmol, 0.5 eq) was added to a dichloromethane solution containing **2a** or **2b** (0.2 mmol, 1.0 eq at -10 ˚C. The reaction was monitored by TLC (chloroform/methanol = 10/1). After 5 hrs., the substrate (Rf, 0.6) was largely consumed and a new spot (Rf, 0.5) was observed. Reactions were then quenched using pre-chilled aqueous NH_4Cl. After the separation, the organic layer was washed with brine. Hexanes was added and the organic layer and the product was obtained by filtration to give **3a** (45 mg, 84%) and **3b** (30 mg, 63%). The chemical structures of these products are determined as (4'-methoxy)cyclopenin (**3a**) and cyclopenin (**3b**).

(4'-Methoxy)cyclopenin (**3a**)[3], ^{1}H NMR (500 MHz, DMSO-d_6) δ 12.18 (1H, s), 9.10 (1H, s), 7.29-7.36 (2H, m), 7.27 (2H, d, 8.7), 7.12 (1H, br. d, 7.6), 7.05-7.09 (3H, m), 3.82 (3H, s); ^{13}C NMR (125 MHz, DMSO-d_6) δ 158.7, 158.3, 142.5, 133.2, 131.1, 126.4, 125.6, 124.4, 123.7, 122.1, 121.2, 115.3, 113.8, 55.1 (Figure S27).

Cyclopenin (**3b**)[3], ^{1}H NMR (500 MHz, DMSO-d_6) δ 12.25 (1H, br. s), 9.19 (1H, s), 7.51 (2H, m), 7.43 (1H, m), 7.37 (1H, br. d, 7.8), 7.29-7.35 (3H, m), 7.06 (1H, m); ^{13}C NMR (125 MHz, DMSO-d_6) δ 158.3, 142.5, 133.8, 133.2, 129.9, 128.4, 127.7, 126.5, 124.3, 124.0, 122.2, 120.9, 115.3 (Figure S28).

Preparation of 7a-7d

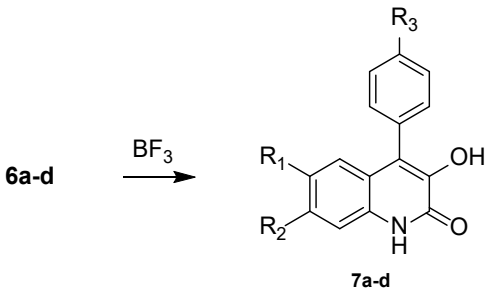

Following the similar conditions as described above, **7a-7d** were prepared (**7a**, 1.09g, 91% over 2 steps, and **7b**, 0.88g, 76% over 2 steps). For **7c** and **7d**, after the reaction, crude products were subjected to silica gel chromatography (chloroform/Methanol = 100:1) to give **7c** (0.57g, 57% over 2 steps) and **7d** (0.87g, 66% over 2 steps).

6-Br-(4'-methoxy)cyclopenin (**7a**), amorphous solid. ^{1}H NMR (500 MHz, DMSO-d_6) δ 12.33 (1H, s), 9.43 (1H, s), 7.47 (1H, dd, 8.6, 2.1), 7.29 (1H, d, 8.6), 7.27 (2H, d, 8.5), 7.16 (1H, d, 2.0), 7.08 (2H, d, 8.5), 3.83 (3H, s); ^{13}C NMR (125 MHz, DMSO-d_6) δ 158.9, 158.1, 143.6, 132.2, 131.1, 128.9, 126.1, 125.0, 123.3, 122.6, 117.4, 114.1, 114.0, 55.1 (Figure S29).

7-Br-(4'-methoxy)cyclopenin (**7b**), amorphous solid. ^{1}H NMR (500 MHz, DMSO-d_6) δ 12.26 (1H, s), 9.34 (1H, s), 7.50 (1H, d, 2.0), 7.24 (2H, d , 8.7), 7.23 (1H, dd, 8.7, 2.1), 7.06 (2H, d, 8.7), 7.04 (2H, d, 8.7), 3.82 (3H, s); ^{13}C NMR (125 MHz, DMSO-d_6) δ 158.8, 158.2, 142.9, 134.2, 131.1, 126.4, 125.1, 124.9, 123.4, 120.5, 118.8, 117.3, 113.9, 55.1 (Figure S30).

6-Br-cyclopenin (**7c**), amorphous solid. ^{1}H NMR (500 MHz, DMSO-d_6) δ 12.36 (1H, s), 9.53 (1H, s), 7.53 (2H, m), 7.48 (1H, dd, 8.7, 2.0), 7.46 (1H, m), 7.34 (2H, m), 7.30 (1H, d, 8.7), 7.08 (H, d, 2.1); ^{13}C NMR (125 MHz, DMSO-d_6) δ 158.1, 143.5, 133.1, 132.2, 129.8, 129.0, 128.6, 128.0, 126.0, 123.0, 122.9, 117.5, 114.1 (Figure S31).

7-Br-cyclopenin (**7d**), amorphous solid. ^{1}H NMR (500 MHz, DMSO-d_6) δ 12.31 (1H, s), 9.44 (1H, s), 7.52 (3H, m), 7.45 (1H, m), 7.33 (2H, m), 7.25 (1H, dd, 8.7, 2.0), 6.98 (1H, d, 8.7); ^{13}C NMR (125 MHz, DMSO-d_6) δ 158.2, 142.9, 134.2, 133.3, 129.8, 128.5, 127.9, 126.3, 125.0, 123.6, 120.2, 118.9, 117.4 (Figure S32).

Synthesis of quinolone analogs

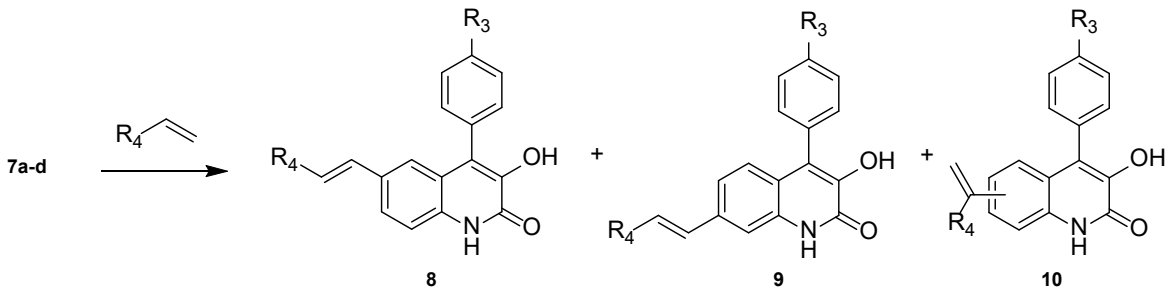

To a reaction mixture containing brominated viridicatin (**7a-b**, 34.6 mg; **7c-d**, 31.6 mg; 0.1 mmol, 1.0 eq), $Pd(OAc)_2$ (3.36 mg, 0.015 mmol, 15 mmol%), $P(otol)_3$ (9.1mg, 0.030 mmol, 30 mmol%) and Et_3N(15.1 mg, 21 uL, 0.15 mmol, 1.5 eq) in anaerobic acetonitrile (10mL) was added alkene (0.5 mmol, 5.0 eq). The reaction was then kept refluxing for 16 hrs. For those reactions using styrenes (**I-V**) and 4-vinyl-1-cyclohexene (**VI**) as the coupling partner, the products were purified using silica gel chromatography (dichloromethane/methanol = 200:1, 0.01% acetic acid) to yield **8a-(I-VI)**, **9b-(I-VI)**, **8c-(I-VI)**, **9d-(I-VI)** (0.074-0.097 mmol, 74%-97%). For those using 4-acryloylmorpholine, 4-vinylpyridine and 4-NH_2 styrene (VI**I-IX**), the products were purified analogously using chloroform/methanol (50:1) as an eluent to give **8a-(VII-IX)**, **9b-(VII-IX)**, **8c-(VII-IX)**, **9d-(VII-IX)** (0.069-0.091 mmol, 69%-91%). For those using 1-vinylpyrrolidin-2-one (**X**), the crude products were first subjected to silica gel chromatography (chloroform/methanol = 50:1) to give products (**10a-X**, 13.0 mg, 0.035 mmol, 35%; **10b-X**, 12.0 mg, 0.032 mmol, 32%; **10c-X**, 13.0 mg, 0.034 mmol, 34%; **10d-X**, 12.0 mg, 0.032 mmol, 32%). Fractions contain other products were concentrated and subjected to a second silica gel chromatography (hexane/acetone = 1:1) to afford **8a-X** (5.5 mg, 0.015 mmol, 15%), **9b-X** (7 mg, 0.018 mmol, 18%), **8c-X** (7.5 mg, 0.020 mmol, 20%), and **9d-X** (6.4 mg, 0.017 mmol, 17%).

For the reactions using D-lemonene (**XI**), after silica gel chromatography (dichloromethane/methanol = 200:1), the partially purified products were purified using semi-preparative HPLC equipped with a Waters Sunfire C18 column (5 um, 19*250 mm, isocratic elution, acetonitrile/ H_2O (0.01% Trifluroacetic acid) = 88:12), to yield **8a-XI** (8 mg, 0.020 mmol, 20%), **10a-XI** (5.0 mg, 0.0125 mmol, 12%) and **9b-XI** (10 mg, 0.0249 mmol, 25%), **10b-XI** (5.5 mg, 0.0137 mmol, 13%).

8a-I, amorphous solid. ^{1}H NMR (500 MHz, DMSO-d_6) δ 12.28 (1H, s), 9.17 (1H, br. s), 7.72 (1H, dd, 8.5, 1.5), 7.55 (2H, d, 7.5), 7.37 (1H, d, 8.5), 7.32 (4H, m), 7.24 (1H, d, 1.5), 7.22 (1H, m), 7.18 (1H, d, 16.5), 7.10 (1H, d, 8.5), 7.04 (1H, d, 16.5), 3.85 (3H, s); ^{13}C NMR (125 MHz, DMSO-d_6) δ 158.7, 158.2, 142.8, 137.1, 132.8, 131.2, 131.2, 128.6, 128.4, 127.4, 127.2, 126.4, 125.5, 123.7, 123.7, 123.6, 121.3, 115.9, 113.9, 55.1 (Figure S33).

9b-I, amorphous solid. ^{1}H NMR (500 MHz, DMSO-d_6) δ 12.25 (1H, s), 9.21 (1H, s), 7.62 (1H, d, 7.5), 7.47 (1H, br. s), 7.41 (1H, dd, 8.4, 1.3), 7.38 (2H, t, 7.6), 7.29 (4H, m), 7.20 (1H, d, 16.0), 7.14 (1H, 8.4), 7.08 (2H, d, 8.7), 3.83 (3H, s); ^{13}C NMR (125 MHz, DMSO-d_6) δ 158.7, 158.5, 142.6, 136.8, 135.2, 133.6, 131.2, 128.9, 128.8, 127.9, 127.8, 126.6, 125.6, 124.8, 123.8, 120.8, 120.1, 113.8, 113.3, 55.1 (Figure S34).

8c-I, amorphous solid. ^{1}H NMR (500 MHz, DMSO-d_6) δ 7.72 (1H, dd, 8.6, 1.6), 7.54 (4H, m), 7.47 (1H, m), 7.38 (3H, m), 7.31 (2H, t, 7.6), 7.21 (1H, m), 7.17 (1H, d, 1.6), 7.15 (1H, d, 16.5), 7.03 (1H, d, 16.6); ^{13}C NMR (125 MHz, DMSO-d_6) δ 158.2, 142.9, 137.0, 133.7, 132.8, 131.2, 130.0, 128.6, 128.5, 128.3, 127.8, 127.4, 127.3, 126.4, 124.0, 123.8, 123.5, 121.1, 116.0 (Figure S35).

9d-I, amorphous solid. ^{1}H NMR (500 MHz, DMSO-d_6) δ 12.29 (1H, s), 9.31 (1H, br. s), 7.62 (2H, d, 7.5), 7.53 (2H, m), 7.49 (1H, br. s), 7.45 (1H, m), 7.38 (5H, m), 7.29 (1H, d, 16.5), 7.27 (1H, m), 7.20 (1H, d,

16.7), 7.06 (2H, d, 8.5); ^{13}C NMR (125 MHz, DMSO-d_6) δ 158.6, 136.8, 135.4, 133.7, 133.6, 129.9, 129.0, 128.8, 128.5, 127.9, 127.9, 127.8, 126.7, 124.8, 124.2, 120.6, 120.3, 113.4 (Figure S36).

8a-II, amorphous solid. ^{1}H NMR (500 MHz, DMSO-d_6) δ 12.26 (1H, br. s), 9.14 (1H, br. s), 7.70 (1H, dd, 8.6, 1.8), 7.45 (2H, d, 8.1), 7.35 (1H, d, 8.5), 7.31 (2H, d, 8.7), 7.21 (1H, d, 1.5), 7.13 (2H, d, 8.0), 7.12 (1H, d, 16.6), 7.11 (2H, d, 8.7), 7.00 (1H, d, 16.3), 3.85 (3H, s), 2.28 (3H, s); ^{13}C NMR (125 MHz, DMSO-d_6) δ 158.7, 158.1, 142.8, 136.8, 134.3, 132.6, 131.3, 131.2, 129.2, 127.3, 127.1, 126.3, 125.5, 123.7, 123.6, 123.4, 121.3, 115.9, 113.9, 55.1, 20.8 (Figure S37).

9b-II, amorphous solid ^{1}H NMR (500 MHz, DMSO-d_6) δ 12.24 (1H, br. s), 9.19 (1H, br. s), 7.50 (2H, d, 8.1), 7.45 (1H, d, 1.2), 7.38 (1H, dd, 8.5, 1.4), 7.29 (2H, d, 8.7), 7.22 (1H, d, 16.2), 7.17 (2H, d, 8.0), 7.15 (1H, d, 16.2), 7.13 (1H, d, 8.4), 7.08 (2H, d, 8.8), 3.83 (3H, s), 2.30 (3H, s); ^{13}C NMR (125 MHz, DMSO-d_6) δ 158.7, 158.5, 142.5, 137.2, 135.4, 134.0, 133.6, 131.2, 129.3, 128.8, 126.9, 126.6, 125.6, 124.8, 123.8, 120.6, 120.1, 113.8, 113.1, 55.1, 20.9 (Figure S38).

8c-II, amorphous solid. ^{1}H NMR (500 MHz, DMSO-d_6) δ 12.31 (1H, s), 9.25 (1H, br. s), 7.70 (1H, dd, 8.6, 1.8), 7.55 (2H, m), 7.47 (1H, m), 7.42 (2H, d, 8.1), 7.38 (2H, m), 7.37 (1H, d, 8.6), 7.15 (1H, d, 1.7), 7.12 (2H, d, 8.1), 7.08 (1H, d, 16.3), 6.98 (1H, d, 16.3), 2.27 (3H, s); ^{13}C NMR (125 MHz, DMSO-d_6) δ 158.1, 142.8, 136.8, 134.2, 133.6, 132.6, 131.3, 129.9, 129.2, 128.4, 127.8, 127.2, 127.2, 126.3, 123.9, 123.7, 123.2, 121.1, 115.9, 20.8 (Figure S39).

9d-II, amorphous solid. ^{1}H NMR (500 MHz, DMSO-d_6) δ 7.51 (4H, m), 7.45 (2H, m), 7.36 (3H, m), 7.21 (1H, d, 16.2), 7.17 (2H, d, 8.0), 7.15 (1H, d, 16.2), 7.05 (1H, d, 8.4), 2.30 (3H, s); ^{13}C NMR (125 MHz, DMSO-d_6) δ 158.9, 142.9, 137.7, 135.9, 134.5, 134.2, 134.0, 130.3, 129.8, 129.3, 128.8, 128.2, 127.3, 127.0, 125.1, 124.6, 120.8, 120.6, 113.6, 21.3 (Figure S40).

8a-III, amorphous solid, ^{1}H NMR (500 MHz, DMSO-d_6) δ 12.25 (1H, s), 9.14 (1H, s), 7.68 (1H, dd, 8.6, 1.8), 7.50 (2H, d, 8.7), 7.34 (1H, d, 8.5), 7.31 (2H, d, 8.7), 7.19 (1H, d, 1.7), 7.10 (2H, d, 8.7), 7.02 (1H, d, 16.5), 6.98 (1H, d, 16.5), 6.89 (1H, d, 8.8), 3.85 (3H, s), 3.76 (3H, s); ^{13}C NMR (125 MHz, DMSO-d_6) δ 158.8, 158.7, 158.2, 142.8, 132.5, 131.6, 131.2, 129.7, 127.7, 126.9, 126.1, 125.5, 123.7, 123.5, 123.2, 121.3, 115.9, 114.1, 113.9, 55.1 (Figure S41).

9b-III, amorphous solid. ^{1}H NMR (500 MHz, DMSO-d_6) δ 12.22 (1H, br. s), 9.16 (1H, br. s), 7.56 (2H, d, 8.7), 7.43 (1H, d, 1.2), 7.36 (1H, dd, 8.6, 1.2), 7.29 (2H, d, 8.7), 7.15 (1H, d, 16.5), 7.12 (1H, d, 8.6), 7.11 (1H, d, 16.5), 7.08 (2H, d, 8.8), 6.94 (2H, d, 8.8), 3.83 (3H, s), 3.77 (3H, s); ^{13}C NMR (125 MHz, DMSO-d_6) δ 159.1, 158.7, 158.5, 142.4, 135.7, 133.6, 131.2, 129.5, 128.6, 128.0, 125.6, 125.6, 124.8, 123.9, 120.4, 119.9, 114.2, 113.8, 112.9, 55.2, 55.1 (Figure S42).

8c-III, amorphous solid. ^{1}H NMR (500 MHz, DMSO-d_6) δ 7.68 (1H, dd, 8.6, 1.8), 7.55 (2H, m), 7.48 (2H, d, 8.8), 7.47 (1H, m), 7.38 (2H, m), 7.36 (1H, d, 8.6), 7.12 (1H, d, 1.7), 7.00 (1H, d, 16.3), 6.96 (1H, d, 16.3), 6.88 (2H, d, 8.7), 3.75 (3H, s); ^{13}C NMR (125 MHz, DMSO-d_6) δ 158.8, 158.1, 142.8, 133.7, 132.5, 131.6, 129.9, 129.7, 128.4, 127.8, 127.7, 126.9, 126.0, 123.9, 123.5, 122.9, 121.1, 115.9, 114.1, 55.1 (Figure S43).

9d-III, amorphous solid. ^{1}H NMR (500 MHz, DMSO-d_6) δ 12.26 (1H, s), 9.26 (1H, s), 7.50-7.58 (4H, m), 7.45 (2H, m), 7.35 (3H, br. d, 7.6), 7.15 (1H, d, 16.3), 7.11 (1H, d, 16.3), 7.04 (1H, d, 8.3), 6.93 (2H, d, 8.5), 3.77 (3H, s); ^{13}C NMR (125 MHz, DMSO-d_6) δ 159.2, 158.5, 142.3, 135.8, 133.8, 133.6, 129.9, 129.5, 128.7, 128.4, 128.0, 127.8, 125.6, 124.7, 120.2, 120.1, 114.2, 112.9, 55.2 (Figure S44).

8a-IV, amorphous solid, ^{1}H NMR (500 MHz, DMSO-d_6) δ 7.70 (1H , dd, 8.5, 1.7), 7.60 (2H, dd, 8.7, 5.6), 7.36 (1H, d, 8.5), 7.31 (2H, d, 8.7), 7.23 (1H, d, 1.7), 7.14 (2H, dd, 8.7, 8.5), 7.13 (1H, d, 16.3), 7.10 (2H,

d, 8.7), 7.04 (1H, d, 16.3), 3.84 (3H, s); ^{13}C NMR (125 MHz, DMSO-d_6) δ 161.5 (d, 243.8), 158.8, 158.2, 142.9, 133.7 (d, 2.8), 132.8, 131. 2, 131.1, 128.3 (d, 8.3), 126.0, 125.5, 123.8, 123.7, 123.6, 121.4, 115.9, 115.5 (d, 21.4), 113.9, 55.1 (Figure S45).

9b-IV, amorphous solid, ^{1}H NMR (500 MHz, DMSO-d_6) δ 12.25 (1H, s), 9.20 (1H, br. s), 7.68 (2H, dd, 8.7, 5.6), 7.45 (1H, d, 1.2), 7.39 (1H, dd, 8.5, 1.4), 7.29 (2H, d, 8.7), 7.25 (1H, d, 16.6), 7.21 (2H, dd, 8.7, 8.5), 7.19 (1H, d, 16.6), 7.13 (1H, d, 8.4), 7.08 (2H, d, 8.7), 3.84 (3H, s); ^{13}C NMR (125 MHz, DMSO-d_6) δ 161.7 (d, 244.5), 158.7, 158.4, 142.6, 135.2, 133.5, 133.4 (d, 3.7), 131. 2, 128.6 (d, 8.3), 127.8, 127.7, 125.6, 124.8, 123.8, 120.7, 120.0, 115.6 (d, 21.4), 113.8, 113.4, 55.1 (Figure S46).

8c-IV, amorphous solid. ^{1}H NMR (500 MHz, DMSO-d_6) δ 7.70 (1H , dd, 8.6, 1.8), 7.58 (2H, dd, 8.9, 5.6), 7.54 (2H, m), 7.46 (1H, m), 7.38 (1H, d, 8.6), 7.38 (2H, d, 8.1), 7.16 (1H, d, 1.7), 7.13 (2H, dd, 8.9, 8.8), 7.10 (1H, d, 16.5), 7.02 (1H, d, 16.5); ^{13}C NMR (125 MHz, DMSO-d_6) δ 161.6 (d, 244.5), 158.2, 142.9, 133.7, 132.8, 131.2, 130.0, 128.5, 128.3 (d, 8.3), 128.2, 127.8, 126.1, 124.0, 123.7, 123.5, 121.1, 116.0, 115.5 (d, 22.0) (Figure S47).

9d-IV, amorphous solid. ^{1}H NMR (500 MHz, DMSO-d_6) δ 12.29 (1H, br. s), 9.30 (1H, br. s), 7.68 (2H, dd, 8.5, 5.6), 7.53 (2H, m), 7.45 (2H, m), 7.39 (1H, dd, 8.7, 1.2), 7.36 (2H, d, 7.0), 7.25 (1H, d, 16.5), 7.21 (2H, dd, 8.9, 8.7), 7.19 (1H, d, 16.5), 7.06 (1H, d, 8.4); ^{13}C NMR (125 MHz, DMSO-d_6) δ 161.7 (d, 245.4), 158.4, 142.5, 135.3, 133.7, 133.5, 133.4 (d, 2.8), 129.9, 128.6 (d, 7.3), 128.4, 127.8, 127.7, 127.7, 124.7, 124.1, 120.5, 120.1, 115.6 (d, 21.1), 113.4 (Figure S48).

8a-V, amorphous solid. ^{1}H NMR (500 MHz, DMSO-d_6) δ 7.76 (2H , d, 8.4), 7.74 (1H, dd, 8.4, 1.5), 7.64 (2H, d, 8.4), 7.38 (1H, d, 8.4), 7.35 (1H, d, 16.0), 7.31 (2H, d, 8.7), 7.28 (1H, d, 1.5), 7.13 (1H, d, 16.0), 7.09 (2H, d, 8.7), 3.84 (3H, s); ^{13}C NMR (125 MHz, DMSO-d_6) δ 158.8, 158.2, 142.9, 141.3, 133.2, 131.4, 131.2, 130.6, 127.2 (C_α-CF_3, q, *J*=32), 126.9, 125.5, 125.4 (C_β-CF_3, q, J=3.7), 124.5 (CF_3, q, J=272) , 124.4, 123.8, 123.7, 121.4, 116.0, 113.9, 55.1 (Figure S49).

9b-V, amorphous solid. ^{1}H NMR (500 MHz, DMSO-d_6) δ 12.30 (1H, br. s), 9.27 (1H, br. s), 7.84 (2H , d, 8.1), 7.70 (2H, d, 8.1), 7.50 (1H, s), 7.46 (1H, d, 16.3), 7.44 (1H, d, 8.4), 7.29 (2H, d, 8.5), 7.28 (1H, d, 16.3), 7.15 (1H, d, 8.4), 7.08 (2H, d, 8.5), 3.83 (3H, s); ^{13}C NMR (125 MHz, DMSO-d_6) δ 158.8, 158.5, 142.9, 141.0, 134.6, 133.5, 131.2, 130.9, 127.6 (C_α-CF_3, q, *J*=31), 127.2, 127.1, 125.5 (C_β-CF_3, q, J=3.7), 124.9, 124.4 (CF_3, q, J=272) , 123.8, 121.3, 120.2, 113.9, 113.8, 55.1 (Figure S50).

8c-V, amorphous solid. ^{1}H NMR (500 MHz, DMSO-d_6) δ 7.75 (1H , dd, 8.5, 1.7), 7.74 (2H, d, 8.2), 7.62 (2H, d, 8.2), 7.54 (1H, m), 7.46 (1H, m), 7.39 (1H, d, 8.5), 7.38 (2H, m), 7.32 (1H, d, 16.3), 7.21 (1H, d, 1.7), 7.11 (1H, d, 16.5); ^{13}C NMR (125 MHz, DMSO-d_6) δ 158.3, 142.9, 141.3, 133.6, 133.3, 131.3, 130.7, 130.0, 128.5, 127.9, 127.2 (C_α-CF_3, q, *J*=31), 126.9, 125.6, 125.4 (C_β-CF_3, q, J=3.7), 124.4 (CF_3, q, J=272) , 124.2, 124.0, 123.9, 121.2, 116.1 (Figure S51).

9d-V, amorphous solid. ^{1}H NMR (500 MHz, DMSO-d_6) δ 12.32 (1H, br. s), 9.37 (1H, br. s), 7.84 (2H , d, 7.8), 7.71 (2H, d, 7.9), 7.41-7.56 (6H, m), 7.35 (2H, d, 7.3), 7.28 (1H, d, 16.3), 7.07 (1H, d, 8.4); ^{13}C NMR (125 MHz, DMSO-d_6) δ 158.4, 142.8, 141.0, 134.7, 133.7, 133.5, 130.9, 129.9, 128.4, 127.8, 127.6 (C_α-CF_3, q, 32), 127.3, 127.1, 125.6 (C_β-CF_3, q, 3.7), 124.8, 124.4 (CF_3, q, 272), 124.0, 121.0, 120.3, 113.9 (Figure S52).

8aVI, amorphous solid. ^{1}H NMR (500 MHz, DMSO-d_6) δ 12.22 (1H, br. s, NH), 9.12 (1H, br. s, OH), 7.47 (1H, dd, 8.5, 1.7), 7.29 (1H, d, 8.5), 7.27 (2H, d, 8.7), 7.07 (2H, d, 8.7), 7.02 (1H, d, 1.5), 6.28 (1H, d, 15.9), 6.09 (1H, dd, 15.9, 7.0), 5.64 (2H, m), 3.83 (3H, s, -OMe), 2.29 (1H, m), 2.07 (1H, m), 2.01 (2H, m), 1.84 (1H, m), 1.73 (1H, m), 1.34 (1H, m); ^{13}C NMR (125 MHz, DMSO-d_6) δ 158.7, 158.1, 142.7, 134.2, 132.3,

131.4, 131.2, 127.5, 126.7, 126.0, 125.5, 123.7, 123.6, 122.4, 121.2, 115.7, 113.8, 55.1, 36.4, 30.9, 28.3 (Figure S53).

9b-VI, amorphous solid. ^{1}H NMR (500 MHz, DMSO-d_6) δ 12.14 (1H, br. s, NH), 9.09 (1H, br.s, OH), 7.28 (1H, d, 1.5), 7.26 (2H, d, 8.5), 7.17 (1H, dd, 8.6, 1.3), 7.07 (1H, d, 8.6), 7.06 (2H, d, 8.5), 6.42 (1H, d, 15.9), 6.27 (1H, dd, 15.9, 7.0), 5.68 (2H, m), 3.83 (3H, s, -OMe), 2.39 (1H, m), 2.14 (1H, m), 2.05 (2H, m), 1.91 (1H, m), 1.79 (1H, m), 1.42 (1H, m); ^{13}C NMR (125 MHz, DMSO-d_6) δ 158.7, 158.4, 142.2, 136.1, 135.6, 133.5, 131.1, 127.3, 126.8, 125.9, 125.6, 124.7, 123.8, 120.2, 119.9, 113.8, 112.4, 55.1, 36.4, 30.8, 28.2, 24.3 (Figure S54).

8c-VI, amorphous solid. ^{1}H NMR (500 MHz, DMSO-d_6) δ 7.51 (2H, m), 7.46 (1H, dd, 8.5, 1.5), 7.43 (1H, m), 7.33 (2H, d, 8.4), 7.30 (1H, d, 8.5), 6.94 (1H, d, 1.5), 6.25 (1H, d, 15.9), 6.06 (1H, dd, 15.9, 7.0), 5.62 (2H, m), 2.28 (1H, m), 2.05 (1H, m), 1.98 (2H, m), 1.82 (1H, m), 1.70 (1H, m), 1.33 (1H, m); ^{13}C NMR (125 MHz, DMSO-d_6) δ 158.6, 143.1, 134.7, 134.1, 132.7, 131.9, 130.3, 128.9, 128.2, 127.9, 127.1, 126.4, 124.4, 124.1, 122.6, 121.4, 116.2, 36.8, 31.3, 28.7, 24.8 (Figure S55).

9d-VI, amorphous solid. ^{1}H NMR (500 MHz, DMSO-d_6) δ 12.16 (1H, br. s), 9.19 (1H, br. s), 7.50 (2H, m), 7.43 (1H, m), 7.32 (2H, d, 7.0), 7.29 (1H, br. s), 7.15 (1H, br. d, 8.4), 6.99 (1H, d, 8.4), 6.41 (1H, d, 15.7), 6.27 (1H, dd, 15.9, 7.0), 5.67 (2H, br. s), 2.38 (1H, m), 2.12 (1H, dd, 16.5, 3.8), 2.04 (2H, m), 1.90 (1H, m), 1.78 (1H, m), 1.40 (1H, m); ^{13}C NMR (125 MHz, DMSO-d_6) δ 158.5, 142.2, 136.2, 135.7, 133.8, 133.5, 129.9, 128.4, 127.7, 127.3, 126.8, 125.9, 124.6, 124.1, 120.1, 120.0, 112.5, 36.5, 30.8, 28.3, 24.4 (Figure S56).

8a-VII, amorphous solid. ^{1}H NMR (500 MHz, DMSO-d_6) δ 12.34 (1H, s), 9.26 (1H, s), 7.86 (1H, dd, 8.5, 1.7), 7.36 (1H, d, 8.5), 7.35 (1H, d, 16.3), 7.31 (2H, d, 8.7), 7.22 (2H, d, 8.7), 7.07 (1H, d, 16.3), 3.84 (3H, s), 3.50-3.70 (8H, m) ; ^{13}C NMR (125 MHz, DMSO-d_6) δ 172.5, 165.0, 159.2, 158.7, 143.4, 142.1, 134.5, 131.7, 129.5, 126.6, 125.6, 124.9, 124.1, 121.6, 116.9, 116.4, 114.3, 66.8, 66.7, 55.6, 46.0, 42.5 (Figure S57).

9b-VII, amorphous solid. ^{1}H NMR (500 MHz, DMSO-d_6) δ 12.23 (1H, br. s), 7.53 (1H, br. d, 8.7), 7.50 (1H, d, 15.4), 7.47 (1H, br. s), 7.28 (2H, d, 8.4), 7.18 (1H, d, 15.4), 7.13 (1H, d, 8.7), 7.08 (2H, d, 8.4), 3.83 (3H, s), 3.50-3.70 (8H, m) ; ^{13}C NMR (125 MHz, DMSO-d_6) δ 172.5, 164.9, 159.2, 158.8, 143.8, 141.6, 133.8, 133.5, 131.6, 125.8, 125.2, 124.1, 122.7, 121.2, 118.6, 116.0, 114.3, 66.8, 66.7, 55.6, 46.1, 42.6 (Figure S58).

8c-VII, amorphous solid. ^{1}H NMR (500 MHz, DMSO-d_6) δ 7.87 (1H, dd, 8.7, 1.5), 7.54 (2H, m), 7.46 (1H, m), 7.37 (3H, m), 7.33 (1H, d, 15.3), 7.14 (1H, d, 1.5), 7.05 (1H, d, 15.4), 3.50-3.70 (8H, m) ; ^{13}C NMR (125 MHz, DMSO-d_6) δ 164.4, 158.3, 142.9, 141.6, 134.1, 133.3, 130.0, 129.2, 128.5, 127.9, 125.9, 124.6, 123.9, 121.0, 116.5, 116.0, 66.4, 66.3, 45.5, 42.2 (Figure S59).

9d-VII, amorphous solid. ^{1}H NMR (500 MHz, DMSO-d_6) δ 12.28 (1H, br. s), 9.46 (1H, br. s), 7.48-7.55 (5H, m), 7.45 (1H, m), 7.35 (2H, br. d, 7.2), 7.17 (1H, d, 15.3), 7.06 (1H, d, 8.5), 3.55-3.75 (8H, m) ; ^{13}C NMR (125 MHz, DMSO-d_6) δ 164.4, 158.3, 143.3, 141.1, 133.5, 133.3, 133.1, 129.9, 128.4, 127.8, 124.7, 123.8, 122.0, 120.8, 118.2, 115.6, 66.3, 66.2, 45.6, 42.1 (Figure S60).

8a-VIII, amorphous solid ^{1}H NMR (500 MHz, DMSO-d_6) δ 12.33 (1H, br. s), 9.23 (1H, br. s), 8.48 (2H, d, 6.0), 7.78 (1H, dd, 8.5, 1.7), 7.54 (2H, d, 6.0), 7.50 (1H, d, 16.5), 7.38 (1H, d, 8.5), 7.31 (2H, d, 8.7), 7.30 (1H, d, 1.7), 7.11 (1H, d, 8.7), 7.05 (1H, d, 16.3), 3.85 (3H, s); ^{13}C NMR (125 MHz, DMSO-d_6) δ 158.8, 158.2, 149.9, 144.4, 143.0, 133.5, 133.1, 131.2, 130.3, 125.4, 124.8, 124.6, 123.9, 123.7, 121.4, 120.8, 116.0, 113.9, 55.2 (Figure S61).

9b-VIII, amorphous solid. ^{1}H NMR (500 MHz, DMSO-d_6) δ 12.38 (1H, s), 9.30 (1H, s), 8.54 (2H, br. s), 7.59 (4H, m), 7.45 (1H, dd, 8.5, 1.1), 7.29 (2H, d, 8.5), 7.18 (1H, d, 16.3), 7.15 (1H, d, 8.5), 7.08 (2H, d, 8.7), 3.83 (3H, s); ^{13}C NMR (125 MHz, DMSO-d_6) δ 158.8, 158.4, 150.0, 144.1, 143.0, 134.2, 133.5, 132.6, 131.2, 126.3, 125.5, 124.9, 123.7, 121.5, 121.0, 120.4, 114.3, 113.9, 55.2 (Figure S62).

8c-VIII, amorphous solid, ^{1}H NMR (500 MHz, DMSO-d_6) δ 12.38 (1H, s), 9.34 (1H, s), 8.47 (2H, d, 6.0), 7.78 (1H, dd, 8.5, 1.5), 7.55 (2H, m), 7.51 (1H, d, 6.0), 7.48 (1H, m), 7.46 (1H, d, 16.5), 7.40 (1H, d, 8.5), 7.38 (2H, d, 8.5), 7.23 (1H, d, 1.2), 7.03 (1H, d, 16.3); ^{13}C NMR (125 MHz, DMSO-d_6) δ 158.3, 149.9, 144.3, 143.0, 133.5, 133.5, 133.0, 130.4, 130.0, 128.5, 127.9, 124.7, 124.6, 124.0, 121.1, 120.8, 116.1 (Figure S63).

9d-VIII, amorphous solid. ^{1}H NMR (500 MHz, DMSO-d_6) δ 12.35 (1H, s), 9.41 (1H, s), 8.54 (2H, d, 5.2), 7.59 (2H, d, 8.5), 7.58 (1H, d, 16.3), 7.53 (3H, m), 7.45 (2H, m), 7.36 (2H, m), 7.17 (1H, d, 16.33), 7.08 (1H, d, 8.4); ^{13}C NMR (125 MHz, DMSO-d_6) δ 158.4, 150.0, 144.0, 143.0, 134.3, 133.6, 133.5, 132.5, 129.9, 128.4, 127.8, 126.3, 124.8, 124.0, 121.3, 121.0, 120.4, 114.2 (Figure S64).

8a-IX, amorphous solid. ^{1}H NMR (500 MHz, DMSO-d_6) δ 12.20 (1H, s), 9.09 (1H, s), 7.60 (1H, dd, 8.6, 1.8), 7.31 (1H, d, 8.5), 7.30 (2H, d, 8.5), 7.22 (2H, d, 8.5), 7.12 (1H, d, 1.5), 7.09 (2H, d, 8.7), 6.85 (1H, d, 16.0), 6.79 (1H, d, 16.0), 6.51 (2H, d, 8.5), 3.84 (3H, s); ^{13}C NMR (125 MHz, DMSO-d_6) δ 158.7, 158.1, 148.6, 142.7, 132.1, 132.0, 131.2, 128.0, 127.5, 125.6, 124.7, 123.7, 123.3, 122.7, 122.4, 121.3, 115.8, 113.9, 55.1 (Figure S65).

9b-IX, amorphous solid. ^{1}H NMR (500 MHz, DMSO-d_6) δ 7.35 (1H, d, 1.2), 7.29 (5H, m), 7.07 (2H, d, 8.5), 7.07 (1H, d, 8.5), 7.02 (1H, d, 16.3), 6.91 (1H, d, 16.3), 6.56 (1H, d, 8.4), 3.84 (3H, s); ^{13}C NMR (125 MHz, DMSO-d_6) δ 158.7, 158.4, 149.0, 142.0, 136.3, 133.6, 131.1, 129.7, 127.8, 125.7, 124.7, 124.4, 123.9, 122.1, 119.8, 119.7, 113.9, 113.8, 112.2, 55.1 (Figure S66).

8c-IX, amorphous solid. ^{1}H NMR (500 MHz, DMSO-d_6) δ 12.27 (1H, br. s), 7.65 (1H, dd, 8.5, 1.5), 7.54 (2H, m), 7.47 (1H, m), 7.36 (3H, m), 7.34 (2H, d, 8.5), 7.08 (1H, d, 1.4), 6.92 (1H, d, 16.6), 6.90 (1H, d, 16.6), 6.76 (2H, d, 8.4); ^{13}C NMR (125 MHz, DMSO-d_6) δ 158.1, 142.8, 133.7, 132.4, 131.8, 130.0, 128.5, 127.8, 127.6, 127.4, 124.9, 124.0, 123.5, 122.8, 121.1, 117.0, 115.9 (Figure S67).

9d-IX, amorphous solid. ^{1}H NMR (500 MHz, DMSO-d_6) δ 12.18 (1H, s), 7.52 (2H, m), 7.44 (1H, m), 7.35 (3H, m), 7.30 (3H, m), 7.02 (1H, d, 16.3), 7.00 (1H, d, 8.2), 6.91 (1H, d, 16.3), 6.56 (2H, d, 8.4); ^{13}C NMR (125 MHz, DMSO-d_6) δ 158.4, 149.0, 142.0, 136.4, 133.8, 133.6, 129.9, 129.8, 128.4, 127.9, 127.7, 124.6, 124.4, 124.2, 122.1, 119.8, 119.6, 113.9, 112.2 (Figure S68).

8a-X, amorphous solid. ^{1}H NMR (500 MHz, DMSO-d_6) δ 7.48 (1H, dd, 8.5, 1.7), 7.32 (1H, d, 14.8), 7.28 (1H, br. d, 8.4), 7.27 (2H, d, 8.9), 7.08 (2H, d, 8.9), 7.02 (1H, d, 1.8), 5.94 (1H, d, 14.8), 3.84 (3H, s), 3.55 (2H, t, 7.2), 2.40 (2H, t, 8.1), 2.01 (2H, m) ; ^{13}C NMR (125 MHz, DMSO-d_6) δ 173.0, 158.7, 158.1, 143.0, 131.9, 131.2, 130.6, 125.7, 123.6, 123.1, 122.4, 121.8, 121.5, 116.0, 113.9, 111.1, 55.2, 45.0, 30.8, 17.1 (Figure S69).

9b-X, amorphous solid. ^{1}H NMR (500 MHz, DMSO-d_6) δ 12.10 (1H, s), 9.07 (1H, br. s), 7.51 (1H, d, 14.8), 7.30 (1H, d, 1.2), 7.27 (2H, d, 8.7), 7.17 (1H, dd, 8.5, 1.2), 7.07 (2H, d, 8.7), 7.06 (1H, d, 8.5), 6.04 (1H, d, 14.8), 3.83 (3H, s), 3.64 (2H, t, 7.2), 2.45 (2H, t, 8.1), 2.07 (2H, m) ; ^{13}C NMR (125 MHz, DMSO-d_6) δ 173.2, 158.7, 158.4, 147.5, 142.0, 134.9, 133.6, 131.1, 125.6, 124.9, 123.9, 123.7, 119.7, 113.8, 111.4, 110.4, 55.1, 44.9, 30.7, 17.1 (Figure S70).

8c-X, amorphous solid. ^{1}H NMR (500 MHz, DMSO-d_6) δ 7.53 (2H, m), 7.48 (1H, dd, 8.5, 1.5), 7.45 (1H, m), 7.35 (2H, m), 7.30 (1H, d, 8.5), 7.30 (1H, d, 14.8), 6.95 (1H, d, 1.5), 5.92 (1H, d, 14.8), 3.55 (2H, t,

7.2), 2.39 (2H, t, 8.1), 2.01 (2H, m); ^{13}C NMR (125 MHz, DMSO-d_6) δ 173.3, 158.5, 134.2, 132.3, 131.1, 130.3, 128.9, 128.2, 124.9, 124.3, 123.7, 122.9, 122.0, 121.7, 116.4, 111.4, 45.4, 31.2, 17.5 (Figure S71).

9d-X, amorphous solid. ^{1}H NMR (500 MHz, DMSO-d_6) δ 12.14 (1H, s), 9.17 (1H, br. s), 7.52 (2H, m), 7.51 (1H, d, 14.6), 7.44 (1H, m), 7.34 (2H, m), 7.32 (1H, d, 1.4), 7.17 (1H, dd, 8.5, 1.5), 6.98 (1H, d, 8.5), 6.03 (1H, d, 14.8), 3.64 (2H, t, 7.2), 2.45 (2H, t, 8.0), 2.07 (2H, m) ; ^{13}C NMR (125 MHz, DMSO-d_6) δ 173.2, 158.4, 142.0, 135.0, 133.8, 133.6, 129.8, 128.4, 127.7, 124.8, 124.1, 123.7, 119.8, 119.4, 111.4, 110.3, 44.9, 30.7, 17.1 (Figure S72).

10a-X, amorphous solid. ^{1}H NMR (500 MHz, DMSO-d_6) δ 7.39 (1H, dd, 8.5, 1.9), 7.32 (1H, d, 8.5), 7.29 (2H, d, 8.8), 7.09 (2H, d, 8.7), 7.05 (1H, d, 1.9), 5.21 (1H, s), 5.05 (1H, s), 3.83 (3H, s), 3.48 (2H, t, 6.9), 2.29 (2H, t, 8.0), 1.94 (2H, m) ; ^{13}C NMR (125 MHz, DMSO-d_6) δ 173.4, 158.8, 158.3, 143.4, 142.7, 133.2, 131.2, 129.7, 125.3, 124.4, 123.5, 121.9, 120.8, 115.3, 113.7, 107.4, 55.2, 49.3, 31.3, 18.3 (Figure S73).

10b-X, amorphous solid. ^{1}H NMR (500 MHz, DMSO-d_6) δ 12.14 (1H, br. s), 7.30 (1H, d, 1.4), 7.28 (1H, d, 8.5), 7.12 (1H, dd, 8.4, 1.5), 7.09 (1H, d, 8.4), 7.08 (2H, d, 8.5), 5.35 (1H, s), 5.19 (1H, s), 3.83 (3H, s), 3.58 (2H, t, 6.9), 2.41 (2H, t, 7.9), 2.08 (2H, m) ; ^{13}C NMR (125 MHz, DMSO-d_6) δ 173.6, 158.7, 158.3, 143.4, 142.8, 134.3, 133.1, 125.5, 124.4, 123.6, 121.1, 120.2, 113.8, 112.7, 108.5, 55.2, 49.4, 31.4, 18.4 (Figure S74).

10c-X, amorphous solid. ^{1}H NMR (500 MHz, DMSO-d_6) δ 12.30 (1H, br. s), 9.32 (1H, br. s), 7.53 (2H, m), 7.45 (1H, m), 7.41 (1H, dd, 8.5, 2.0), 7.36 (2H, m), 7.33 (1H, d, 8.5), 6.95 (1H, d, 1.9), 5.22 (1H, s), 5.04 (1H, s), 3.46 (2H, t, 6.9), 2.26 (2H, t, 8.0), 1.91 (2H, m) ; ^{13}C NMR (125 MHz, DMSO-d_6) δ 173.4, 158.3, 143.3, 142.7, 133.5, 133.2, 129.9, 129.7, 128.3, 127.8, 124.5, 123.8, 121.8, 120.6, 115.4, 107.5, 49.3, 31.3, 18.3 (Figure S75).

10d-X, amorphous solid. ^{1}H NMR (500 MHz, DMSO-d_6) δ 12.17 (1H, br. s), 9.32 (1H, br. s), 7.52 (2H, m), 7.44 (1H, m), 7.325(2H, m), 7.31 (1H, d, 1.7), 7.12 (1H, dd, 8.5, 1.8), 7.02 (1H, d, 8.5), 5.35 (1H, s), 5.19 (1H, s), 3.58 (2H, t, 6.9), 2.40 (2H, t, 8.0), 2.07 (2H, m) ; ^{13}C NMR (125 MHz, DMSO-d_6) δ 173.6, 158.3, 143.4, 142.7, 134.4, 133.7, 133.1, 129.8, 128.4, 127.8, 124.2, 123.8, 120.9, 120.3, 112.7, 108.5, 49.4, 31.4, 18.3 (Figure S76).

8a-XI, amorphous solid. ^{1}H NMR (500 MHz, DMSO-d_6) δ 12.19 (1H, br. s, NH), 7.29 (1H, d, 8.4), 7.28 (2H, d, 8.7), 7.22 (1H, dd, 8.4, 1.2), 7.07 (2H, d, 8.7), 6.20 (1H, s), 5.38 (1H, br. s), 3.83 (3H, s, -OMe), 2.15 (1H, m), 1.88-2.05 (4H, m), 1.75 (1H, m), 1.69 (3H, s), 1.61 (3H, s), 1.49 (1H, m); ^{13}C NMR (125 MHz, DMSO-d_6) δ 158.7, 158.2, 142.6, 142.0, 133.1, 131.8, 131.4, 131.1, 127.5, 125.6, 124.2, 123.6, 122.9, 120.9, 120.6, 115.0, 113.8, 55.1, 43.1, 30.1, 30.1, 27.4, 23.3, 15.8 (Figure S77).

9b-XI, amorphous solid. ^{1}H NMR (500 MHz, DMSO-d_6) δ 12.12 (1H, br. s, NH), 9.07 (1H, br. s, OH), 7.27 (2H, d, 8.7), 7.25 (1H, br. s), 7.08 (1H, d, 8.4), 7.06 (2H, d, 8.7), 6.97 (1H, br. d, 8.4), 6.29 (1H, s), 5.41 (1H, br. s), 3.83 (3H, s, -OMe), 2.22 (1H, m), 1.91-2.10 (4H, m), 1.84 (3H, s), 1.78 (1H, m), 1.64 (3H, s), 1.54 (1H, m); ^{13}C NMR (125 MHz, DMSO-d_6) δ 158.7, 158.4, 143.6, 142.2, 136.2, 133.1, 131.1, 125.6, 124.1, 123.7, 123.3, 122.7, 120.5, 119.2, 114.8, 113.8, 55.1, 43.3, 30.2, 30.1, 27.4, 23.3, 16.0 (Figure S78).

10a-XI, amorphous solid. ^{1}H NMR (500 MHz, DMSO-d_6) δ 12.15 (1H, br. s, NH), 9.06 (1H, br. s, OH), 7.27 (1H, d, 8.2), 7.24 (2H, d, 8.5), 7.14 (1H, dd, 8.2, 1.5), 7.06 (2H, d, 8.5), 6.95 (1H, d, 1.5), 5.32 (1H, br. s), 4.76 (1H, s, C=CH_2), 4.59 (1H, s, C=CH_2), 3.83 (3H, s, -OMe), 3.30 (2H, s), 1.84-2.00 (4H, m), 1.78 (1H, m), 1.68 (1H, m), 1.58 (3H, s), 1.35 (1H, m); ^{13}C NMR (125 MHz, DMSO-d_6) δ 158.7, 158.2, 153.2, 142.6, 133.3, 133.1, 131.6, 131.1, 127.5, 125.6, 124.3, 123.5, 121.0, 120.5, 115.3, 113.7, 109.7, 55.1, 41.0, 38.1, 30.8, 30.1, 27.7, 23.2 (Figure S81).

10b-XI, amorphous solid. ^{1}H NMR (500 MHz, DMSO-d_6) δ 12.09 (1H, br. s, NH), 7.27 (2H, d, 8.5), 7.16, (1H, br. s), 7.06 (2H, d, 8.5), 7.05 (1H, d, 8.3), 6.92 (1H, dd, 8.3, 1.1), 5.34 (1H, br. s), 4.86 (1H, s, C=CH_2), 4.72 (1H, s, C=CH_2), 3.82 (3H, s, -OMe), 3.40 (2H, s), 2.07 (1H, m), 1.80-2.00 (4H, m), 1.76 (1H, m), 1.58 (3H, s), 1.41 (1H, m); ^{13}C NMR (125 MHz, DMSO-d_6) δ 158.7, 158.4, 152.8, 142.0, 138.4, 133.2, 133.1, 131.1, 125.7, 124.4, 123.7, 123.3, 120.5, 119.4, 115.2, 113.8, 110.1, 55.1, 41.1, 38.1, 30.7, 30.1, 27.7, 23.2 (Figure S82).

Density Functional Theory Calculations

DFT calculations were performed using Gaussian 09 program (Rev D01).[4] The hybrid functional B3LYP was used in conjunction with the Pople basis set 6-31g.[5-7] The effect of solvent (water or dichloromethane) was included in all calculations and was modeled by self-consistent reaction field (SCRF) method with the Polarizable Continuum Model (PCM) as implemented in Gaussian 09.[8] The empirical dispersion using the D3 version of Grimme's dispersion with the original D3 damping function was also included in all calculations.[9] The initial geometries of the various compounds were taken from the crystal structures (PDB: 6K0F). For cyclopenin and its analogs in the folded (boat-like) configuration, the crystal structure of the Br-substituted cyclopenin at C7 position reported in this study was used as the initial geometric structure for DFT calculations. For cyclopenin and its analogs in the extended flat (chair-like) configuration, the cyclopenin structure in the crystal structure of the AsqJ enzyme bound with cyclopenin (PDB: 6K0F) was used as the initial geometry. The geometry optimization was converged based on the default convergence criteria. The transition states involved in the conversion of cyclopenin to viridicatin were first searched along the coordinate of the C10-C5a distance (for the first transition state) and along the coordinate of the C5a-C5 distance (for the second transition state) via relaxed geometric scans. The transition states were then optimized via the Synchronous Transit-Guided Quasi-Newton (STQN) method as implemented in Gaussian 09 (keyword QST2 or QST3).[10-11] The optimized transition states were further verified by frequency calculations to show a single imaginary frequency and by intrinsic reaction coordinate (IRC) calculations in both the forward and the backward direction starting from the transition state structure.[12-13] The free energies were derived from frequency calculations on the geometry optimized structures. The XYZ coordinates of all the calculated structures were included in a separate SI file.

Molecular Dynamics Simulations

Molecular Dynamics simulations were performed with GROMACS-2018 program. GAFF parameters for ligands were set using ANTECHAMBER and ACPYPE.[14-16] The initial coordinates of the complex of AsqJ with ligands were modeled from the crystal structure of AsqJ-$Fe3^{+}$-2OG-cyclopeptin complex (PDB entry 5Y7R). The geometry of Fe coordination sphere was restrained using distance, valence angle and torsion harmonic restraints. The complex was solvated in a water box with dimensions 80 x 80 x 63 Å. The systems were subjected to energy minimization using Steepest Decent algorithm, followed by 20ns NPT MD equilibration using Langevin integrator (300K, 2ps relaxation time, 2fs time step) and Berendsen barostat (1 atm). Alchemical transformation of DHCP-OME and DCHP-OME ligands to their brominated derivatives were done using 10ns MD calculations for 11 intermediate lambda states of the system. Similar 11 lambda alchemical transformation calculations were performed for ligands solvated in 40 x 40 x 40 Å water box. Bennett acceptance ratio method (BAR) were used to compute free energy changes associated with ligand mutations in protein (ΔG_{prot}) and in water (ΔG_{wat}) from which binding free energy difference were calculated $\Delta\Delta G_{bind} = \Delta G_{prot} - \Delta G_{wat}$. Fe-C10 distance distribution were computed from 10ns long MD simulations for unperturbed ligands (lambda = 0 and lambda = 1).

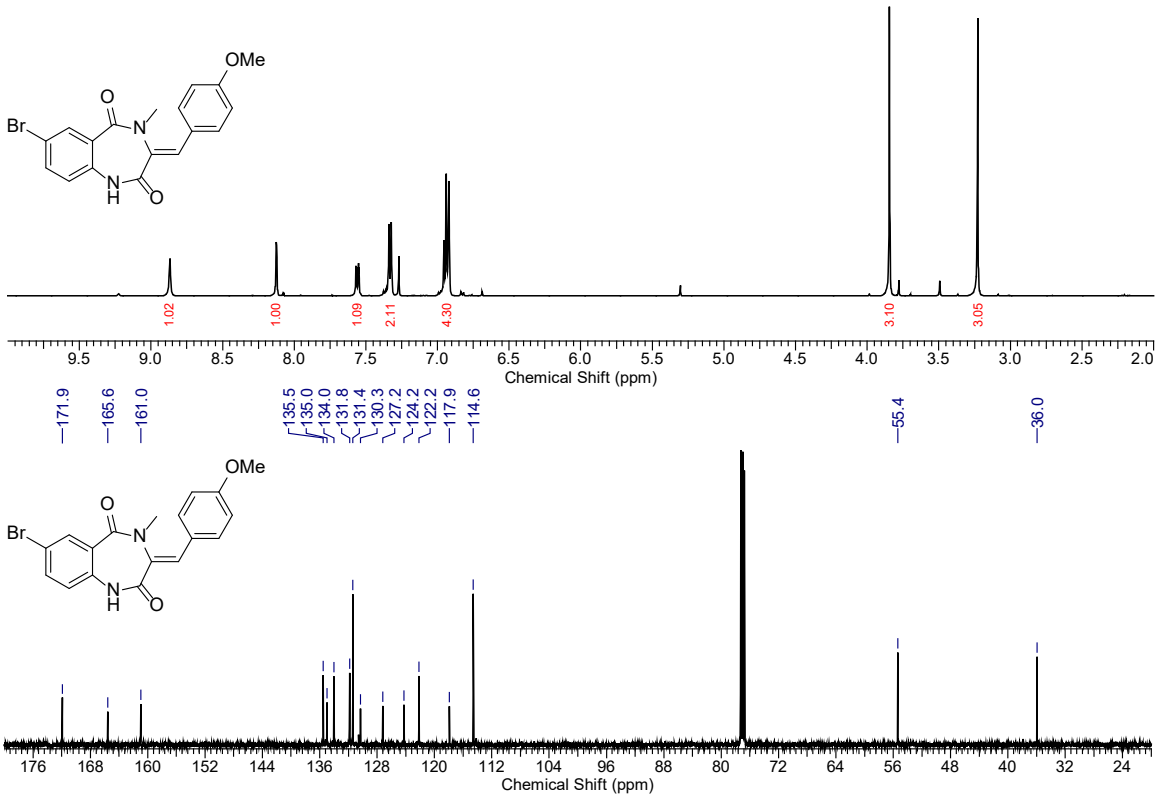

Figure S1. ^{1}H and ^{13}C NMR of 7-Br-(4'-methoxy)dehydrocyclopeptin (**5a**) in $CDCl_3$

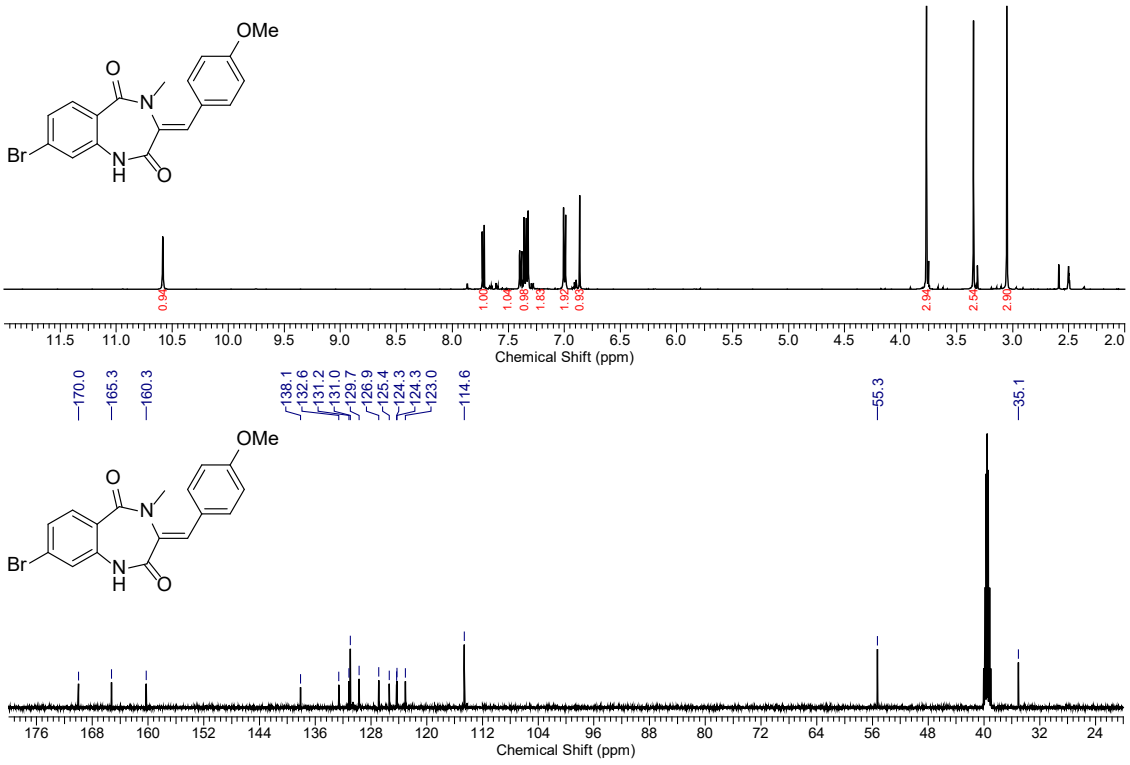

Figure S2. ^{1}H and ^{13}C NMR of 8-Br-(4'-methoxy)dehydrocyclopeptin (**5b**) in DMSO-d_6

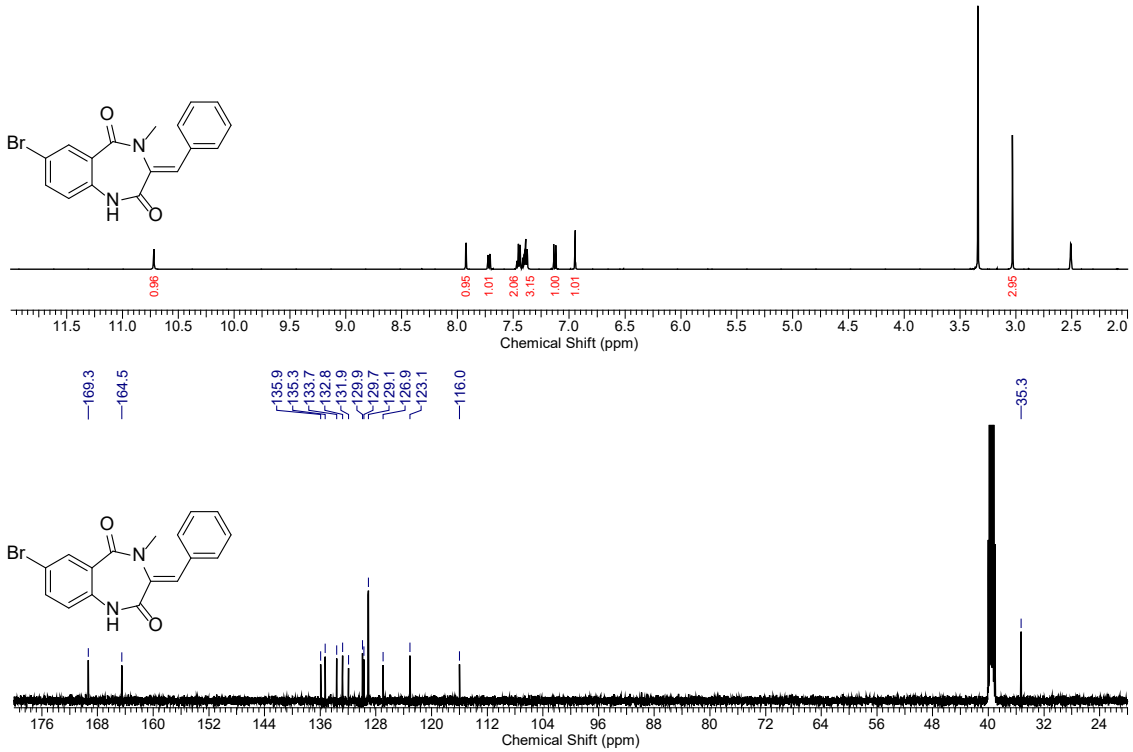

Figure S3. ^{1}H and ^{13}C NMR of 7-Br-dehydrocyclopeptin (**5c**) in DMSO-d_6

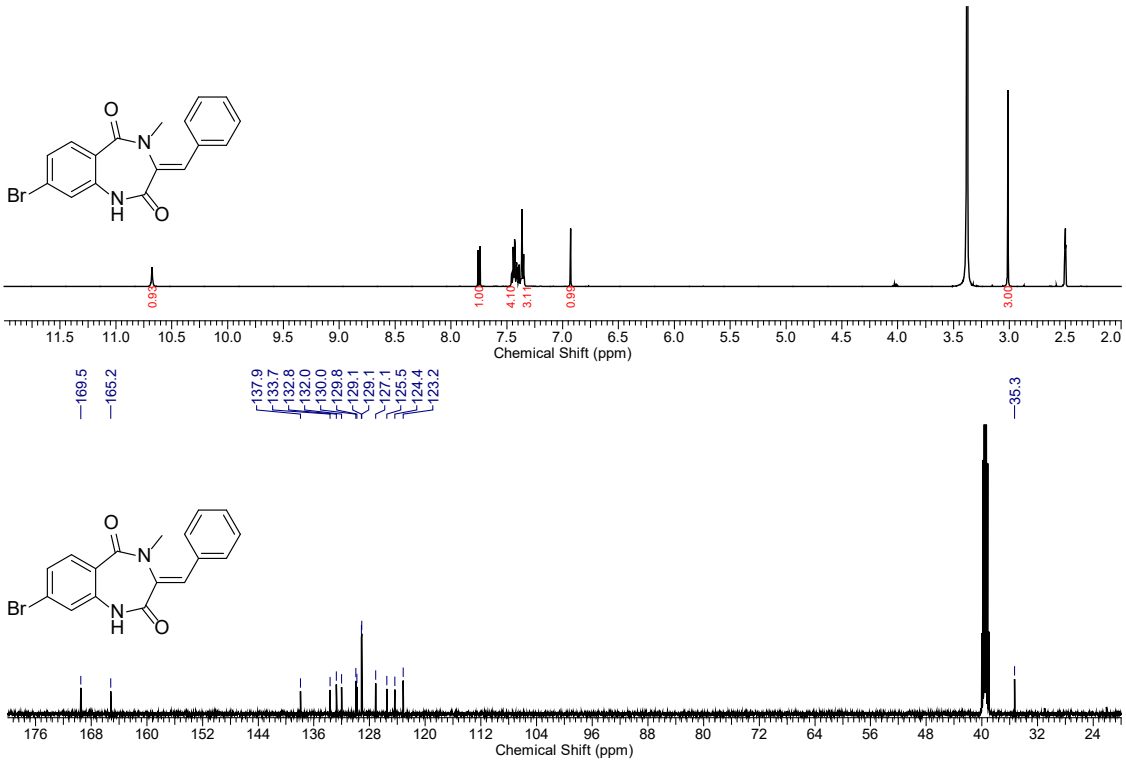

Figure S4. ^{1}H and ^{13}C NMR of 8-Br-dehydrocyclopeptin (**5d**) in DMSO-d_6

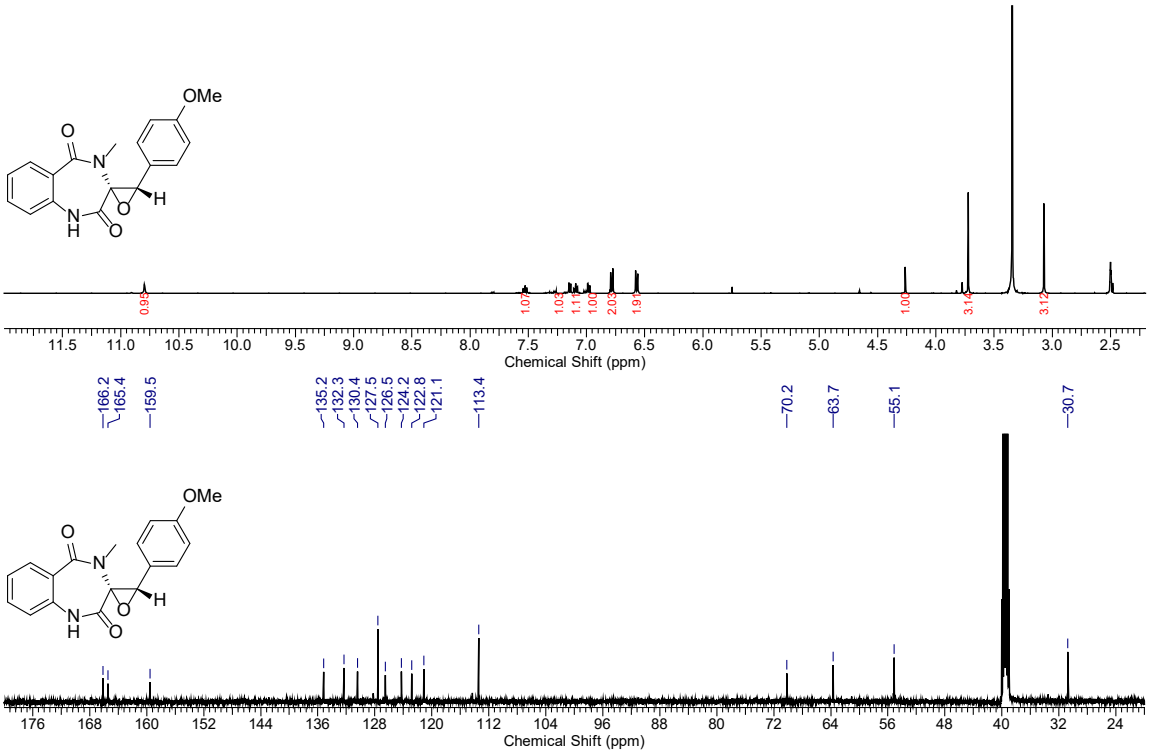

Figure S5. ^{1}H and ^{13}C NMR of (4'-methoxy)cyclopenin (**2a**) in DMSO-d_6

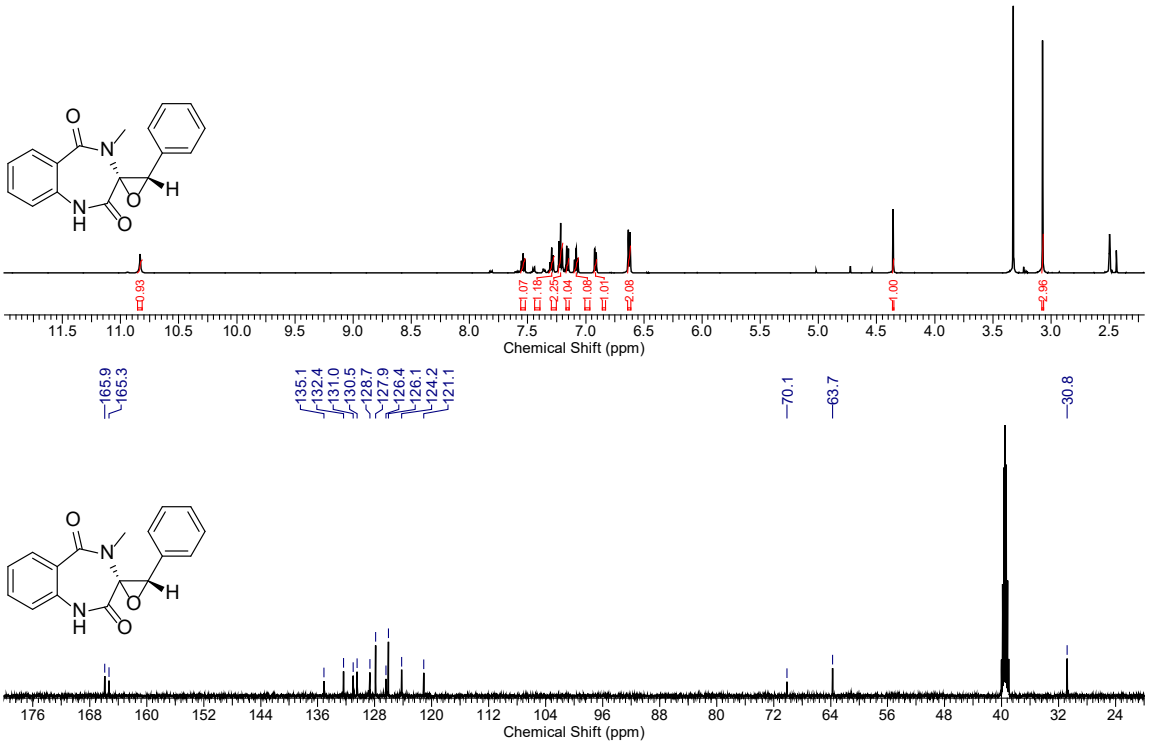

Figure S6. ^{1}H and ^{13}C NMR of cyclopenin (**2b**) in DMSO-d_6

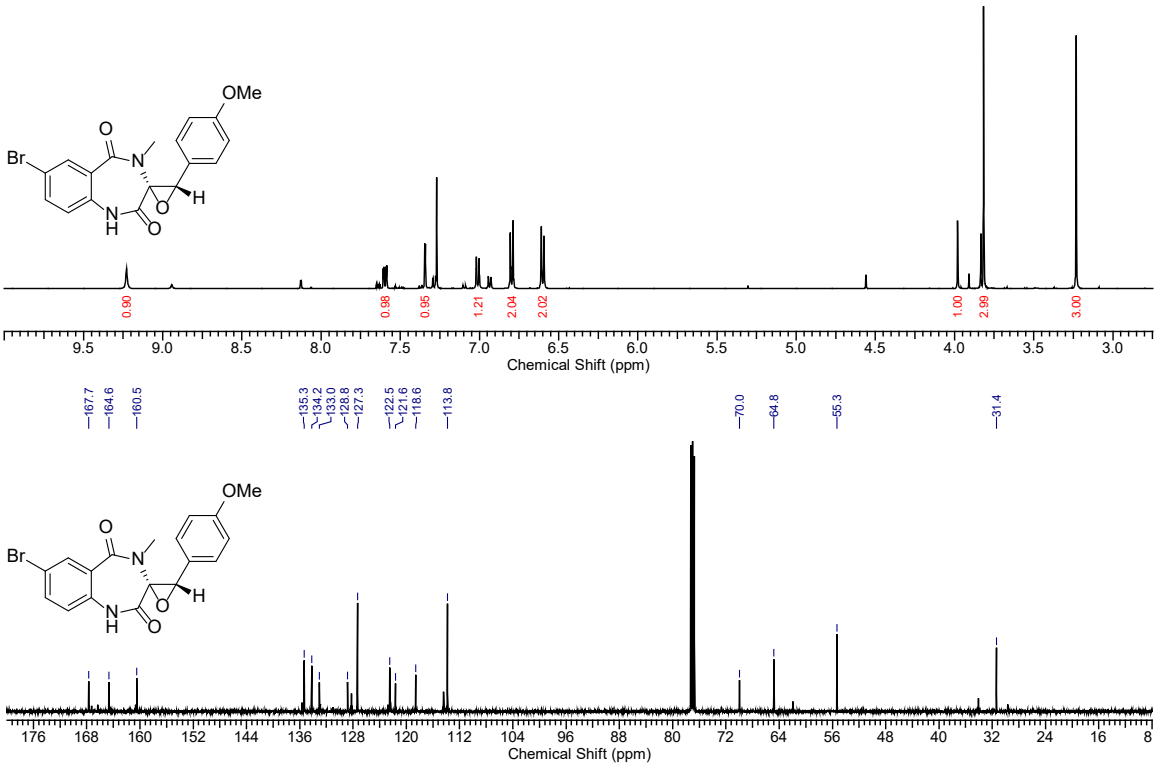

Figure S7. ^{1}H and ^{13}C NMR of 7-Br-(4'-methoxy)cyclopenin (**6a**) in $CDCl_3$

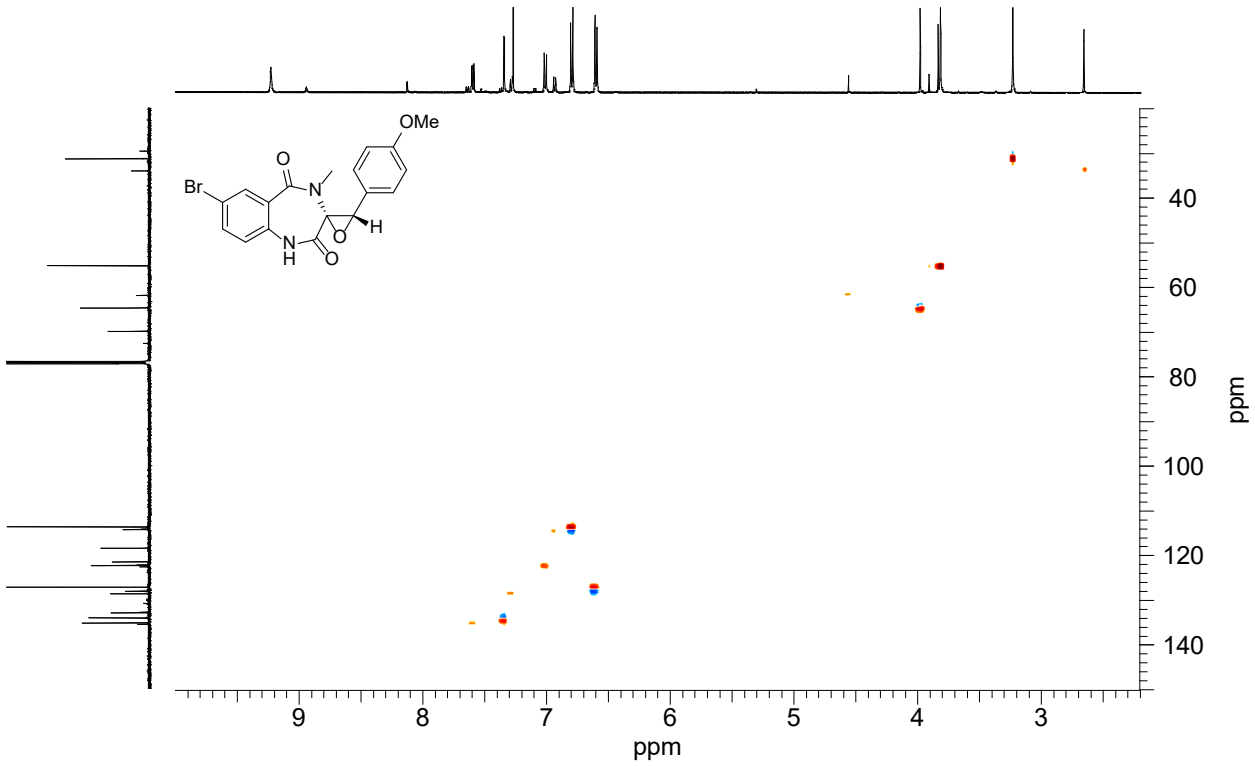

Figure S8. HSQC of 7-Br-(4'-methoxy)cyclopenin (**6a**) in $CDCl_3$

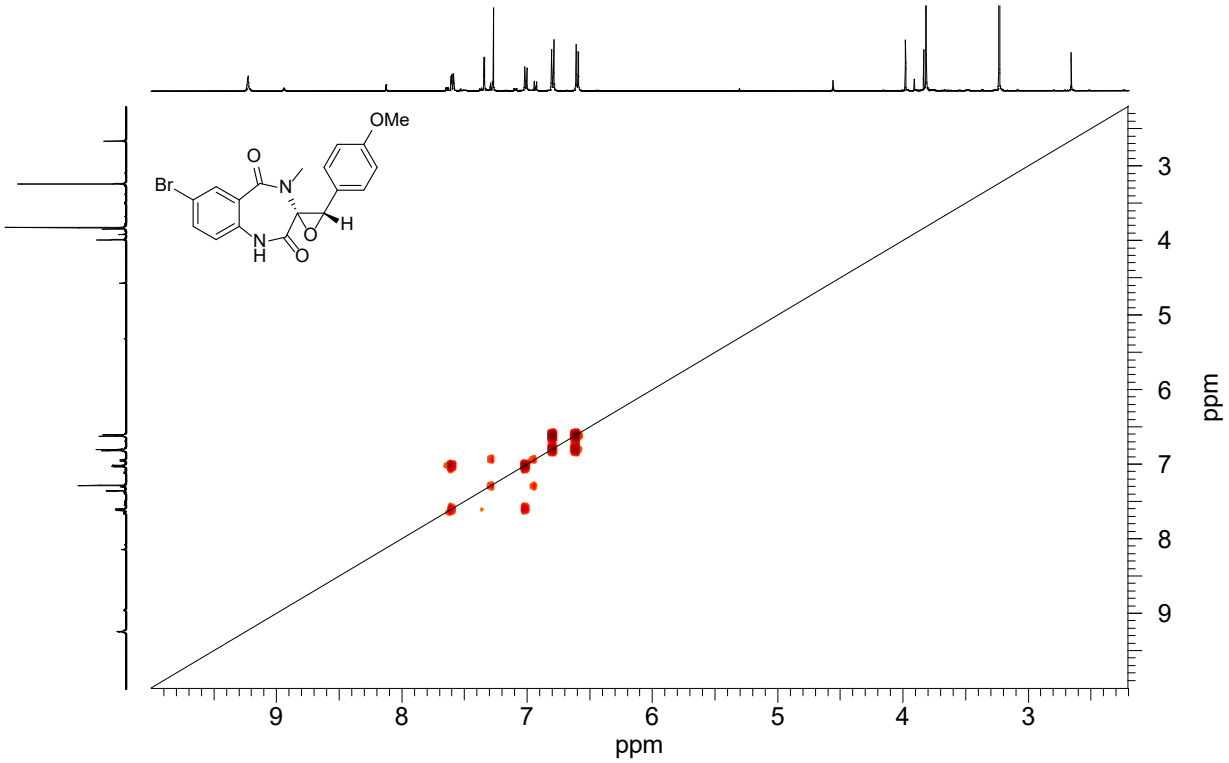

Figure S9. ^{1}H-^{1}H COSY of 7-Br-(4'-methoxy)cyclopenin (**6a**) in $CDCl_3$

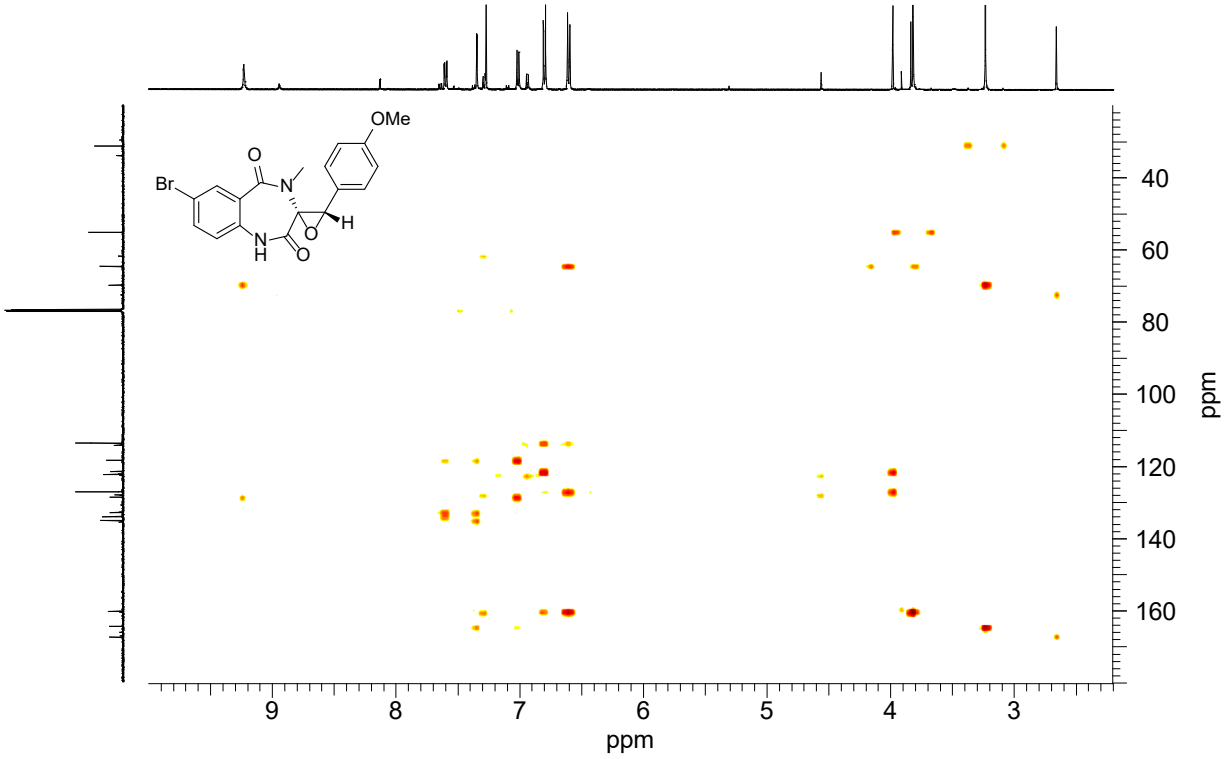

Figure S10. HMBC of 7-Br-(4'-methoxy)cyclopenin (**6a**) in $CDCl_3$

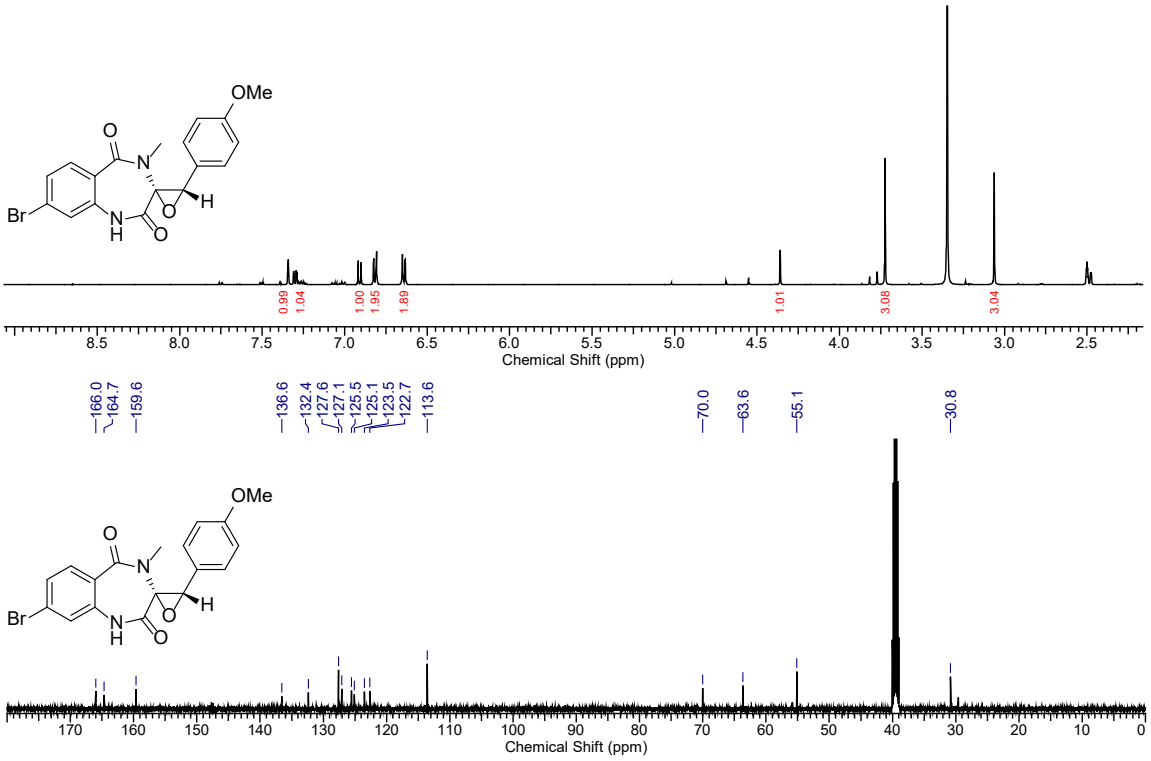

Figure S11. ^{1}H and ^{13}C NMR of 8-Br-(4'-methoxy)cyclopenin (**6b**) in DMSO-d_6

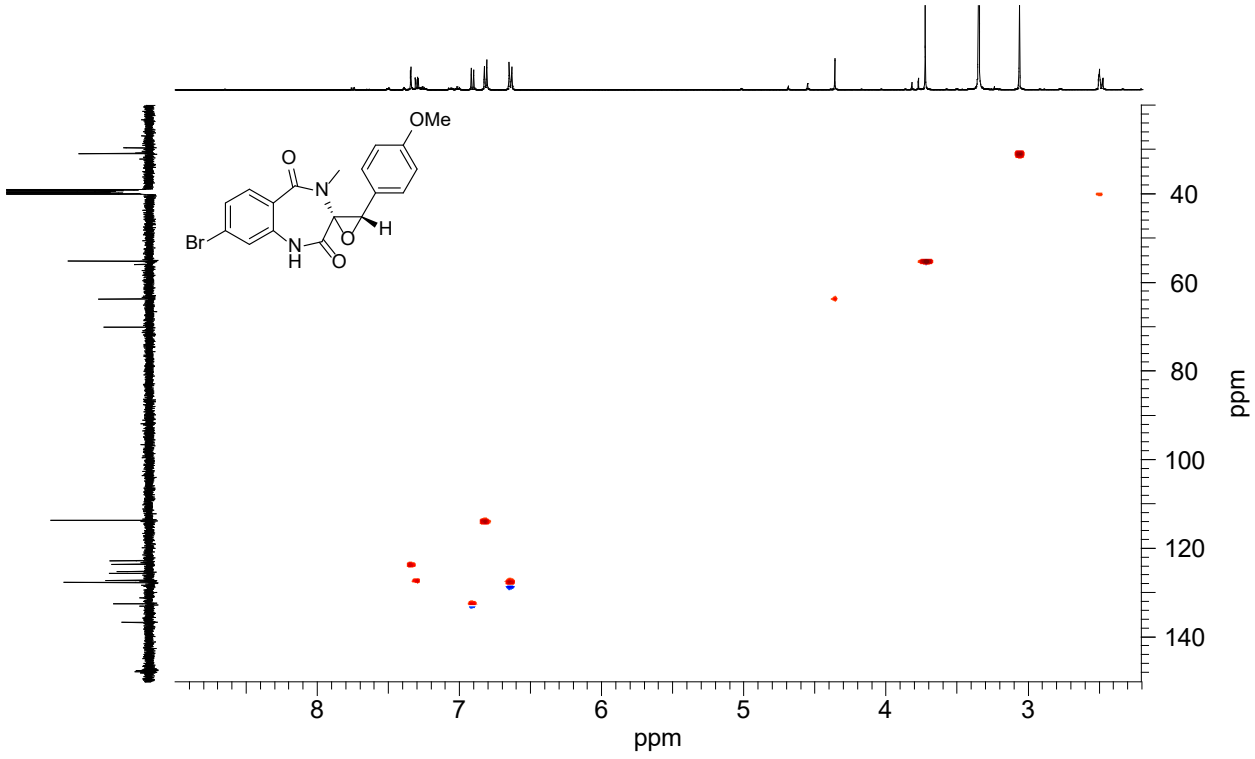

Figure S12. HSQC of 8-Br-(4'-methoxy)cyclopenin (**6b**) in DMSO-d_6

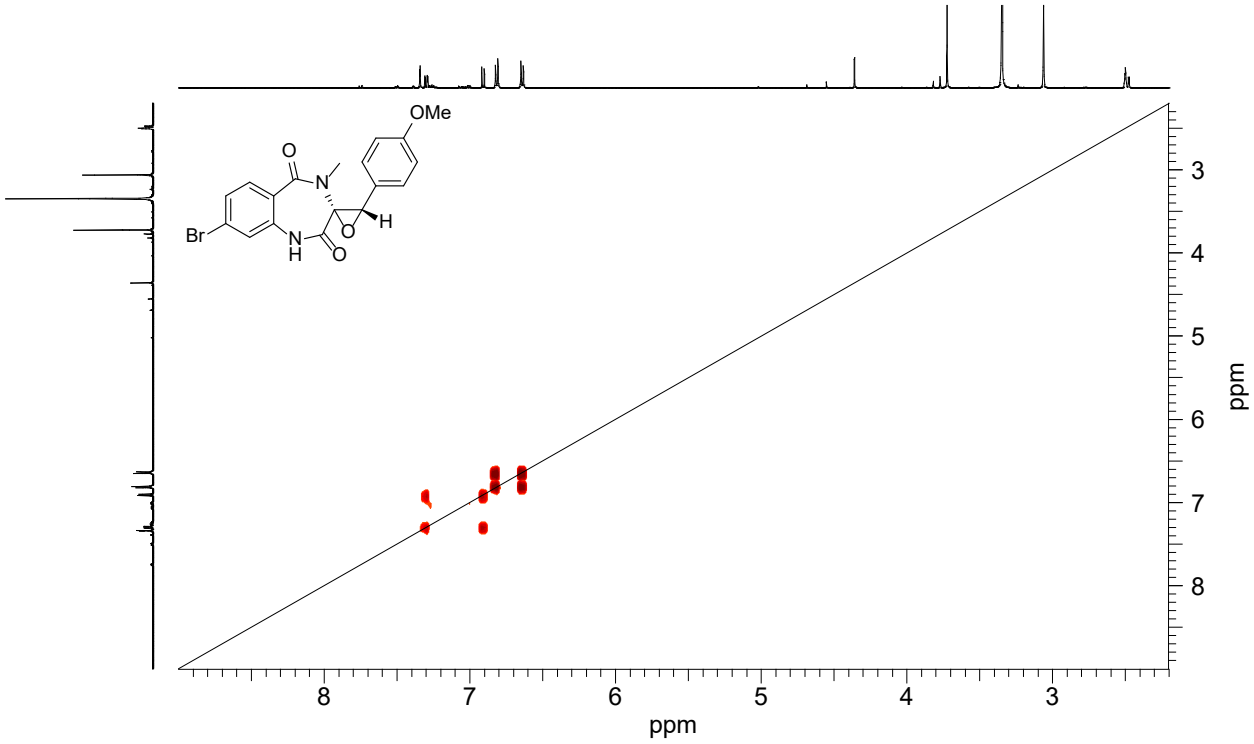

Figure S13. ^{1}H-^{1}H COSY of 8-Br-(4'-methoxy)cyclopenin (**6b**) in DMSO-d_6

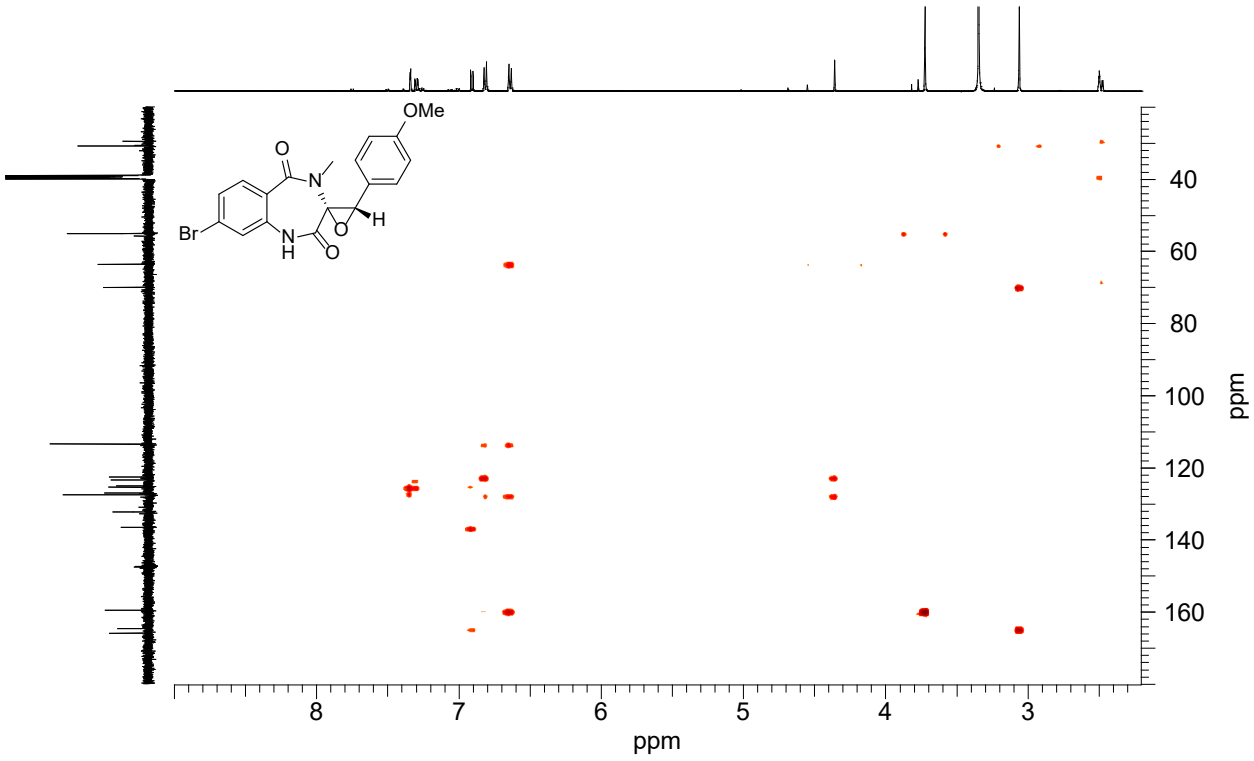

Figure S14. HMBC of 8-Br-(4'-methoxy)cyclopenin (**6b**) in DMSO-d_6

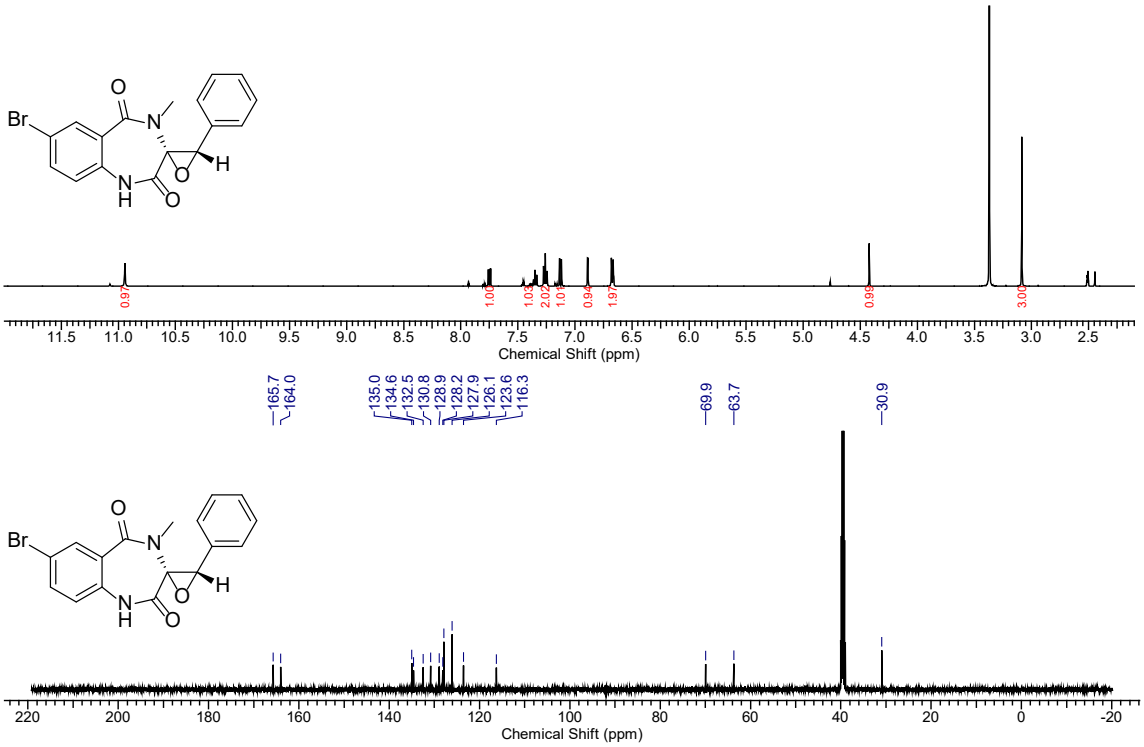

Figure S15. ^{1}H and ^{13}C NMR of 7-Br-cyclopenin (**6c**) in DMSO-d_6

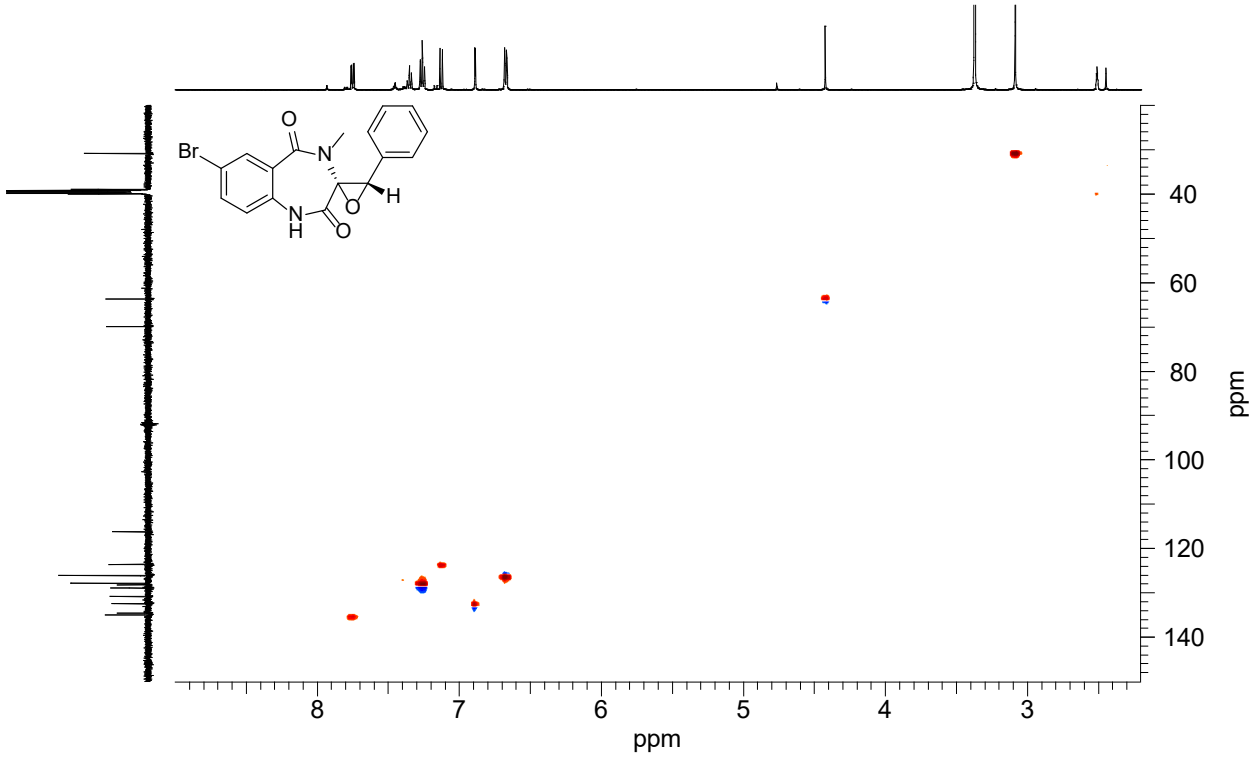

Figure S16. HSQC of 7-Br-cyclopenin (**6c**) in DMSO-d_6

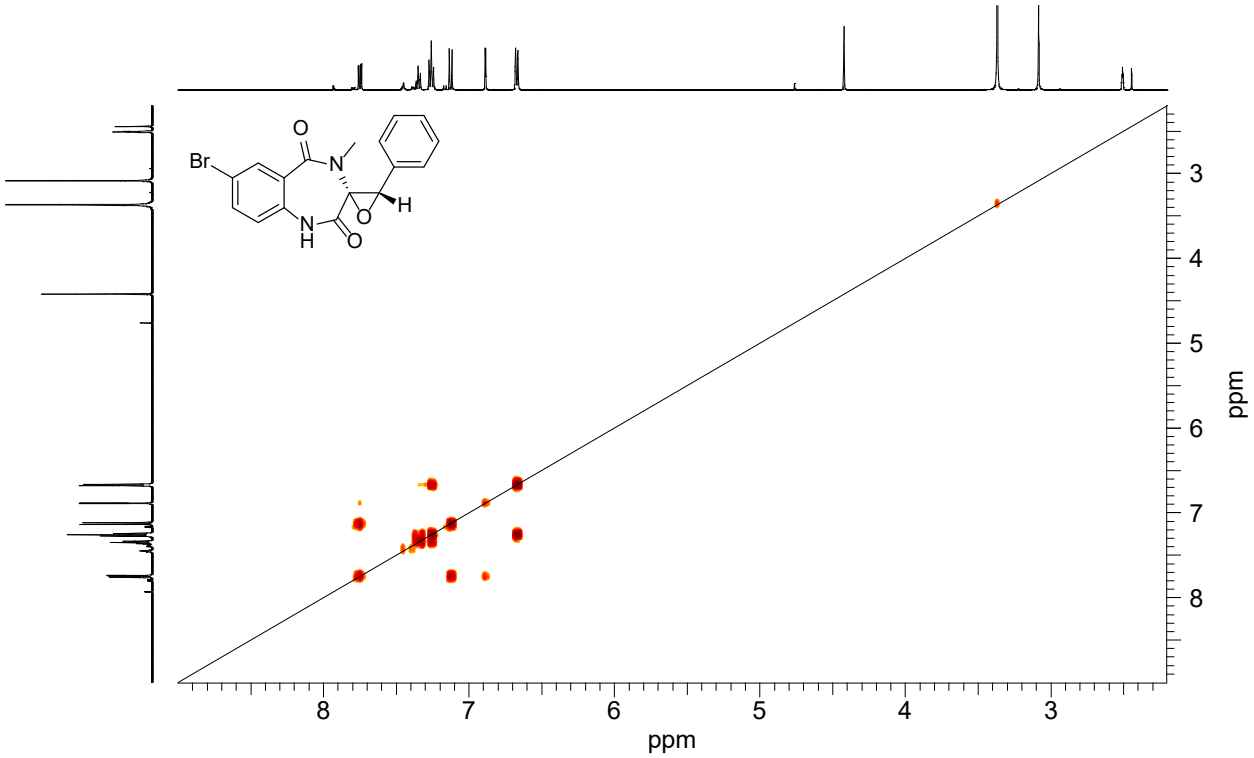

Figure S17. ^{1}H-^{1}H COSY of 7-Br-cyclopenin (**6c**) in DMSO-d_6

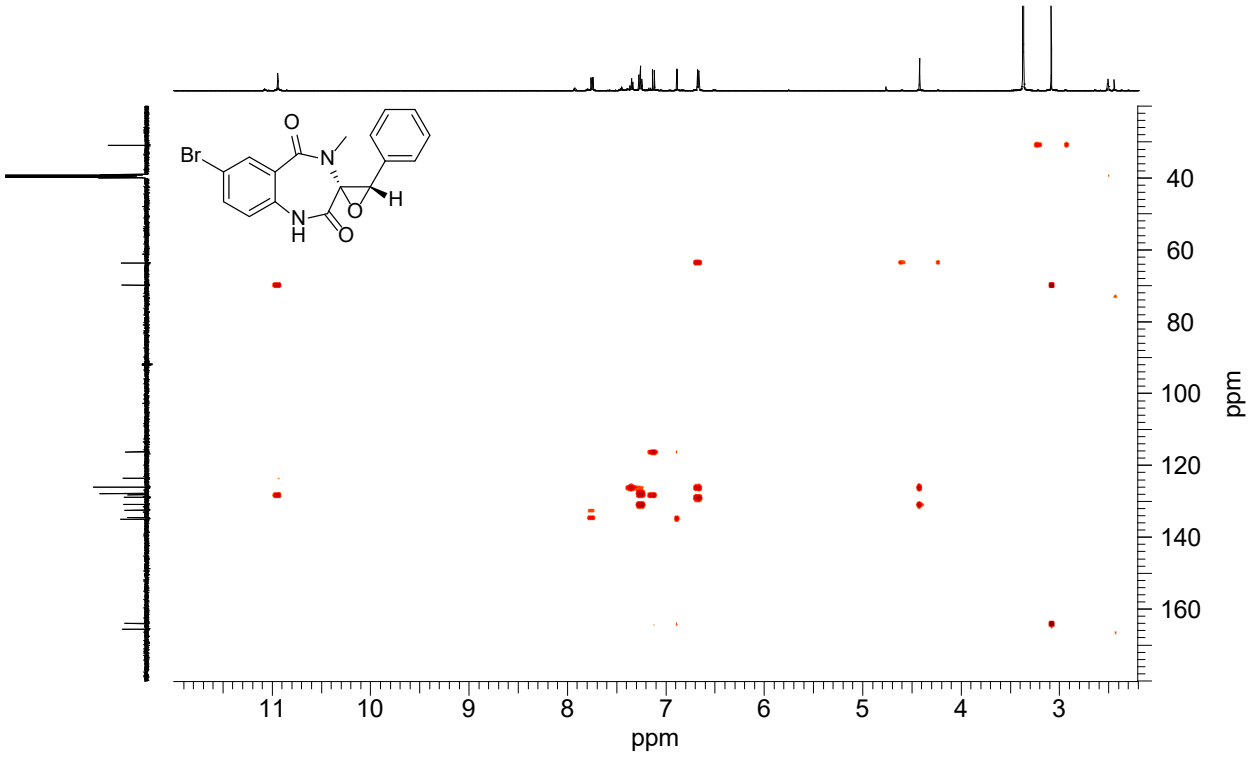

Figure S18. HMBC of 7-Br-cyclopenin (**6c**) in DMSO-d_6

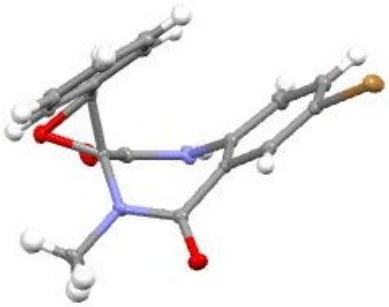

Figure S19. X-ray of 7-Br-cyclopenin (**6c**)

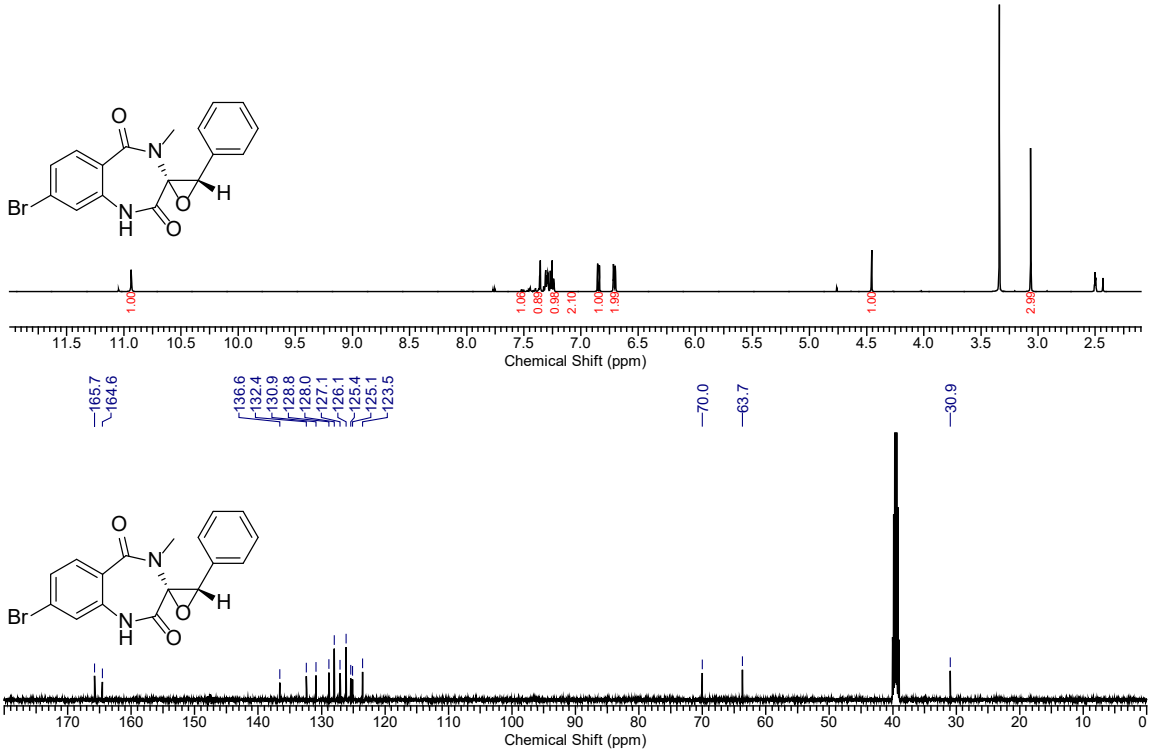

Figure S20. ^{1}H and ^{13}C NMR of 8-Br-cyclopenin (**6d**) in DMSO-d_6

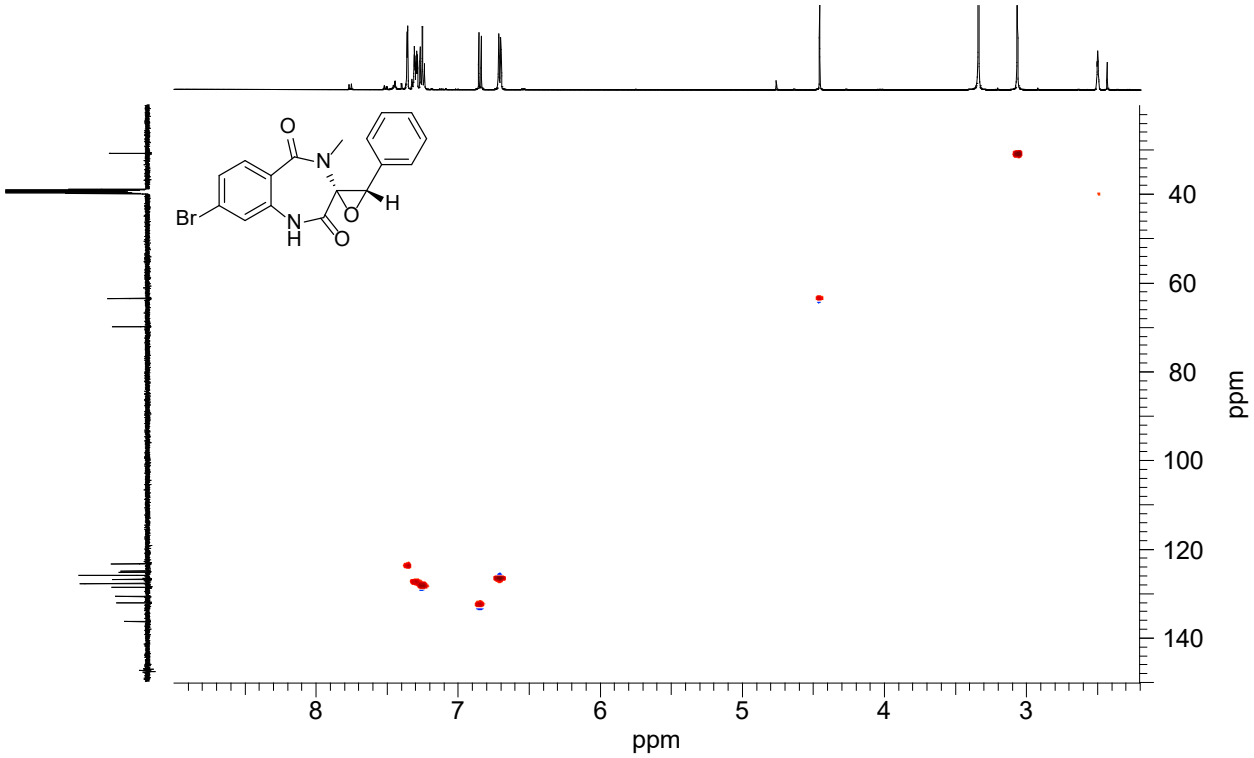

Figure S21. HSQC of 8-Br-cyclopenin (**6d**) in DMSO-d_6

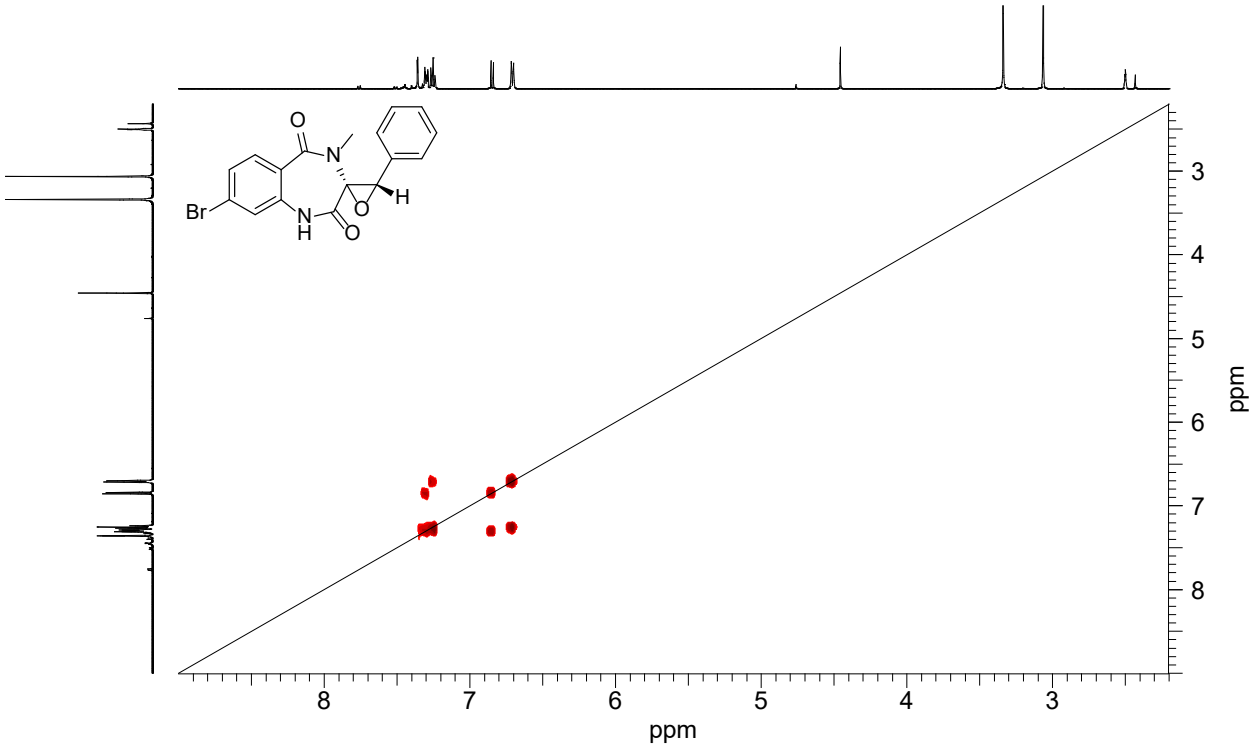

Figure S22. ^{1}H-^{1}H COSY of 8-Br-cyclopenin (**6d**) in DMSO-d_6

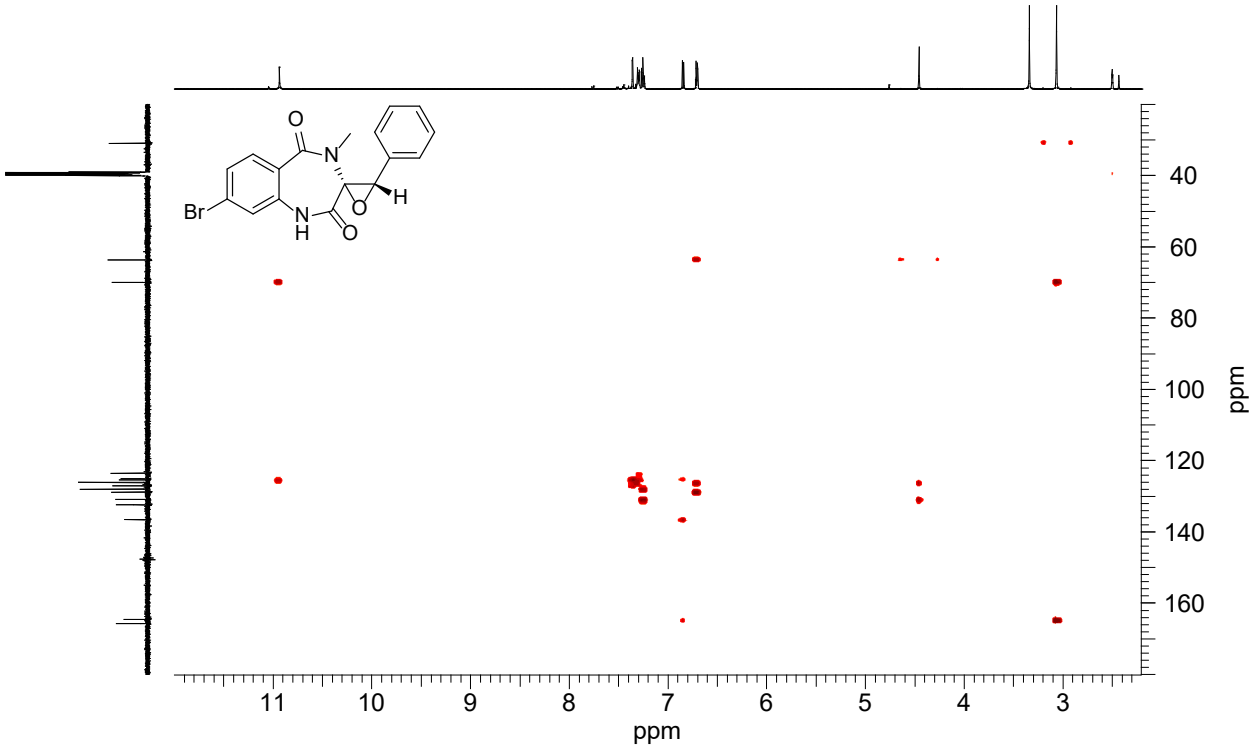

Figure S23. HMBC of 8-Br-cyclopenin (**6d**) in DMSO-d_6

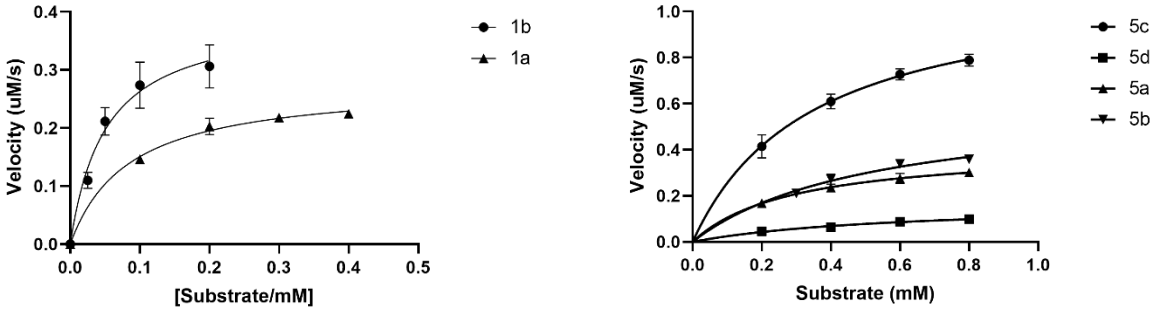

Figure S24. Steady-state enzymatic kinetics of AsqJ catalyzed epoxidation using **1a**, **1b**, **5a-5d**.

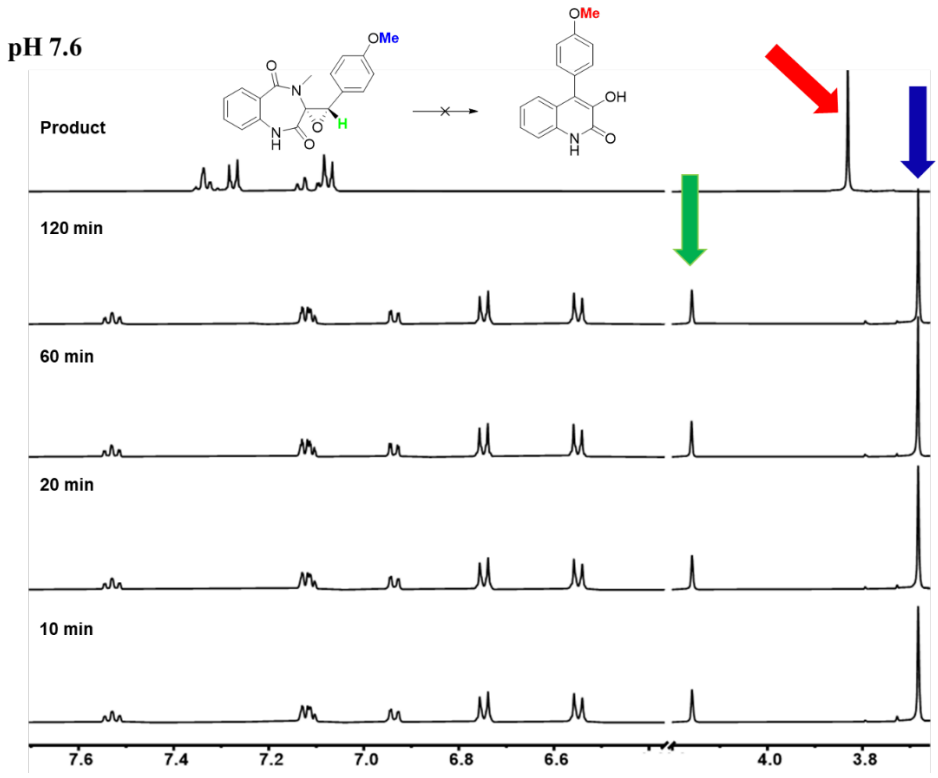
pH 7.6
OMe
O
N
H
O
O
H
OMe
OH
N
H
O
Product
120 min
60 min
20 min
10 min
7.6
7.4
7.2
7.0
6.8
6.6
4.0
3.8

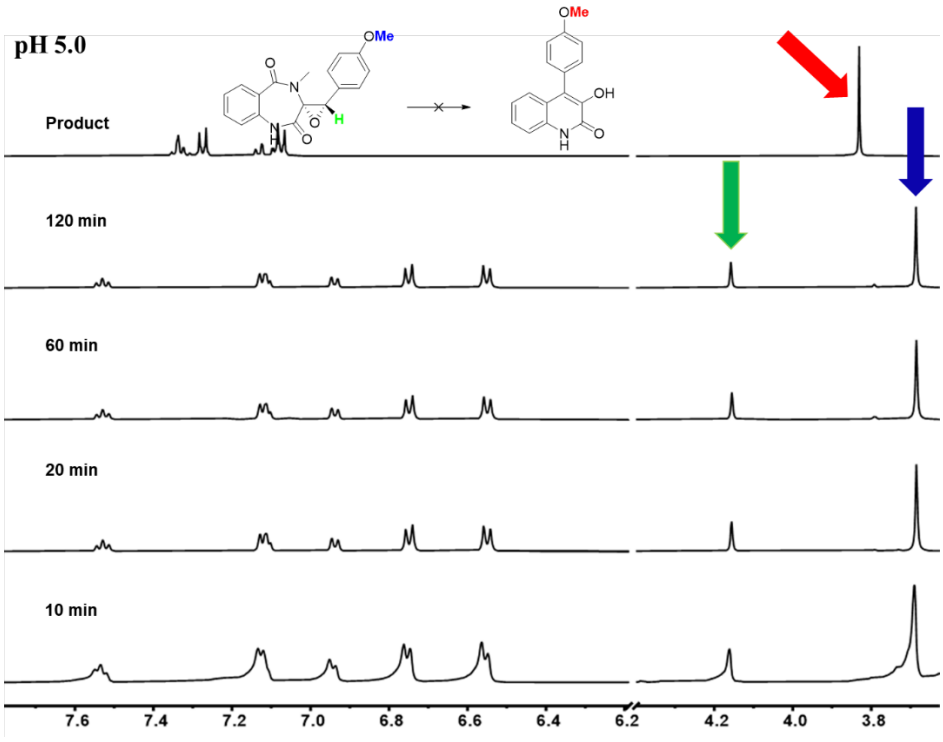
pH 5.0
OMe
O
N
H
O
O
H
OMe
OH
N
H
O
Product
120 min
60 min
20 min
10 min
7.6
7.4
7.2
7.0
6.8
6.6
6.4
6.2
4.2
4.0
3.8

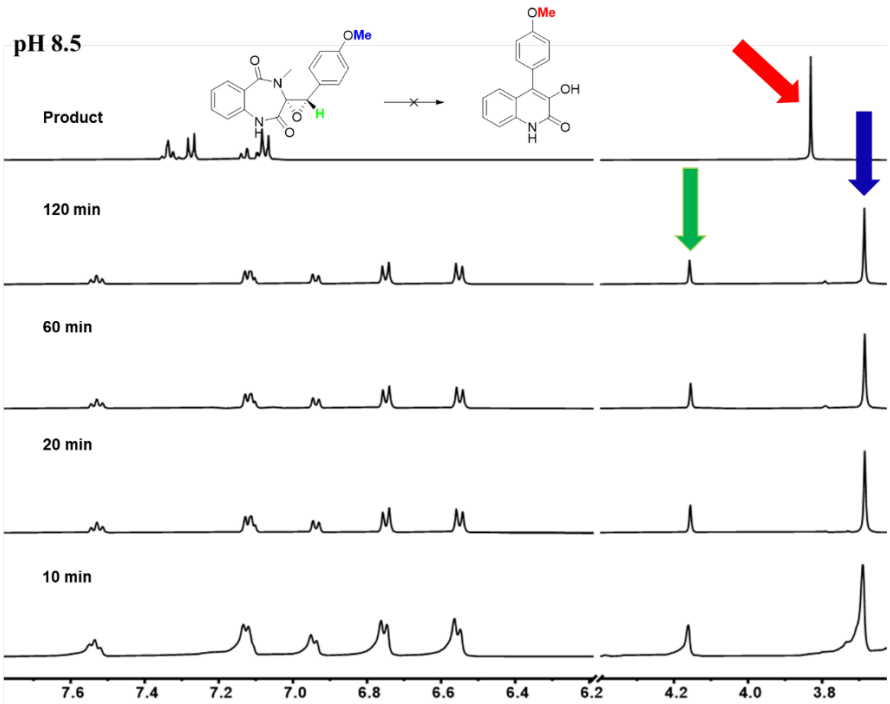

Figure S25. Using ^{1}H-NMR to monitor possible rearrangement of **2a** under pH 7.6, 5.5 and 8.5. Within 120 mins, no obvious rearrangement can be detected (**2a** → **3a**) under pH 7.6, 5.5 and 8.5.

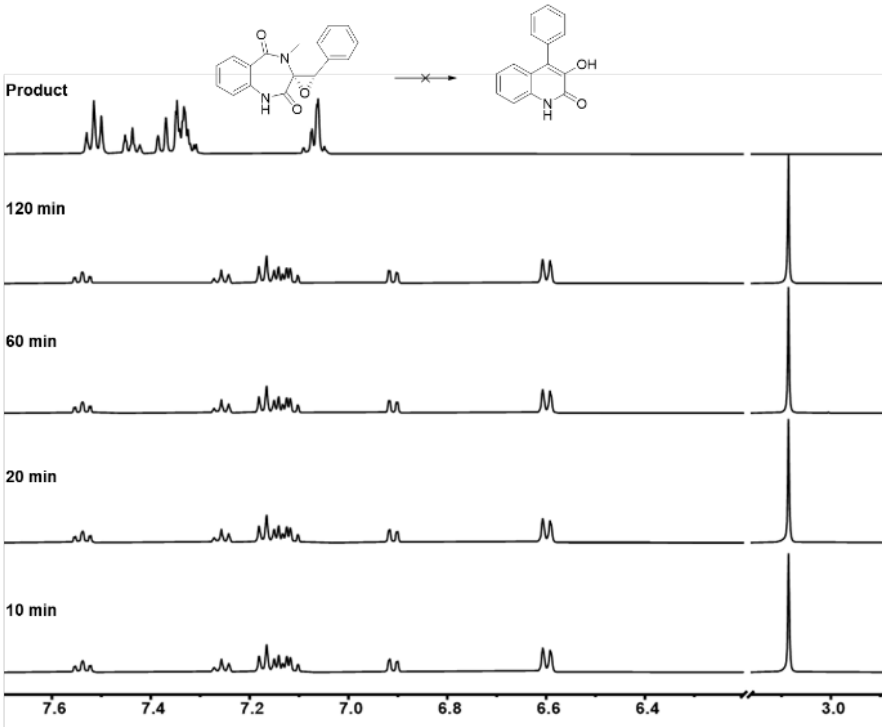

Figure S26. Using ^{1}H-NMR to monitor possible rearrangement of **2b** under pH 7.6. Within 120 mins, no obvious rearrangement can be detected (**2b** → **3b**).

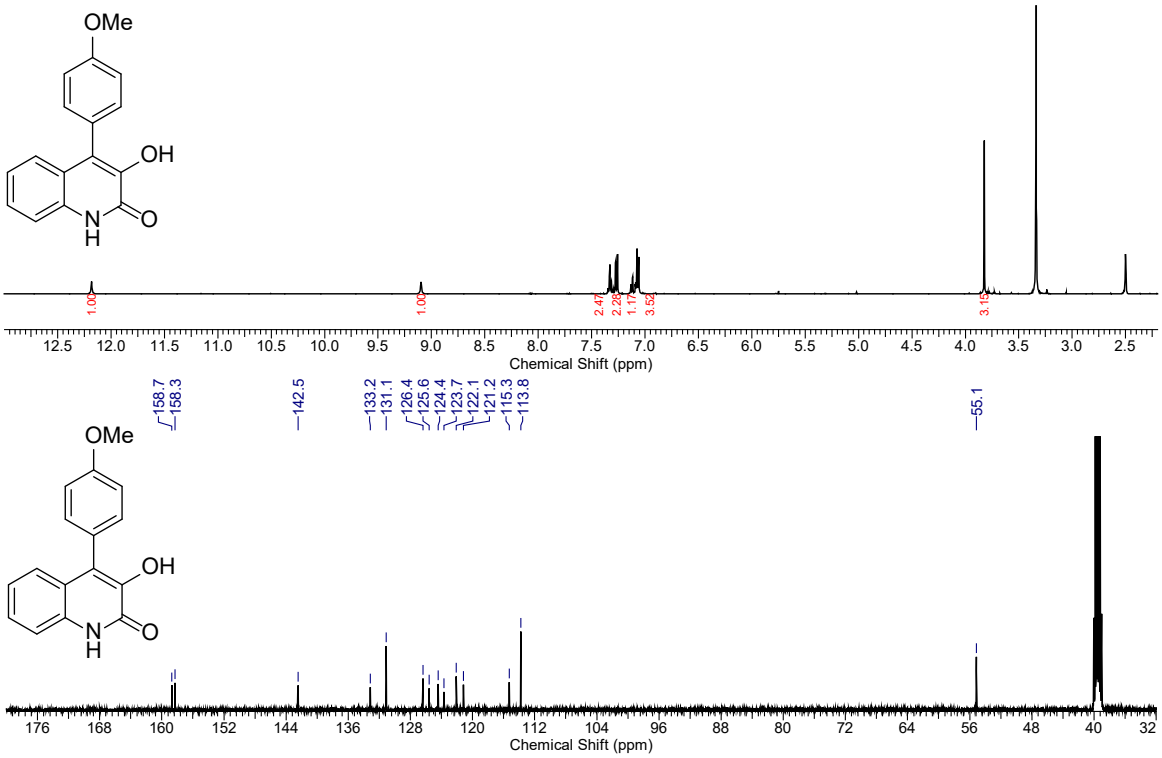

Figure S27. ^{1}H and ^{13}C NMR of (4'-methoxy)viridicatin (**3a**) in DMSO-d_6

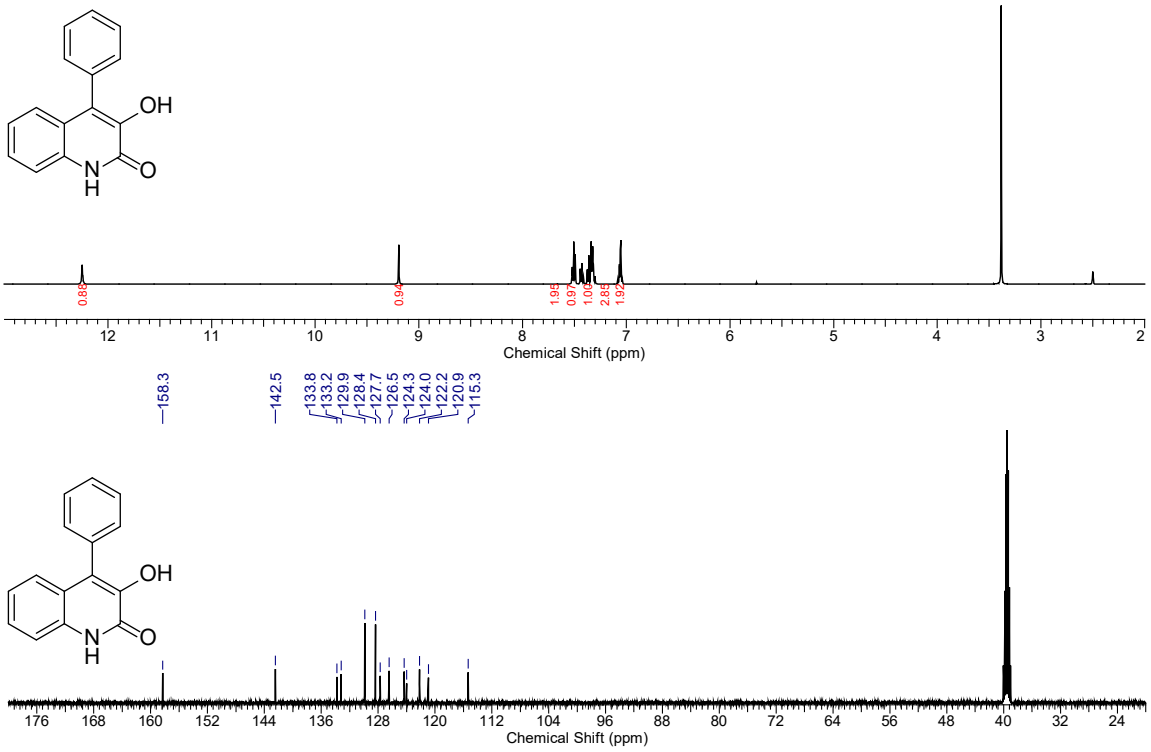

Figure S28. ^{1}H and ^{13}C NMR of viridicatin (**3b**) in DMSO-d_6

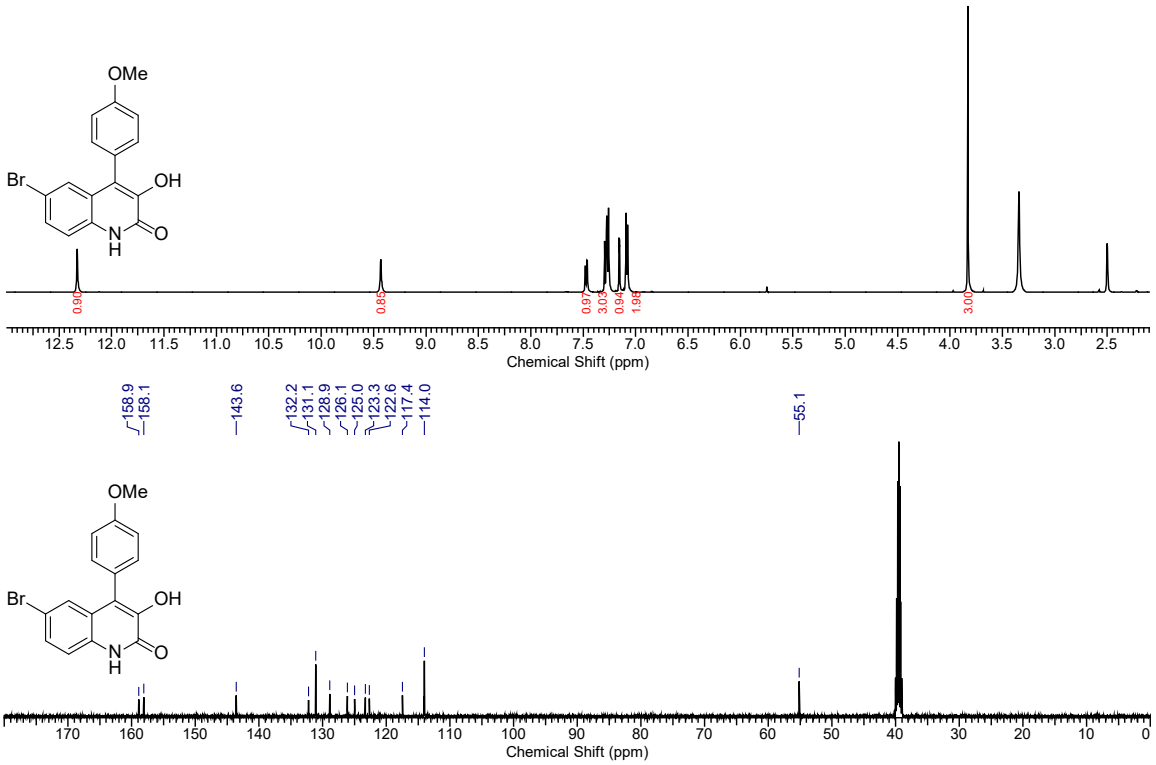

Figure S29. ^{1}H and ^{13}C NMR of 7-Br-(4'-methoxy)viridicatin (**7a**) in DMSO-d_6

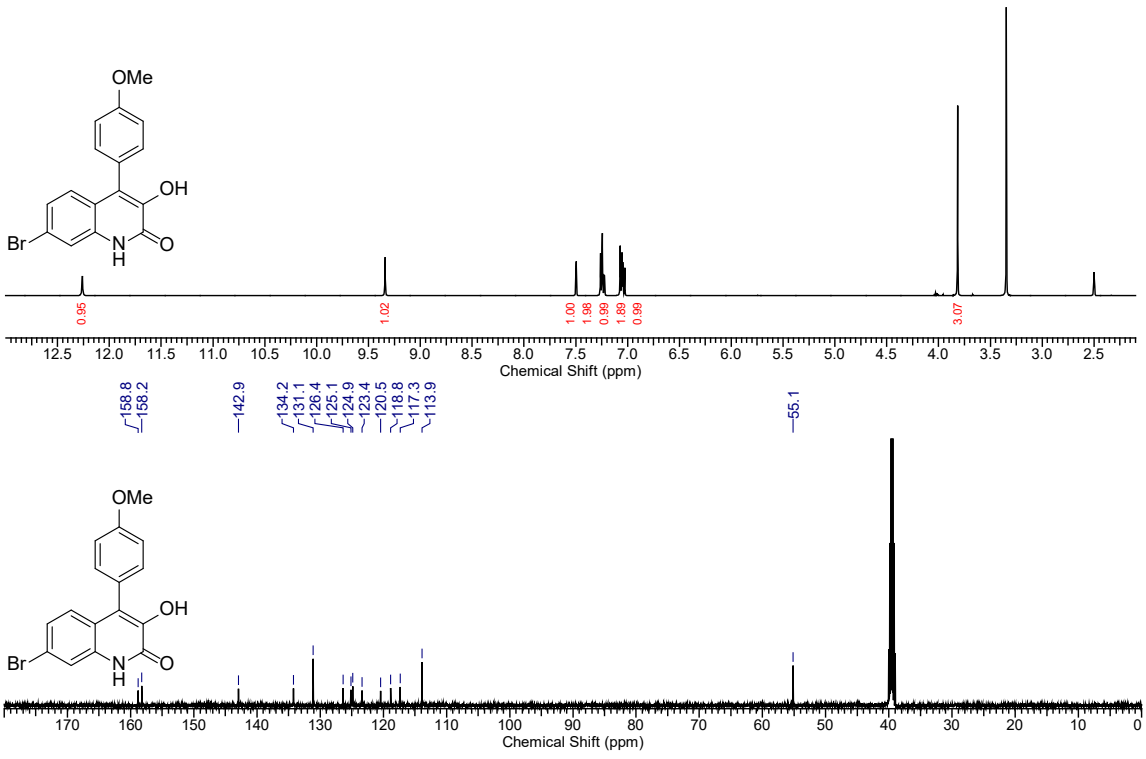

Figure S30. ^{1}H and ^{13}C NMR of 8-Br-(4'-methoxy)viridicatin (**7b**) in DMSO-d_6

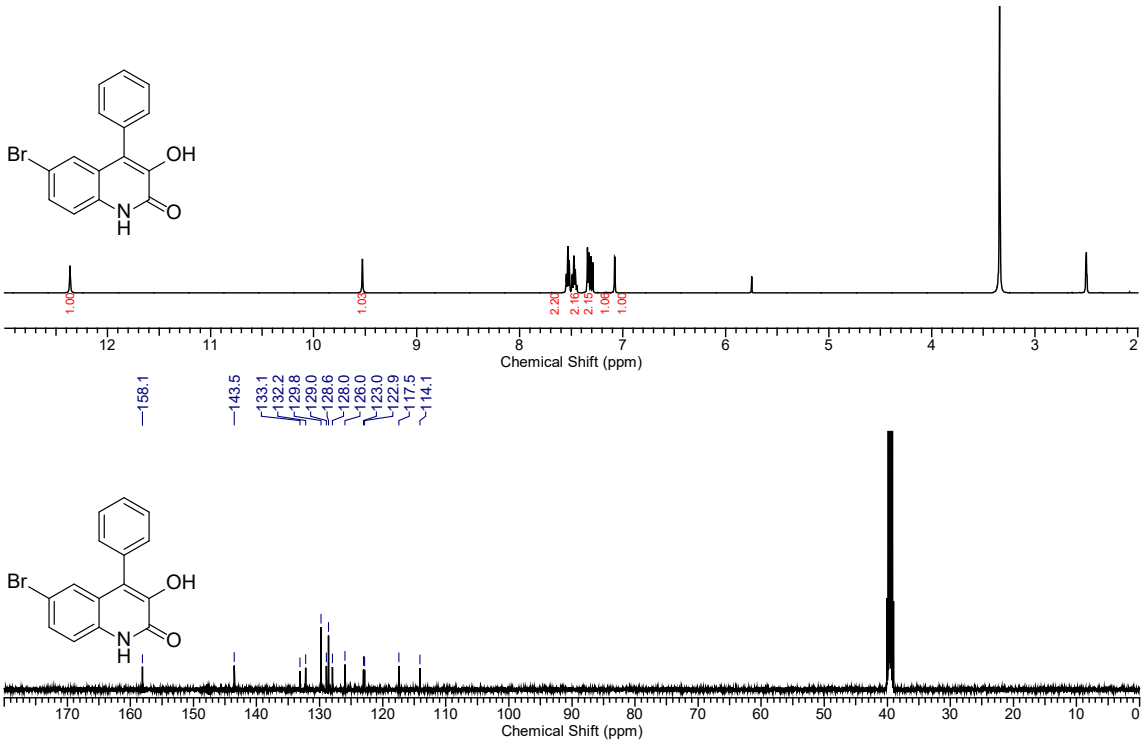

Figure S31. ^{1}H and ^{13}C NMR of 7-Br-viridicatin (**7c**) in DMSO-d_6

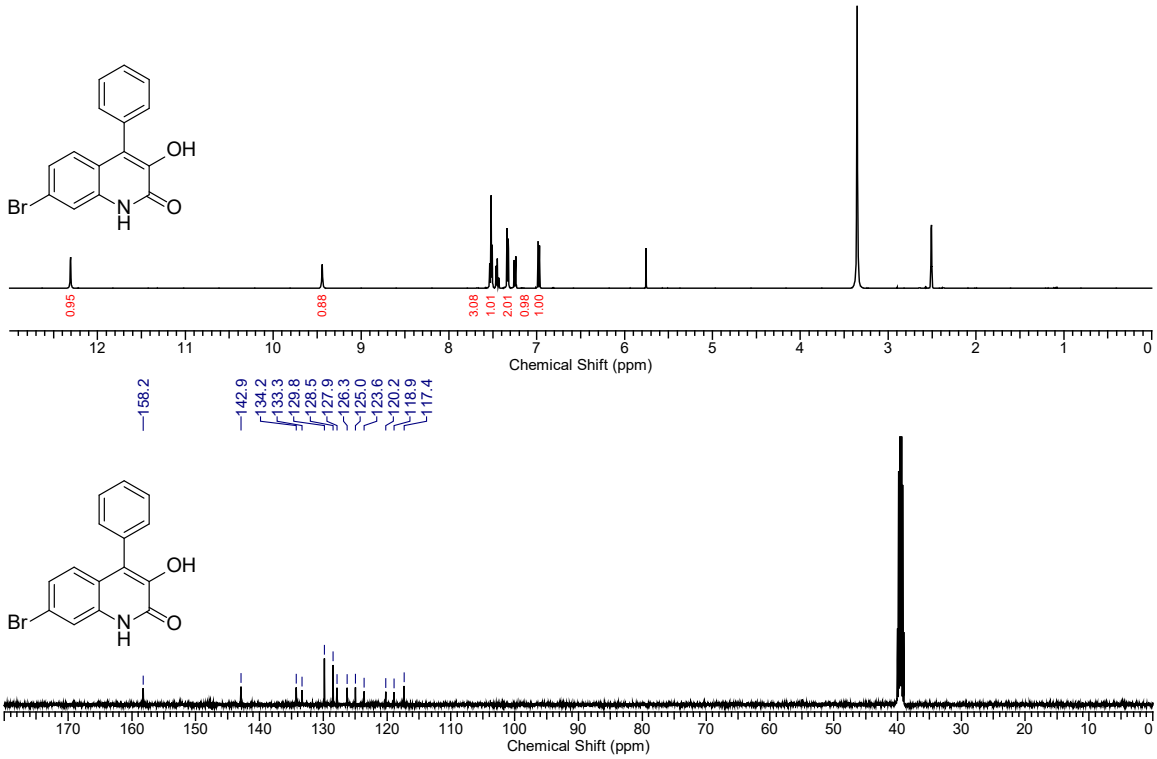

Figure S32. ^{1}H and ^{13}C NMR of 8-Br-viridicatin (**7d**) in DMSO-d_6

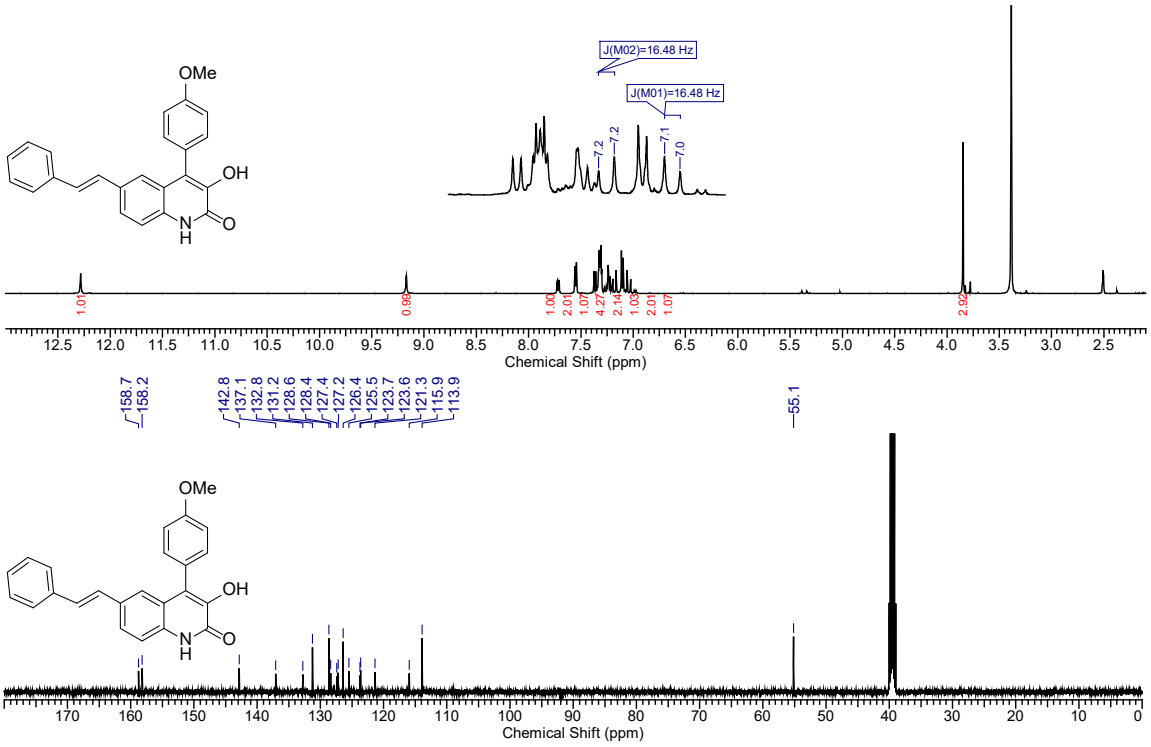

Figure S33. ^{1}H and ^{13}C NMR of **8a-I** in DMSO-d_6

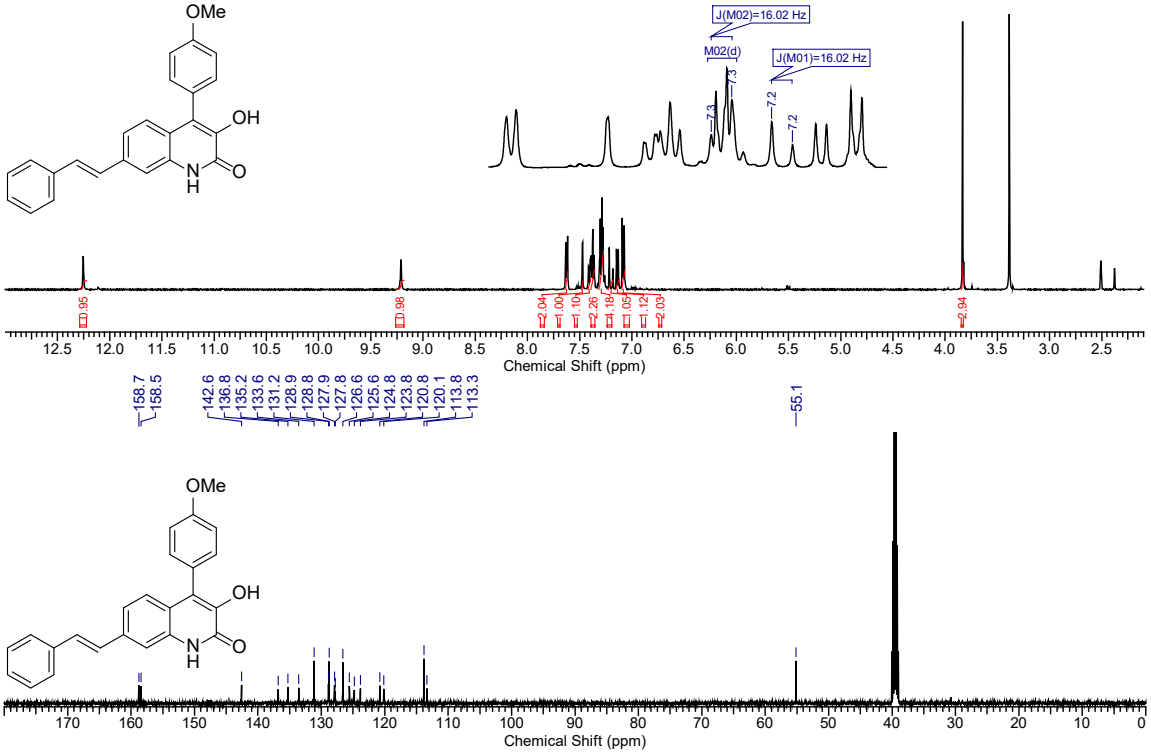

Figure S34. ^{1}H and ^{13}C NMR of **9b-I** in DMSO-d_6

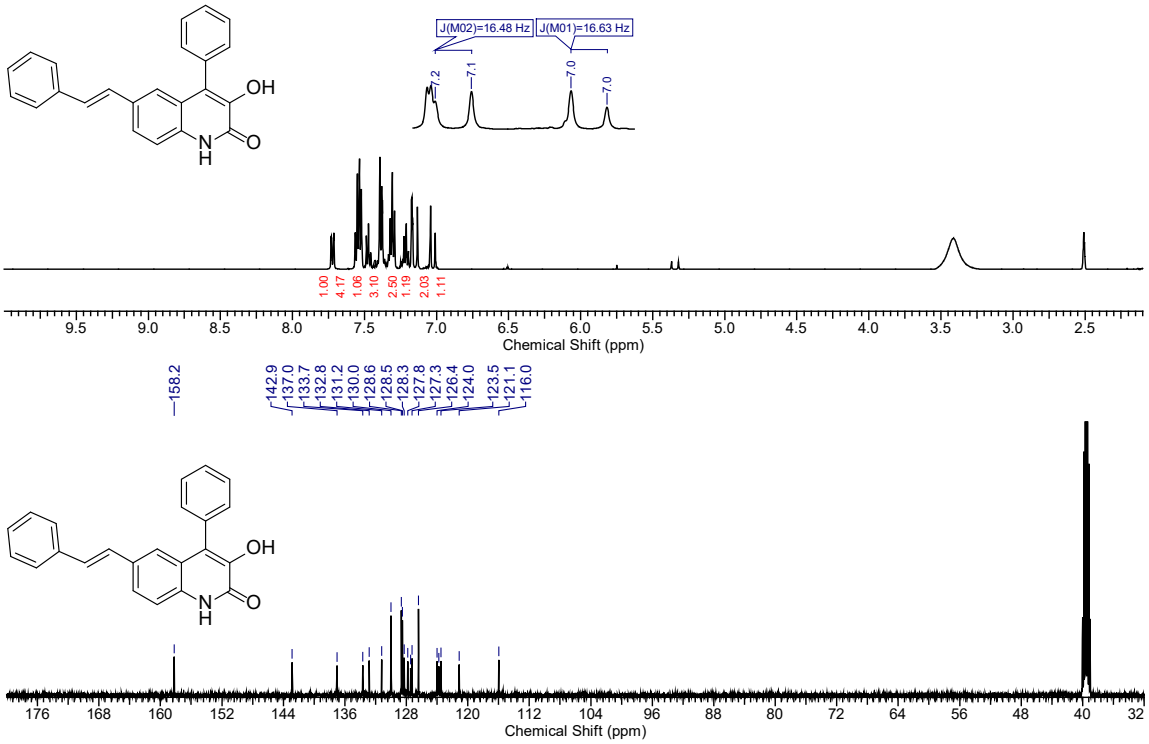

Figure S35. ^{1}H and ^{13}C NMR of **8c-I** in DMSO-d_6

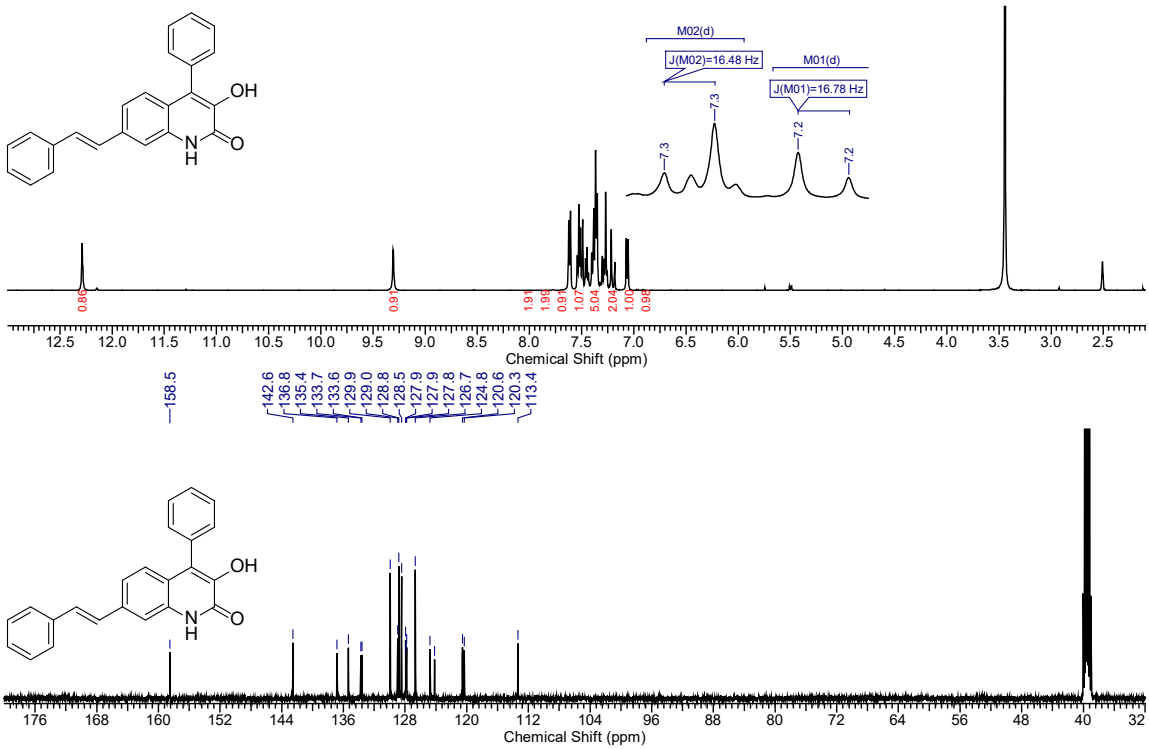

Figure S36. ^{1}H and ^{13}C NMR of **9d-I** in DMSO-d_6

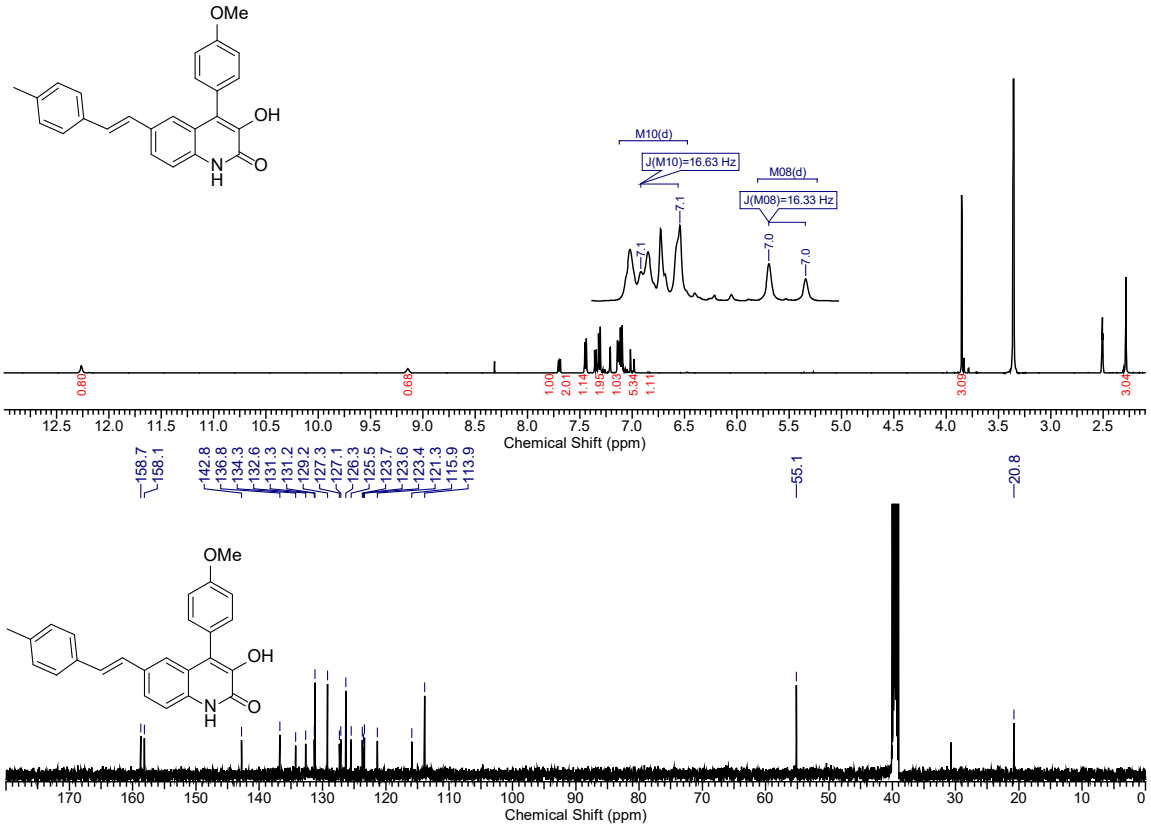

Figure S37. ^{1}H and ^{13}C NMR of **8a-II** in DMSO-d_6

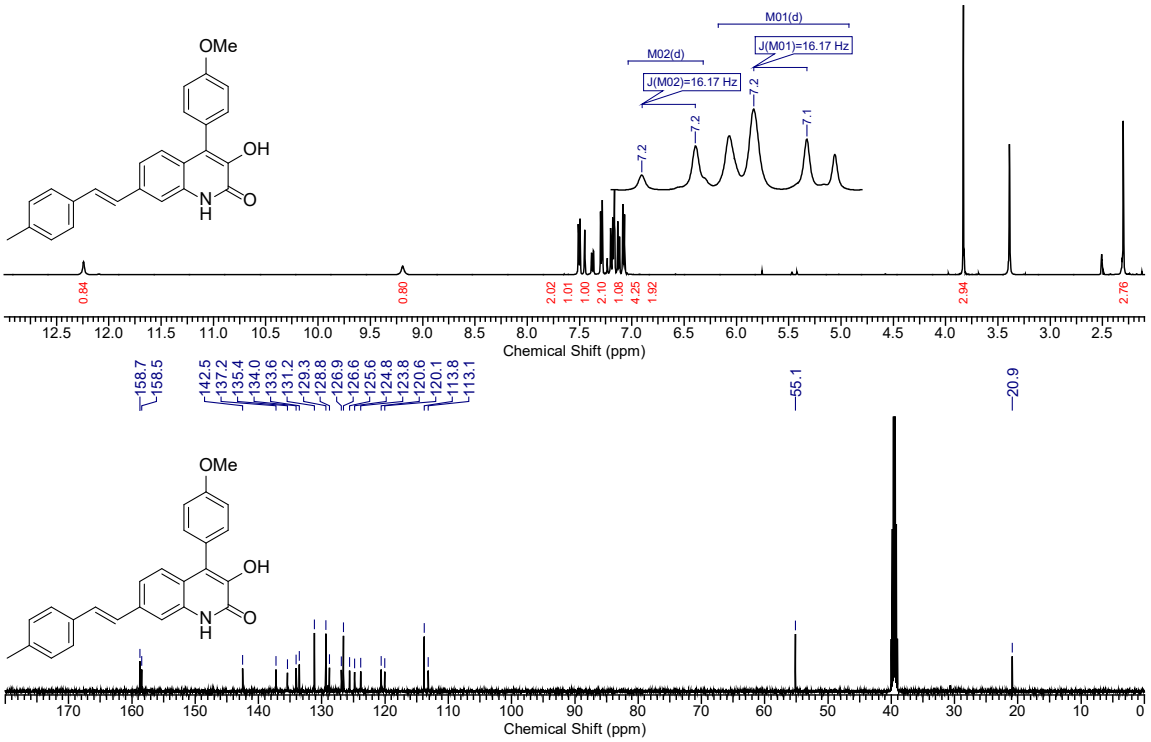

Figure S38. ^{1}H and ^{13}C NMR of **9b-II** in DMSO-d_6

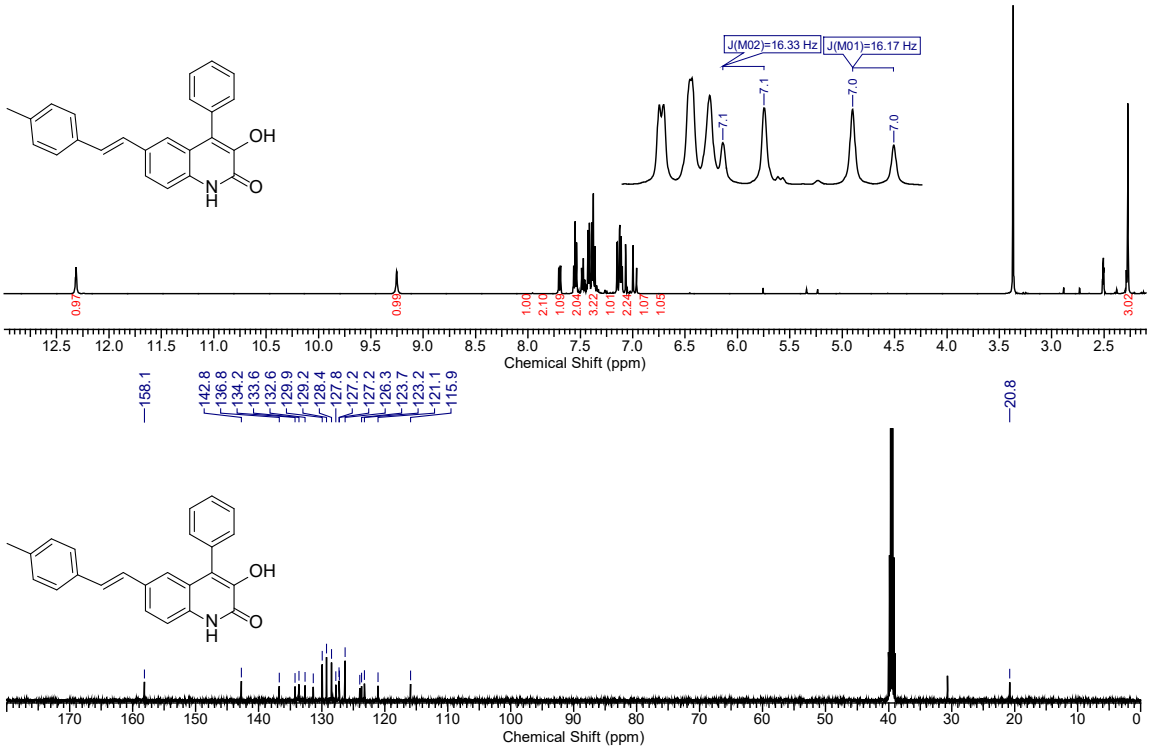

Figure S39. ^{1}H and ^{13}C NMR of **8c-II** in DMSO-d_6

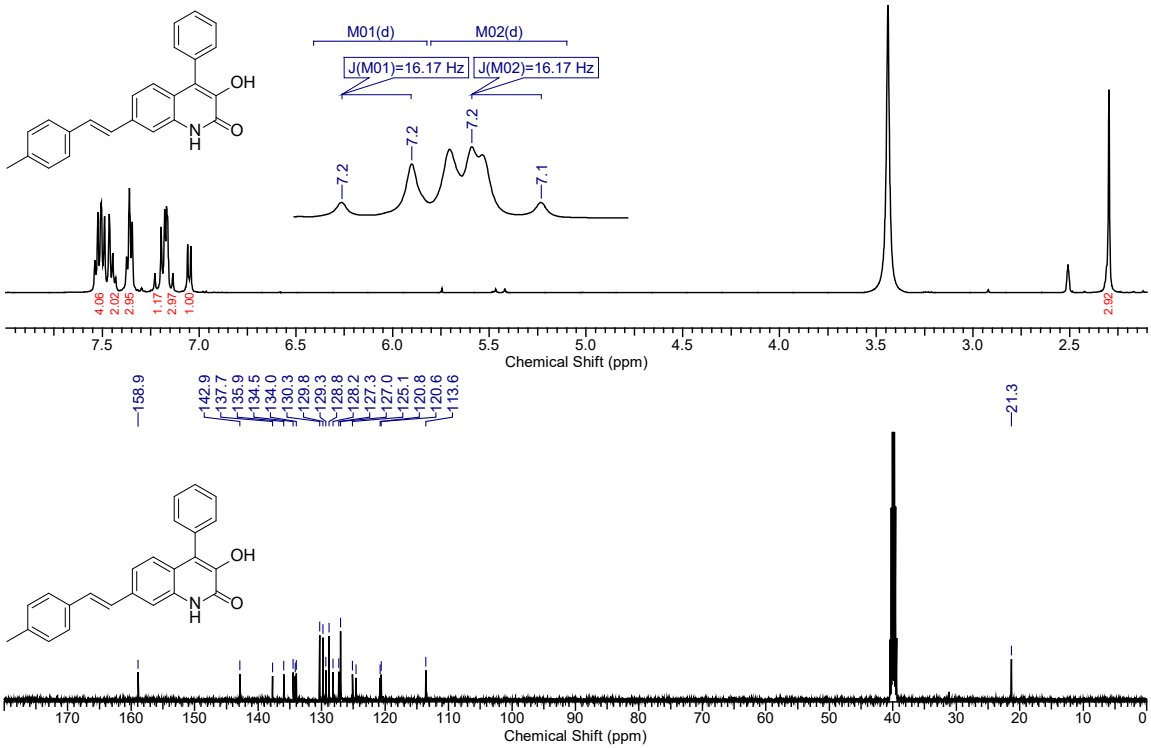

Figure S40. ^{1}H and ^{13}C NMR of **9d-II** in DMSO-d_6

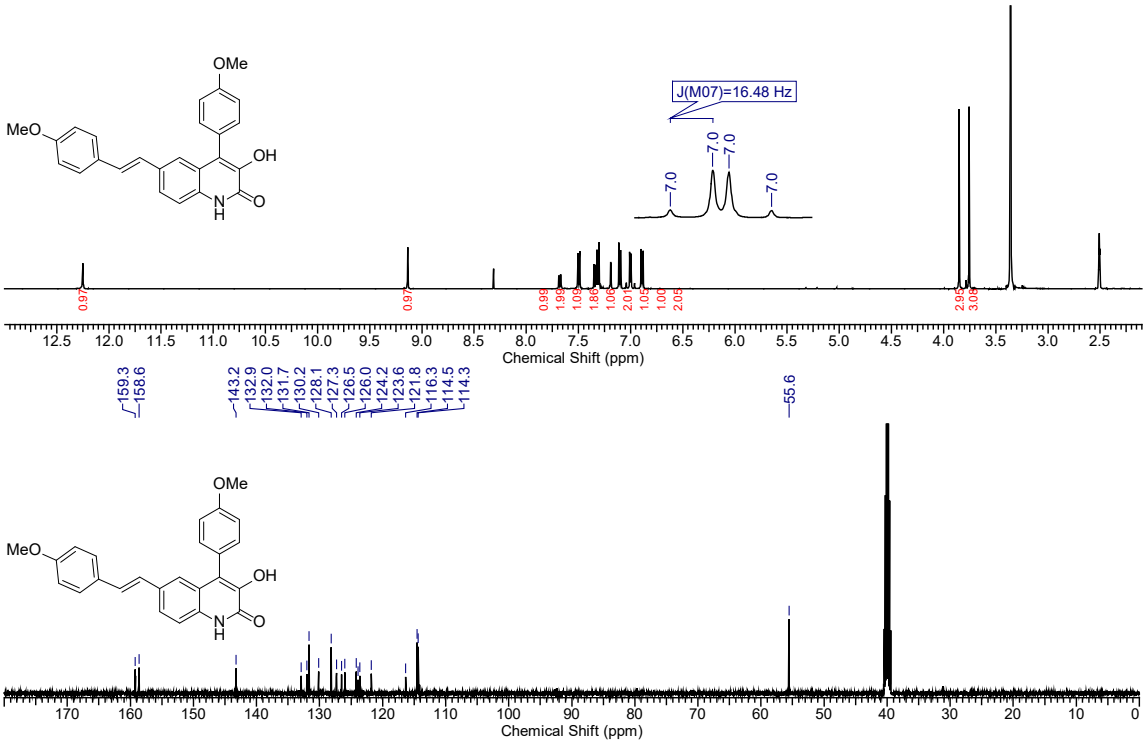

Figure S41. ^{1}H and ^{13}C NMR of **8a-III** in DMSO-d_6

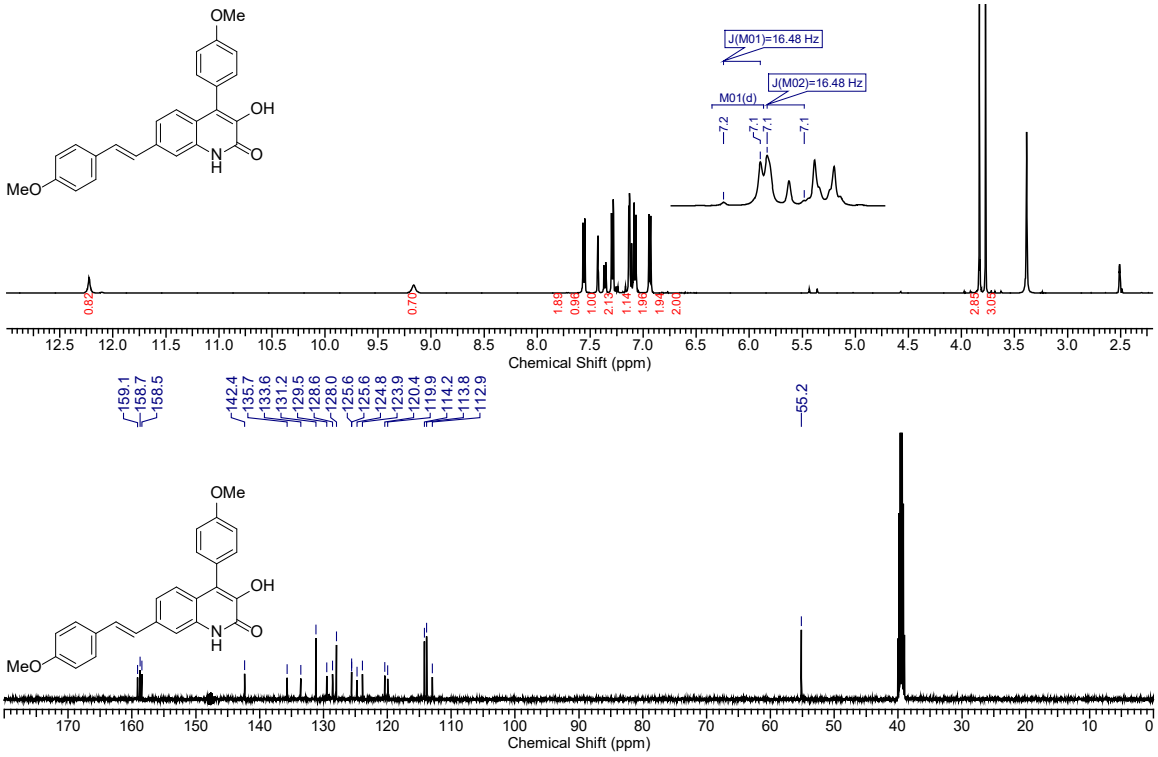

Figure S42. ^{1}H and ^{13}C NMR of **9b-III** in DMSO-d_6

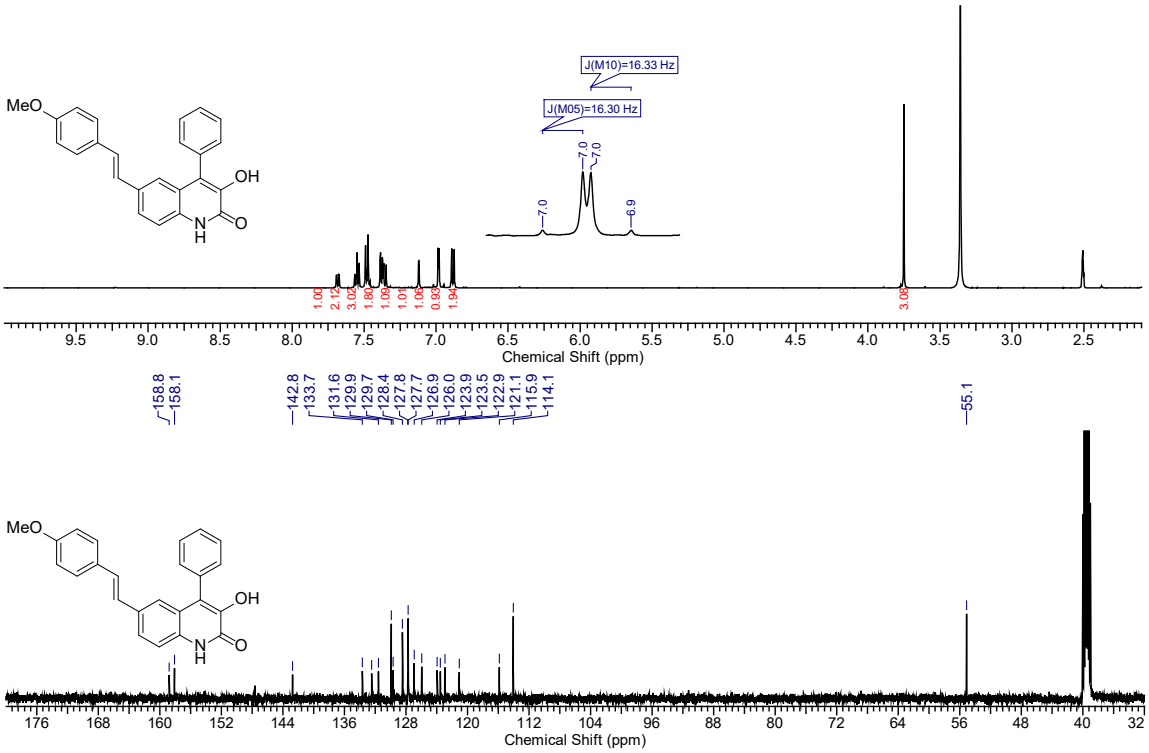

Figure S43. ^{1}H and ^{13}C NMR of **8c-III** in DMSO-d_6

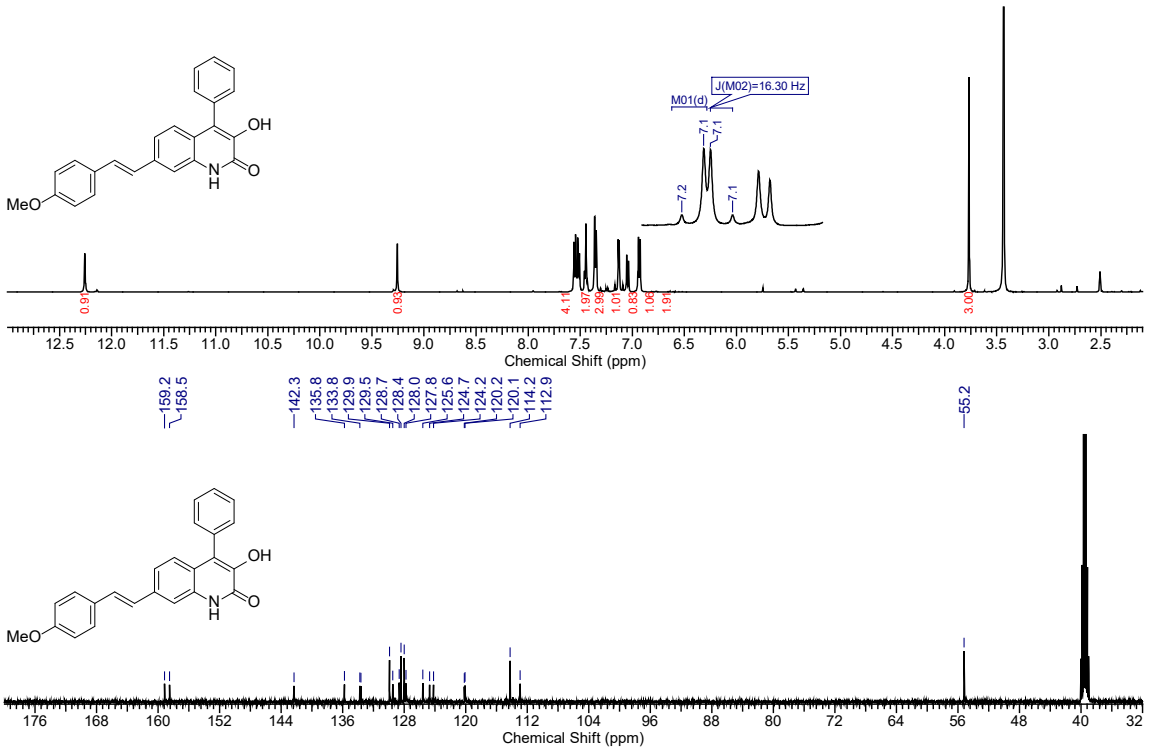

Figure S44. ^{1}H and ^{13}C NMR of **9d-III** in DMSO-d_6

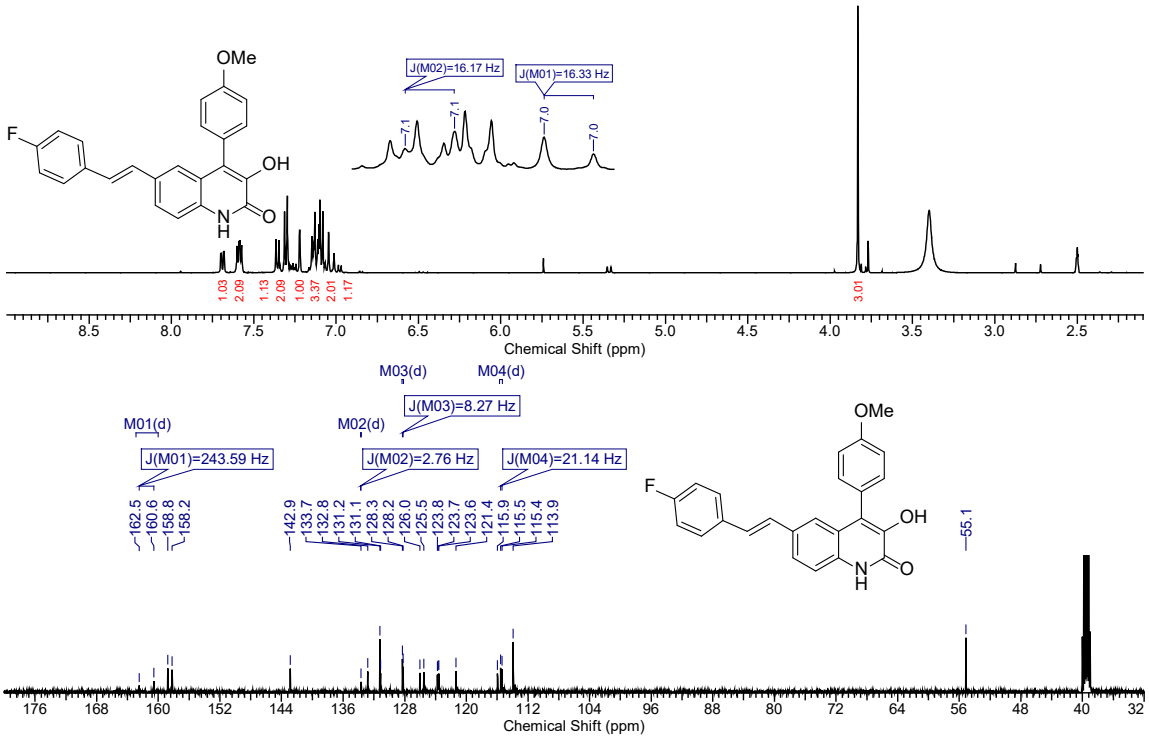

Figure S45. ^{1}H and ^{13}C NMR of **8a-IV** in DMSO-d_6

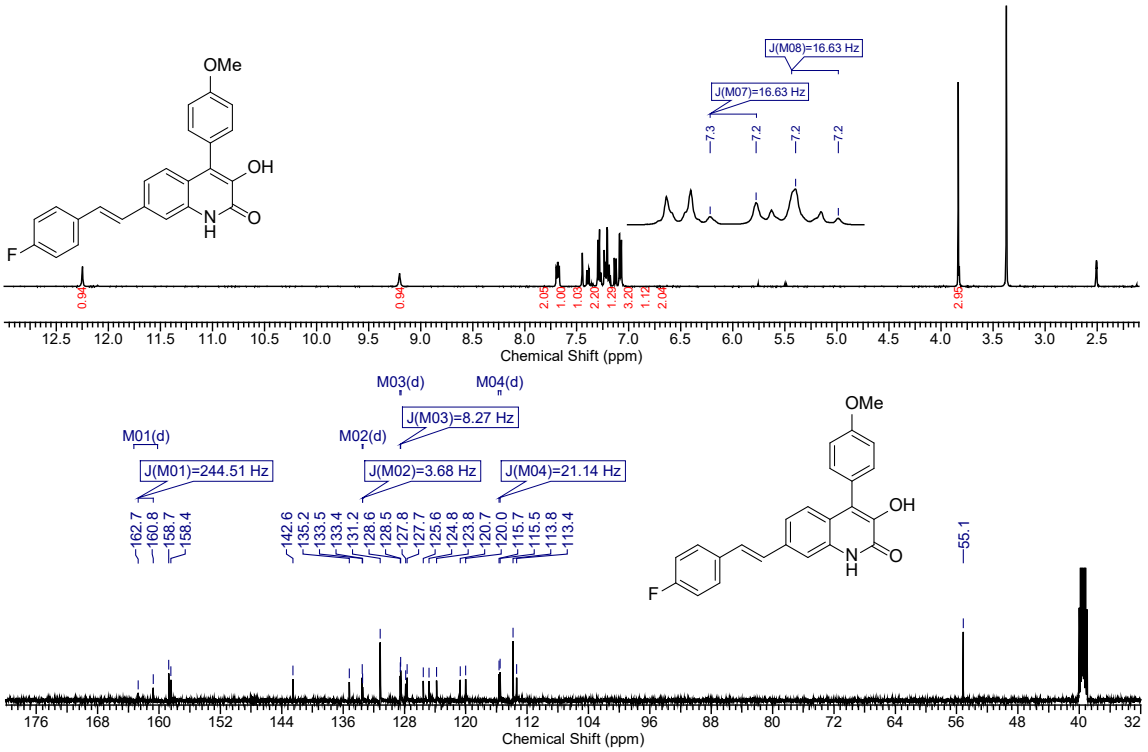

Figure S46. ^{1}H and ^{13}C NMR of **9b-IV** in DMSO-d_6

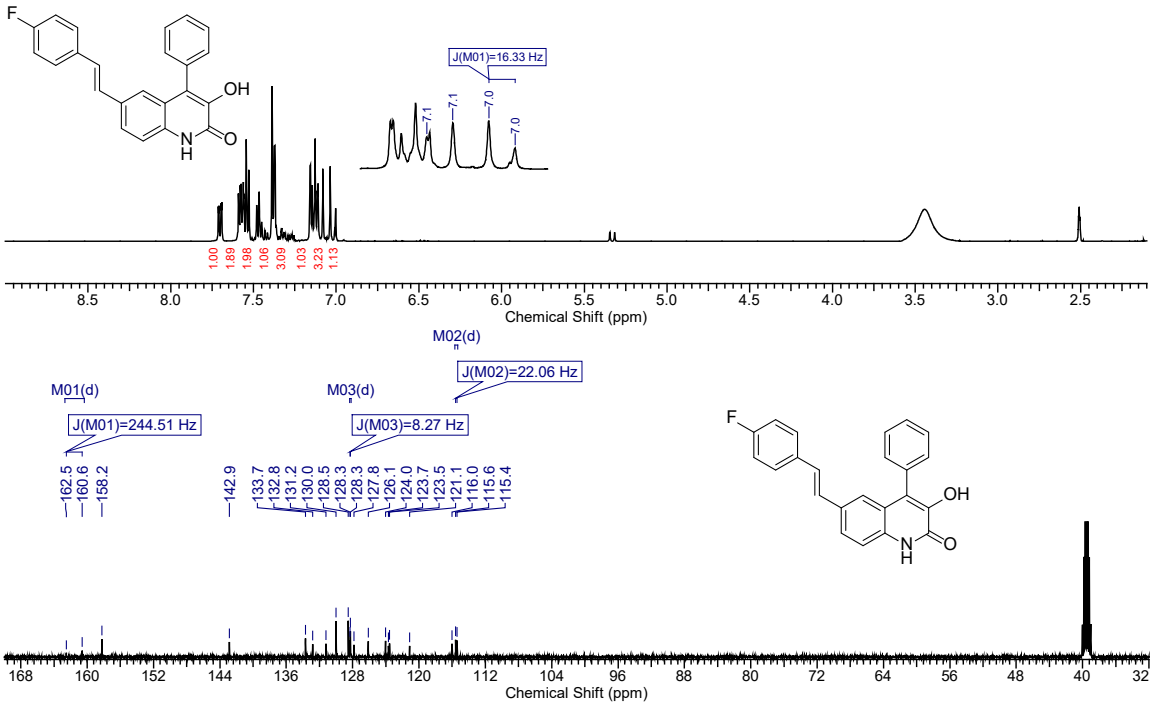

Figure S47. ^{1}H and ^{13}C NMR of **8c-IV** in DMSO-d_6

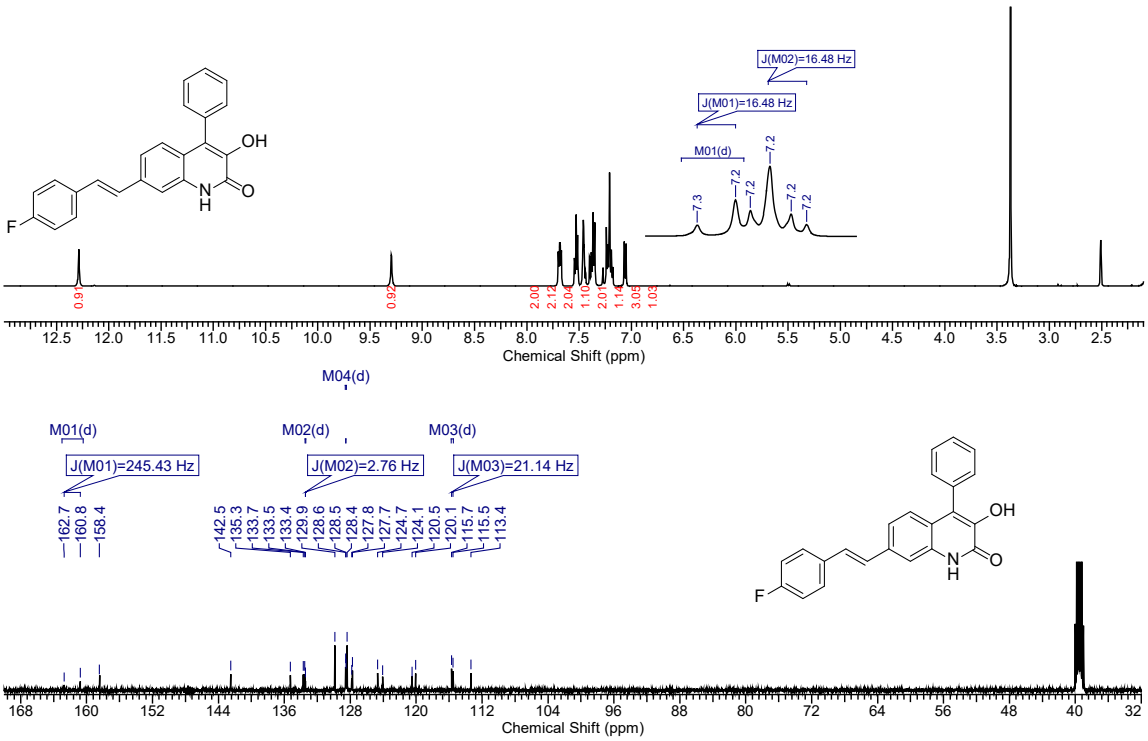

Figure S48. ^{1}H and ^{13}C NMR of **9d-IV** in DMSO-d_6

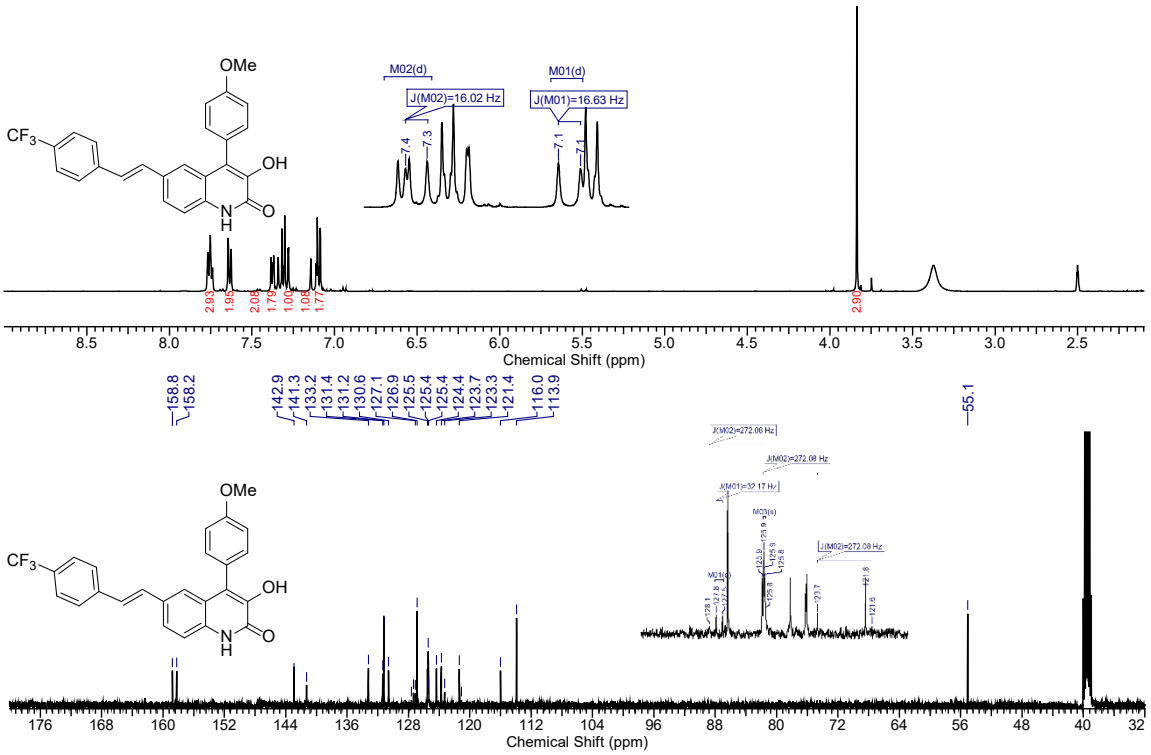

Figure S49. ^{1}H and ^{13}C NMR of **8a-V** in DMSO-d_6

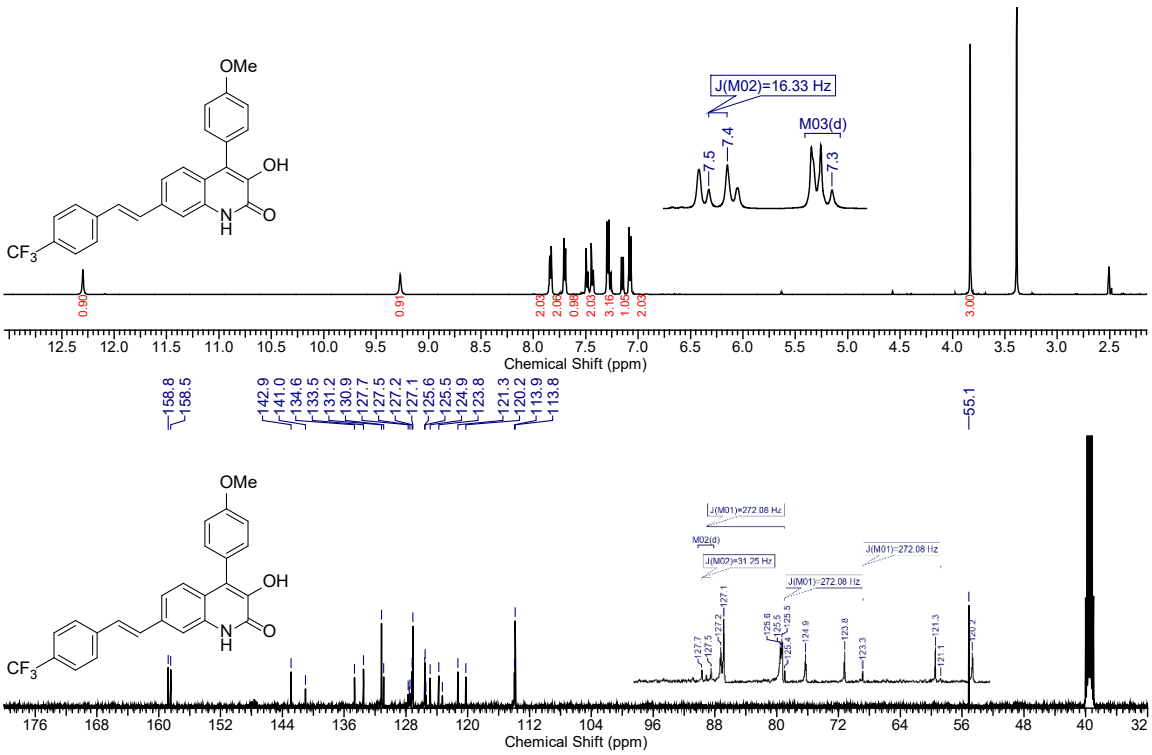

Figure S50. ^{1}H and ^{13}C NMR of **9b-V** in DMSO-d_6

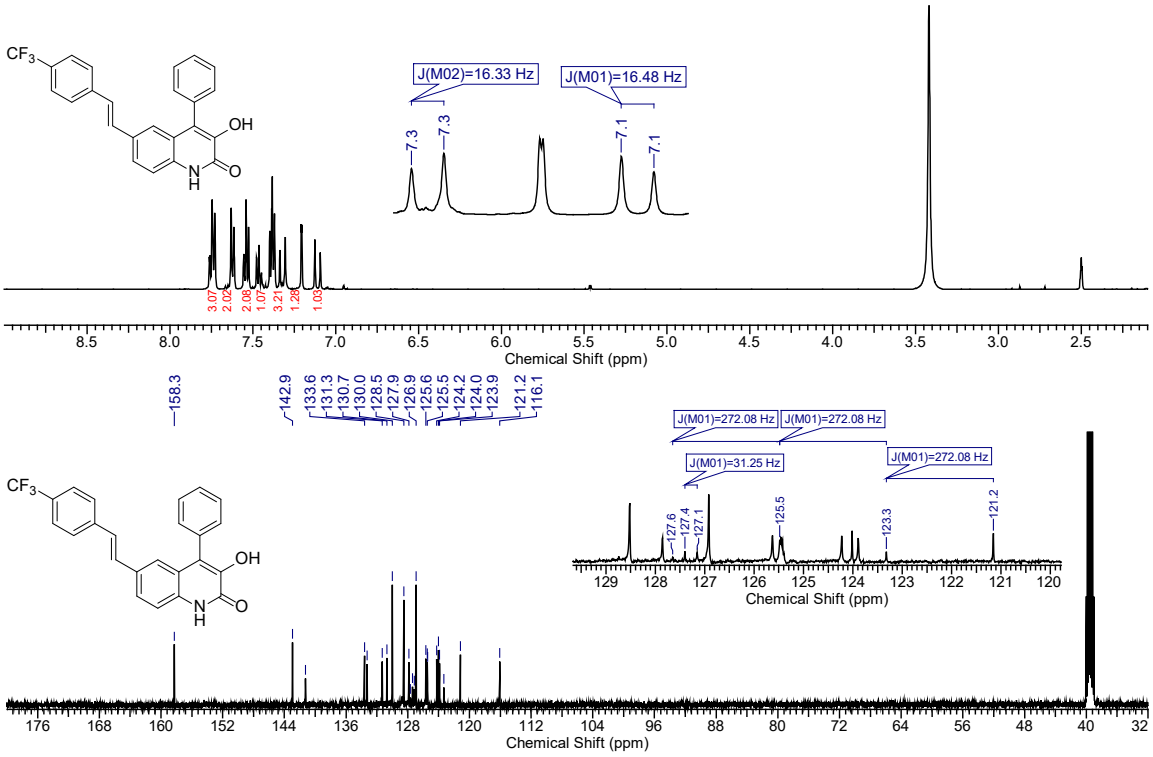

Figure S51. ^{1}H and ^{13}C NMR of **8c-V** in DMSO-d_6

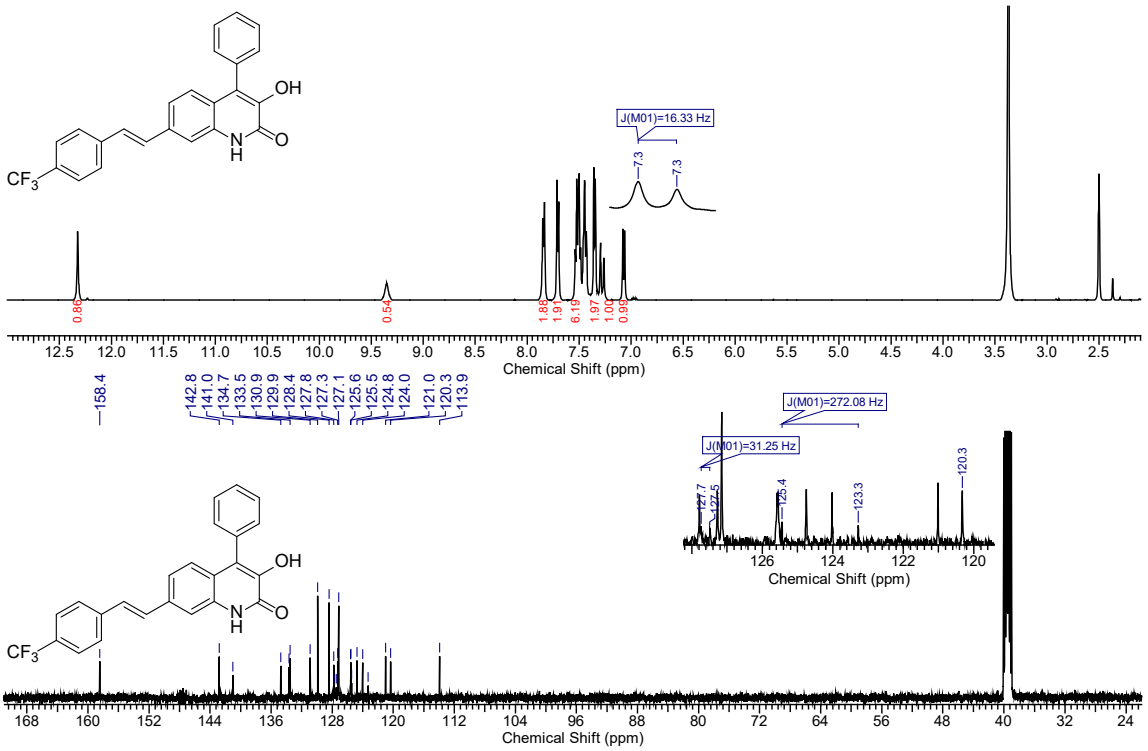

Figure S52. ^{1}H and ^{13}C NMR of **9d-V** in DMSO-d_6

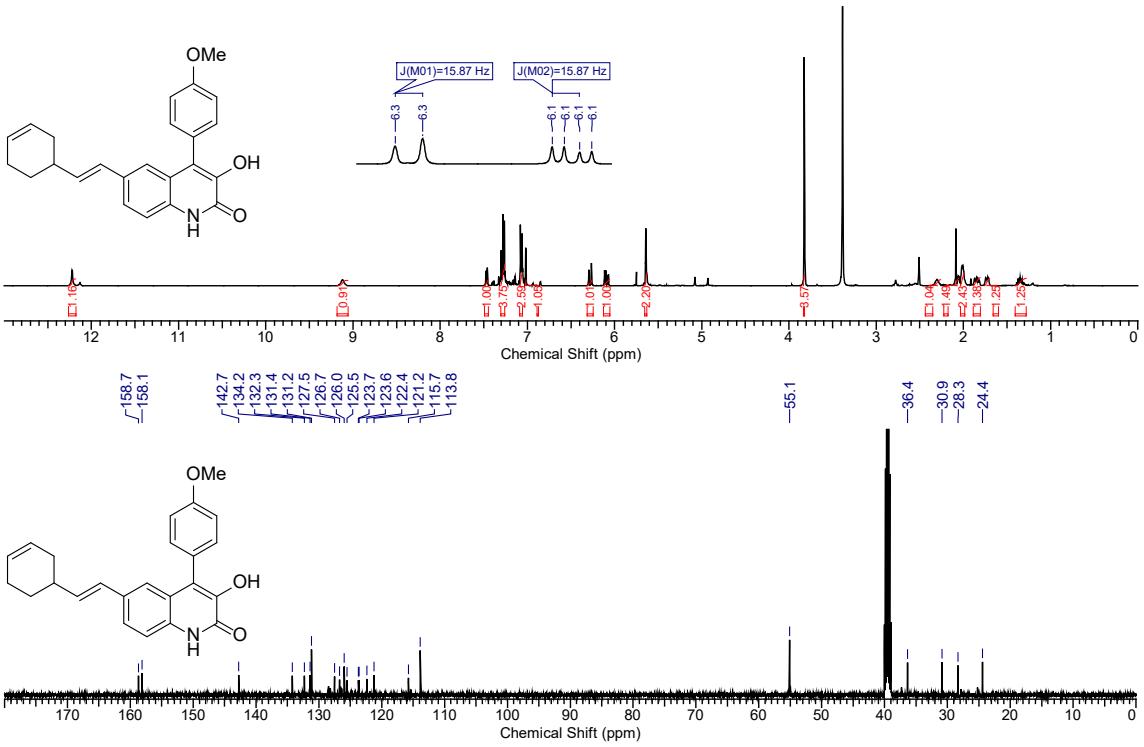

Figure S53. ^{1}H and ^{13}C NMR of **8a-VI** in DMSO-d_6

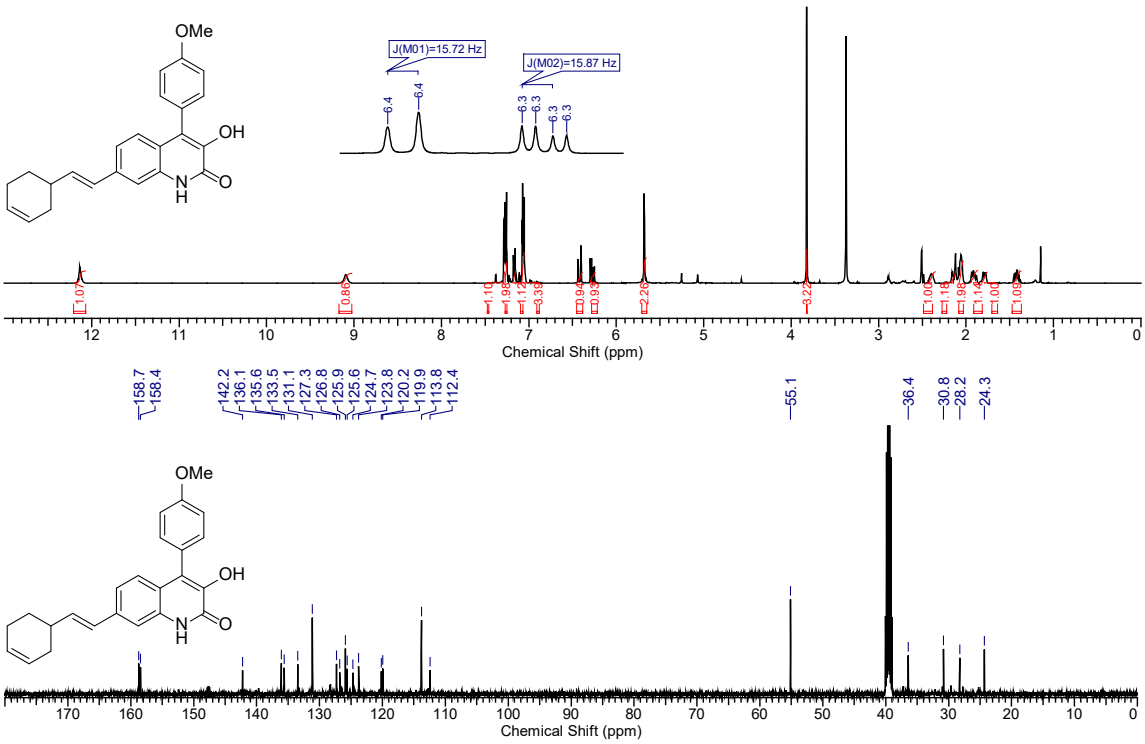

Figure S54. ^{1}H and ^{13}C NMR of **9b-VI** in DMSO-d_6

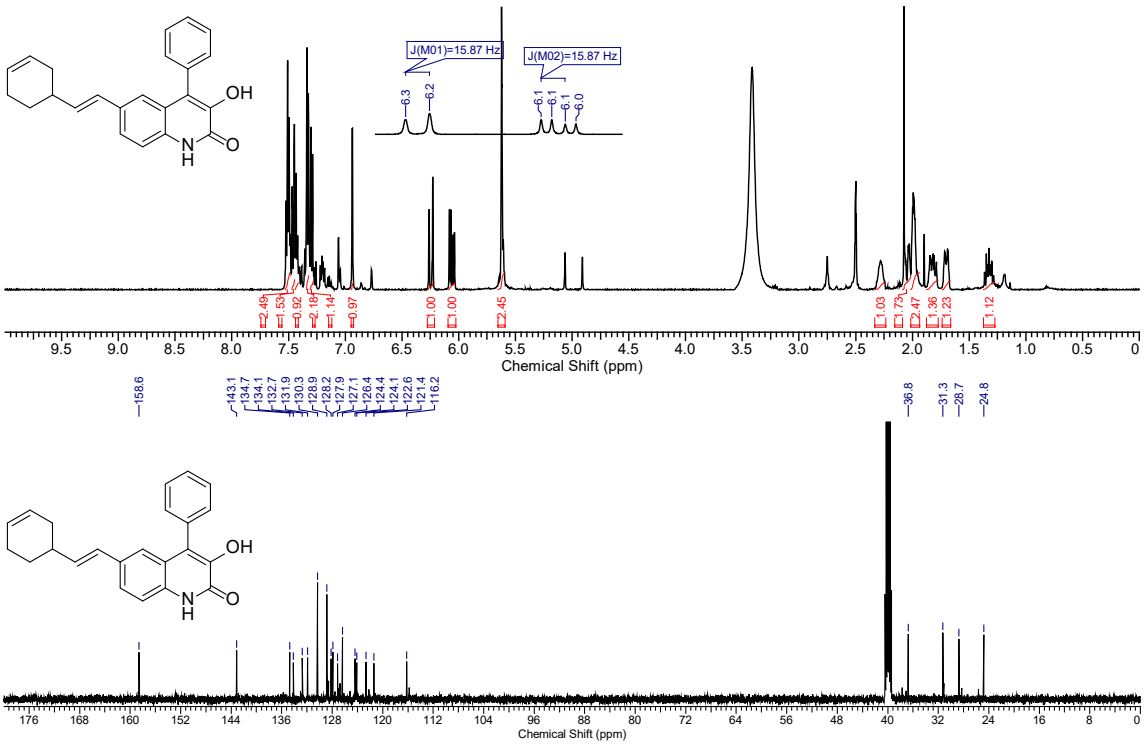

Figure S55. ^{1}H and ^{13}C NMR of **8c-VI** in DMSO-d_6

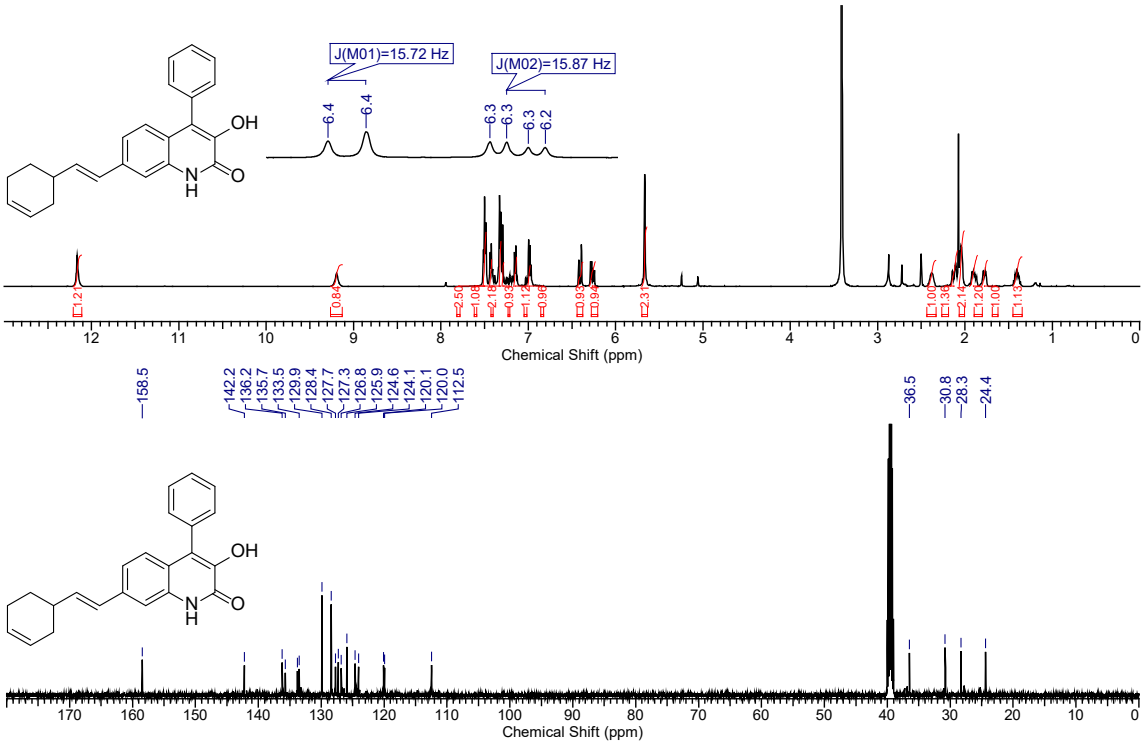

Figure S56. ^{1}H and ^{13}C NMR of **9d-VI** in DMSO-d_6

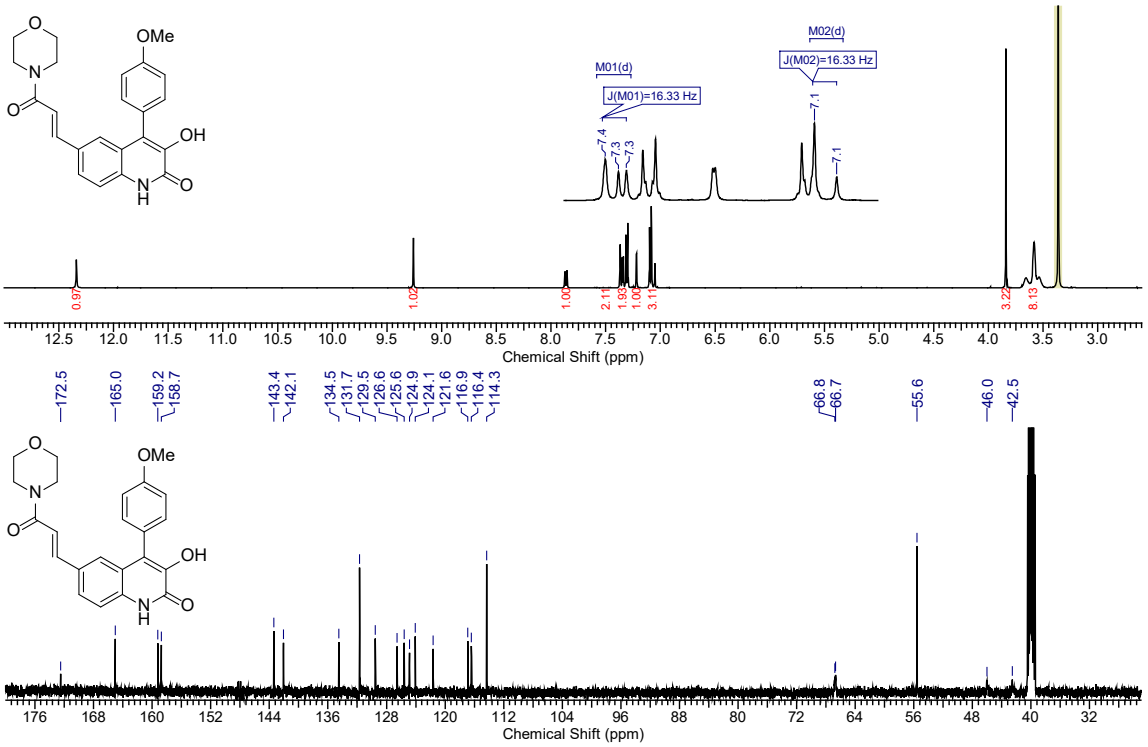

Figure S57. ^{1}H and ^{13}C NMR of **8a-VII** in DMSO-d_6

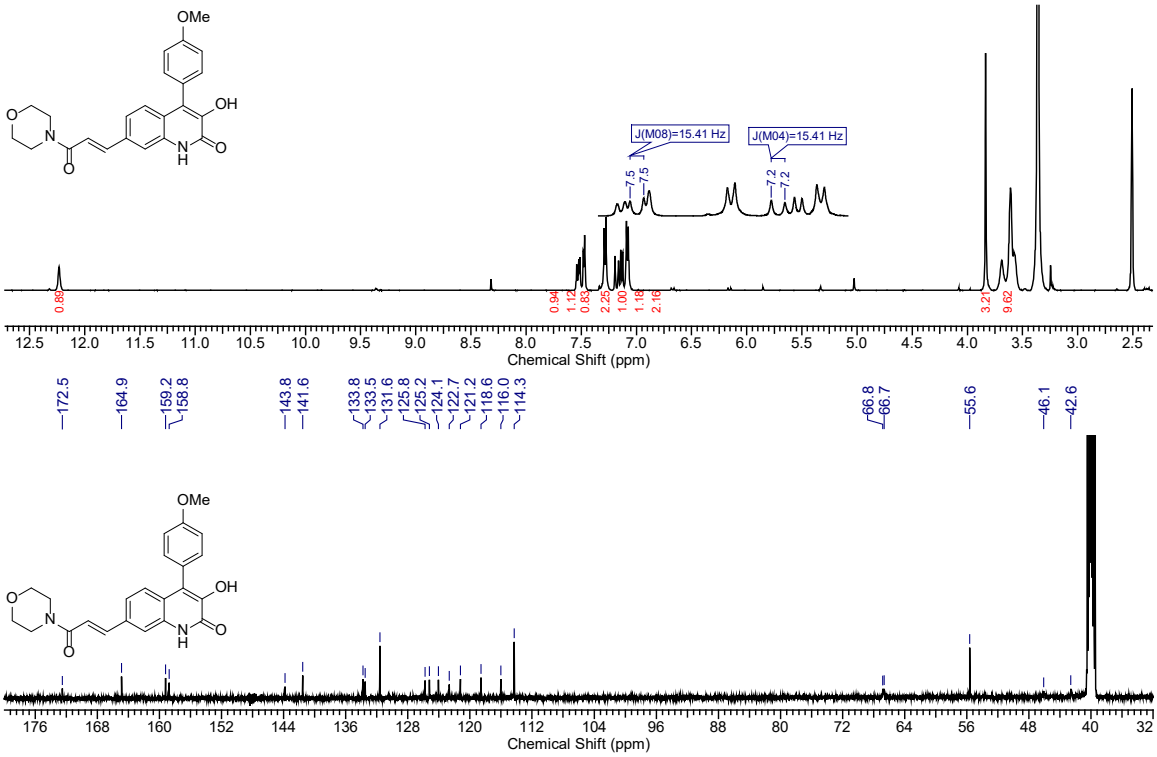

Figure S58. ^{1}H and ^{13}C NMR of **9b-VII** in DMSO-d_6

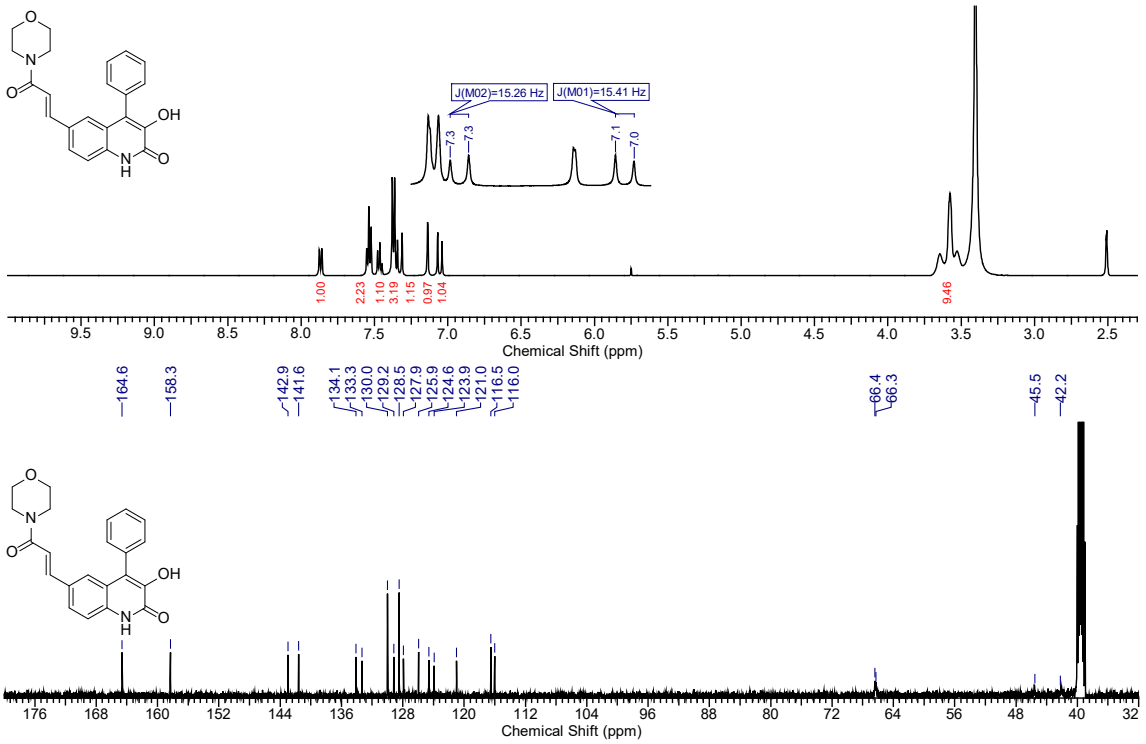

Figure S59. ^{1}H and ^{13}C NMR of **8c-VII** in DMSO-d_6

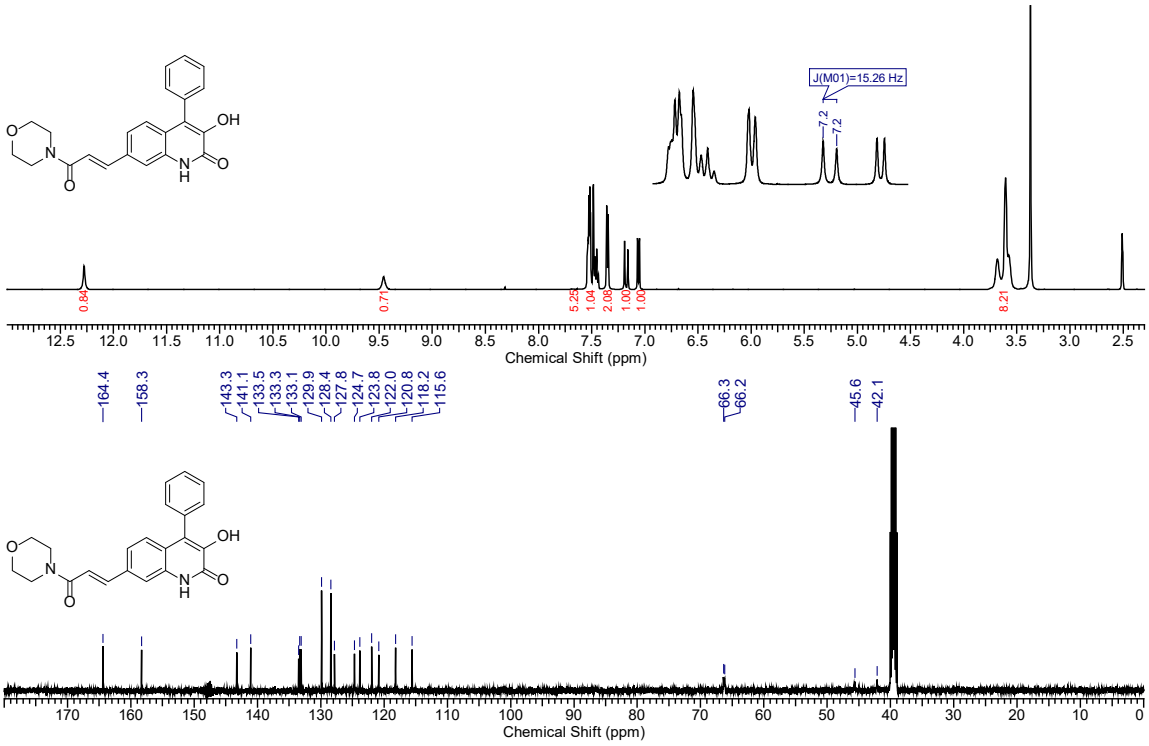

Figure S60. ^{1}H and ^{13}C NMR of **9d-VII** in DMSO-d_6

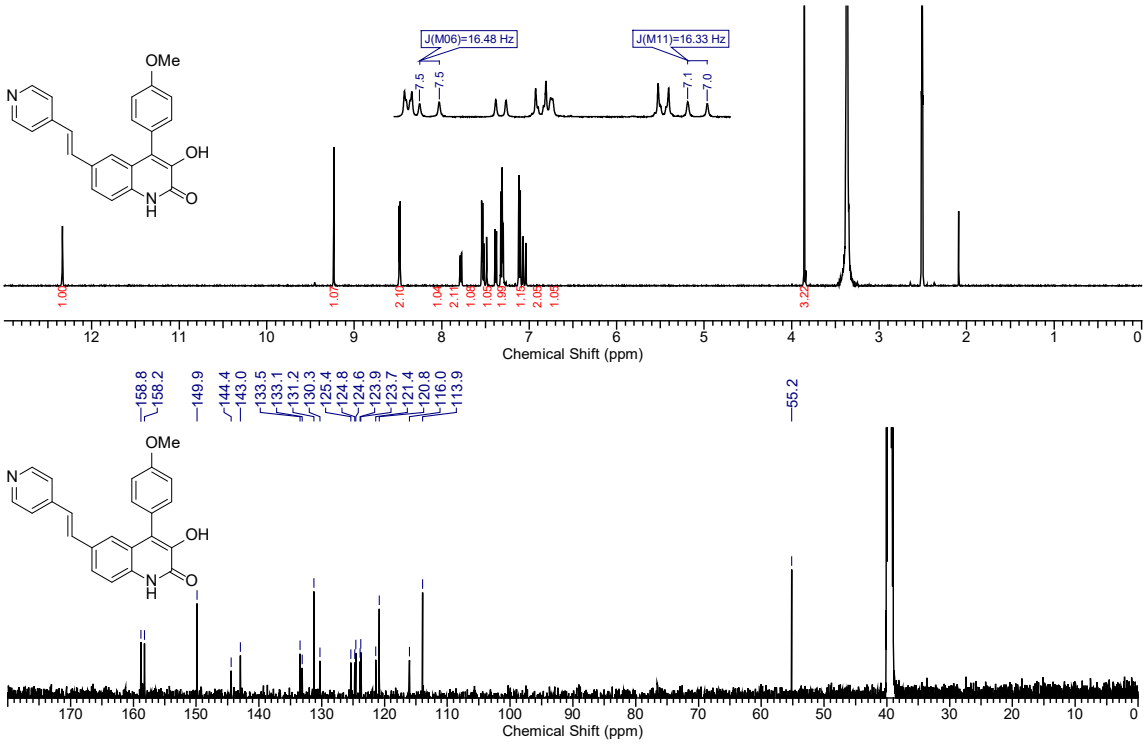

Figure S61. ^{1}H and ^{13}C NMR of **8a-VIII** in DMSO-d_6

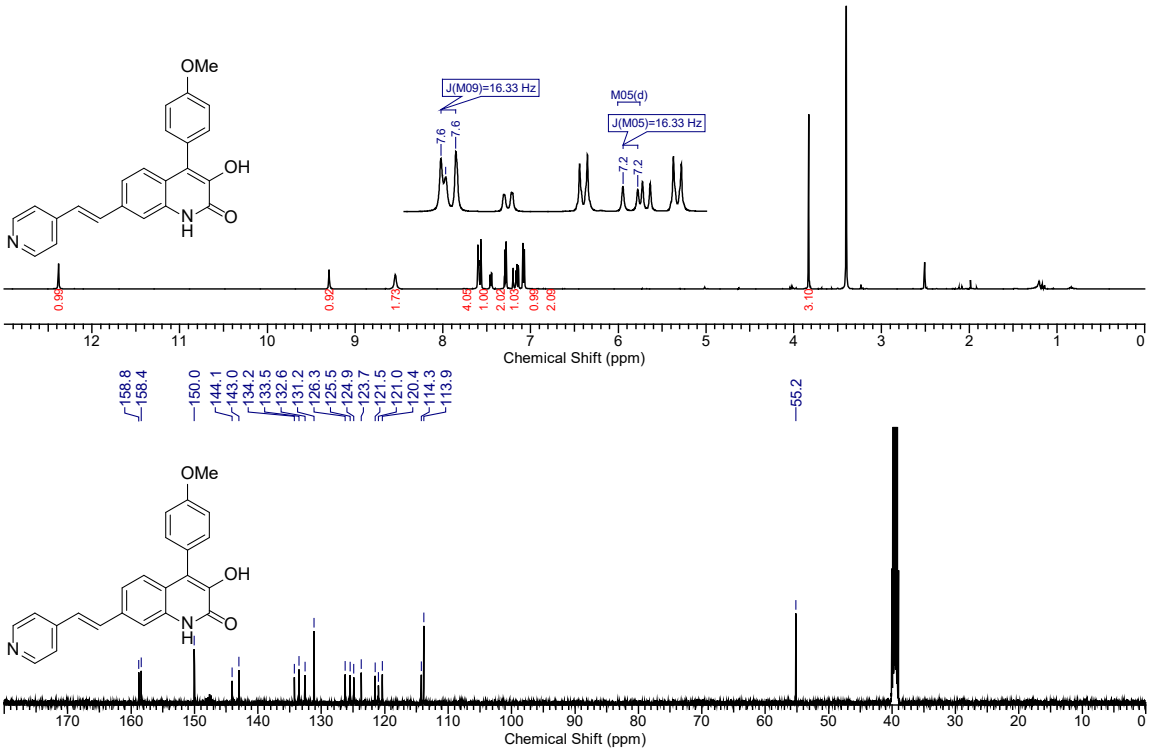

Figure S62. ^{1}H and ^{13}C NMR of **9b-VIII** in DMSO-d_6

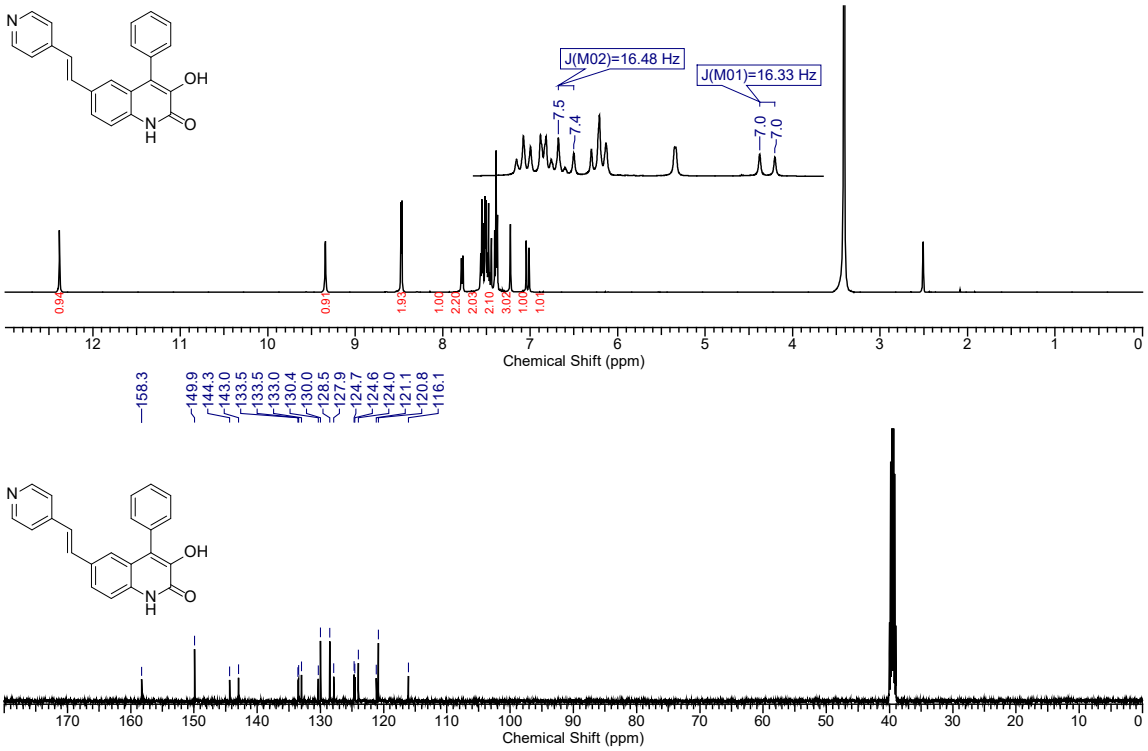

Figure S63. ^{1}H and ^{13}C NMR of **8c-VIII** in DMSO-d_6

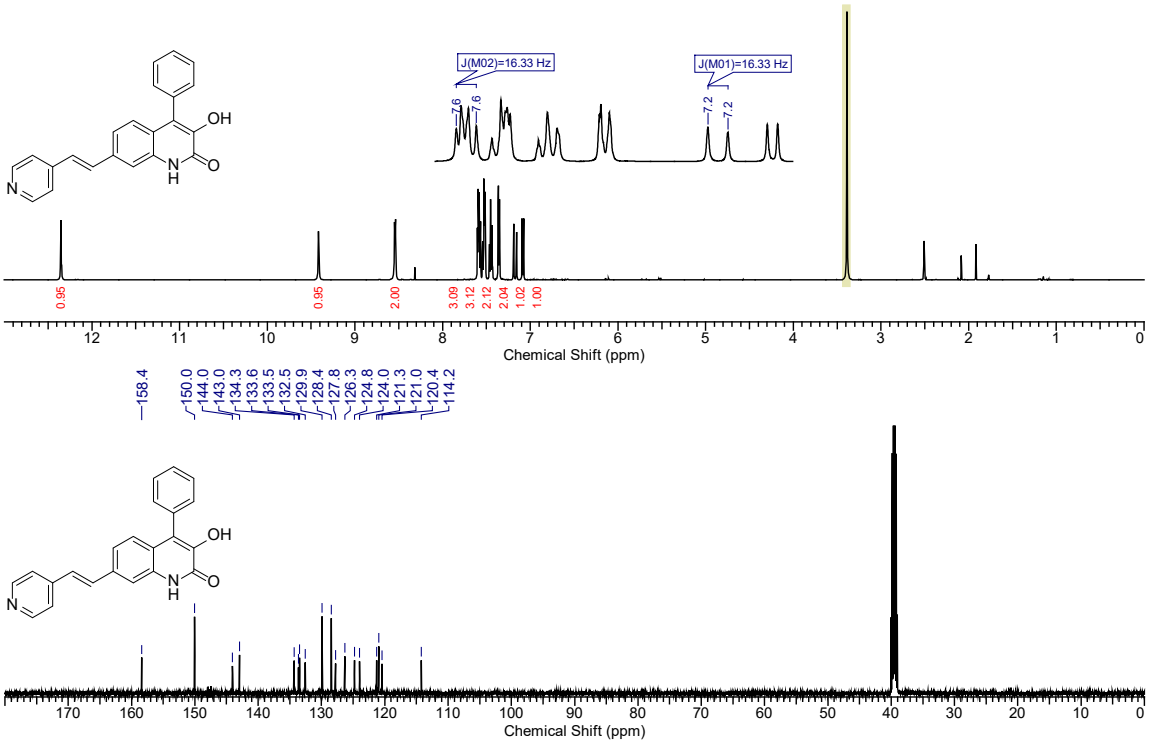

Figure S64. ^{1}H and ^{13}C NMR of **9d-VIII** in DMSO-d_6

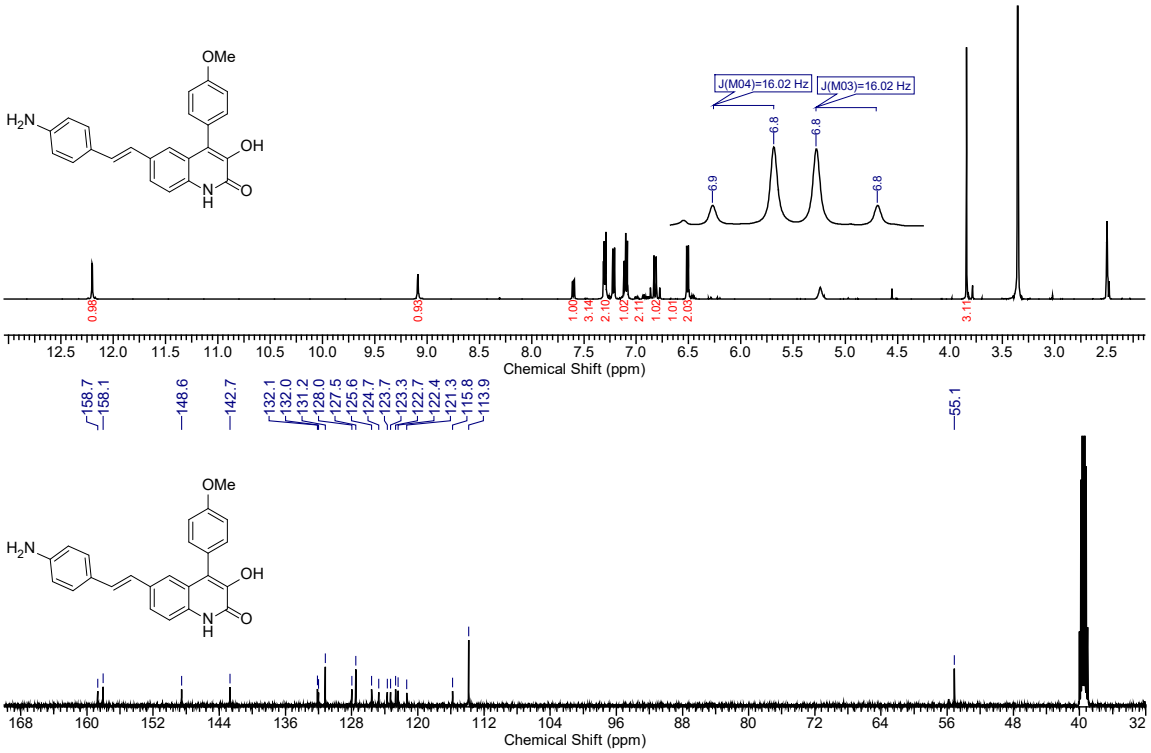

Figure S65. ^{1}H and ^{13}C NMR of **8a-IX** in DMSO-d_6

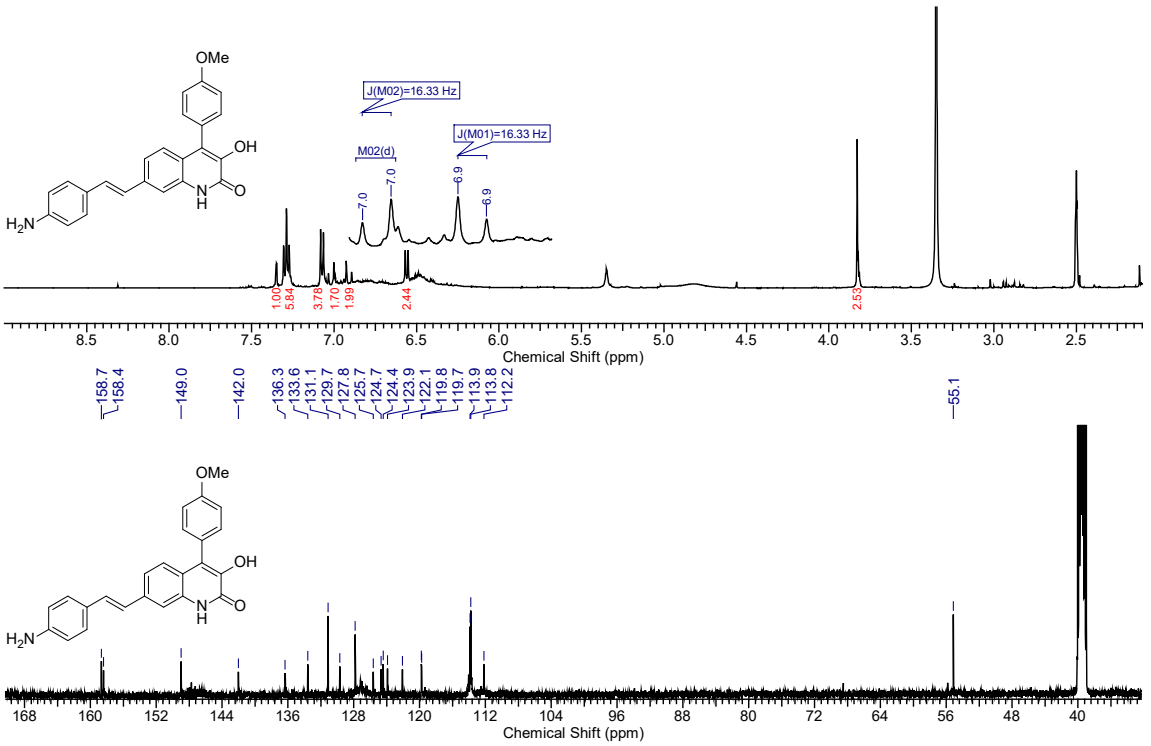

Figure S66. ^{1}H and ^{13}C NMR of **9b-IX** in DMSO-d_6

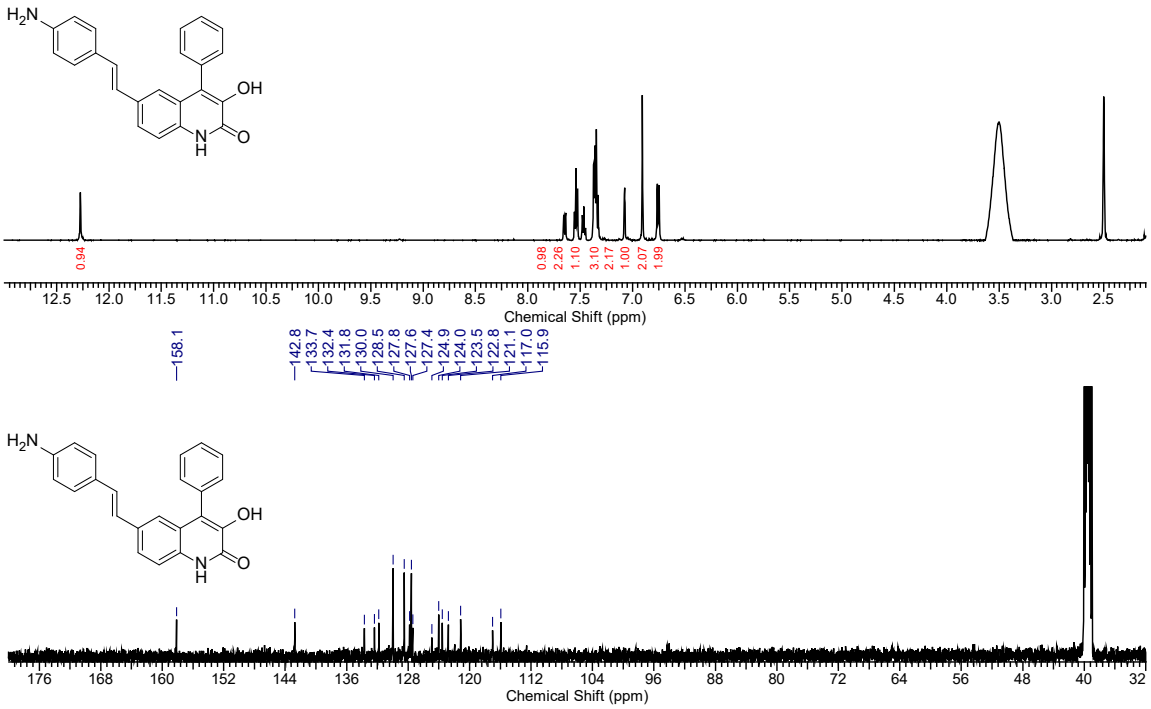

Figure S67. ^{1}H and ^{13}C NMR of **8c-IX** in DMSO-d_6

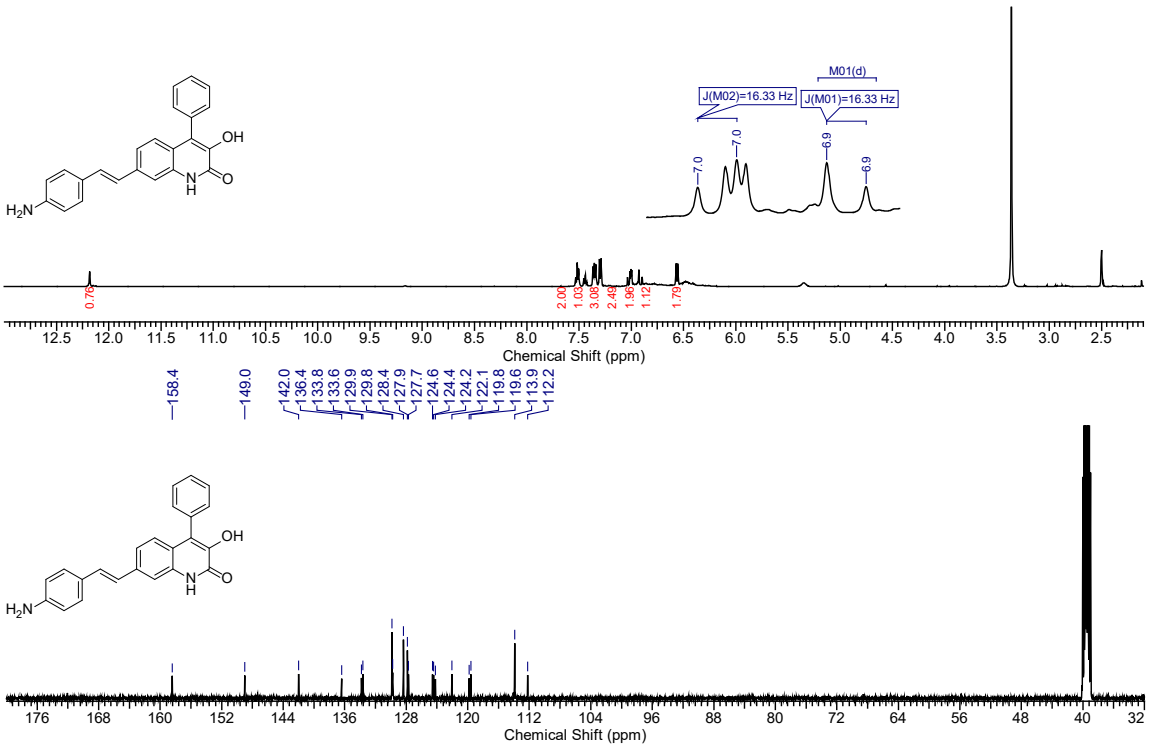

Figure S68. ^{1}H and ^{13}C NMR of **9d-IX** in DMSO-d_6

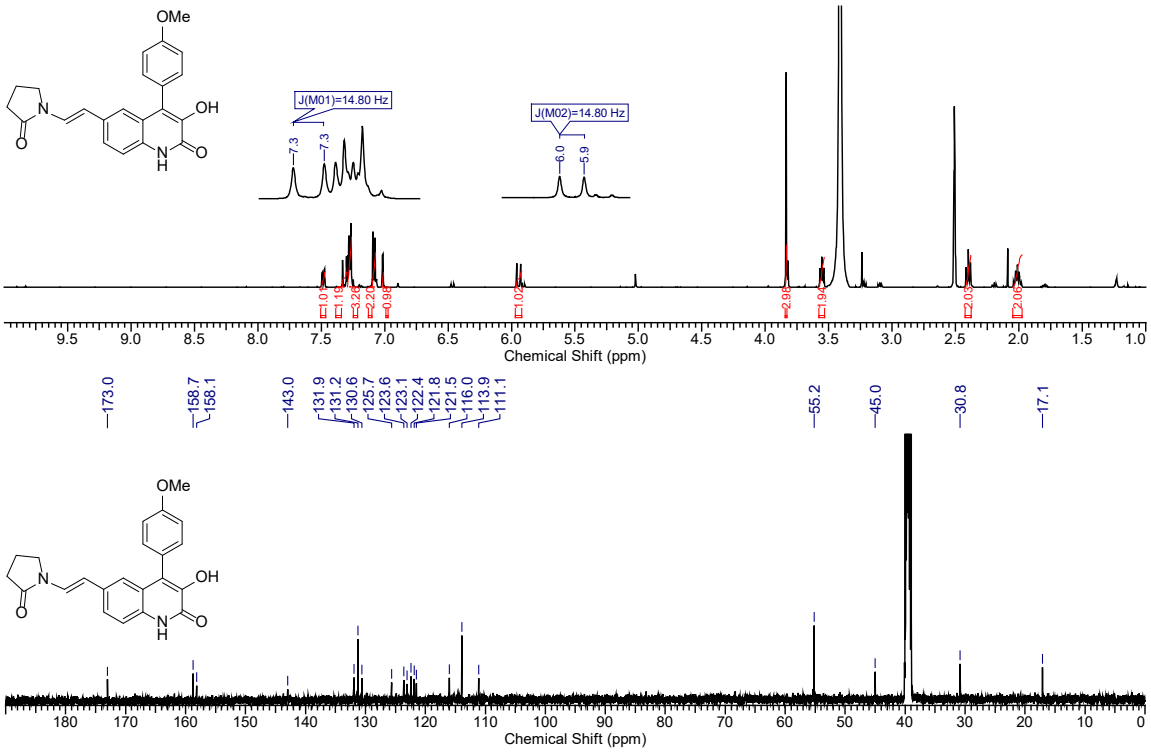

Figure S69. ^{1}H and ^{13}C NMR of **8a-X** in DMSO-d_6

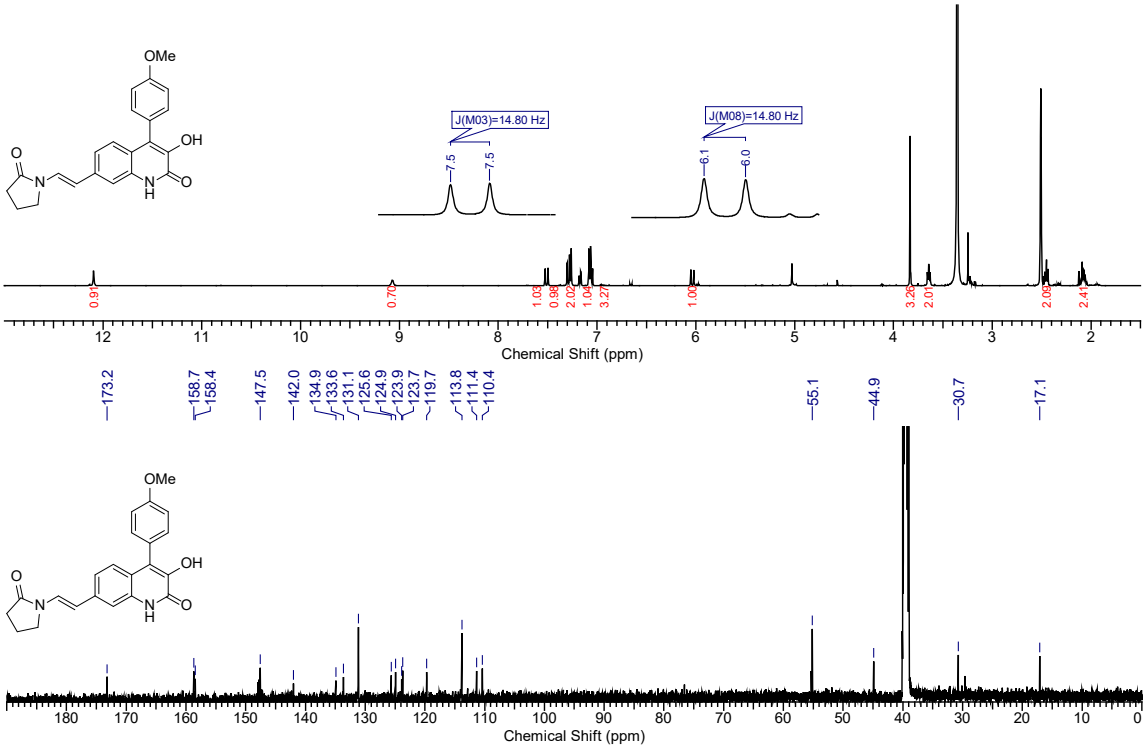

Figure S70. ^{1}H and ^{13}C NMR of **9b-X** in DMSO-d_6

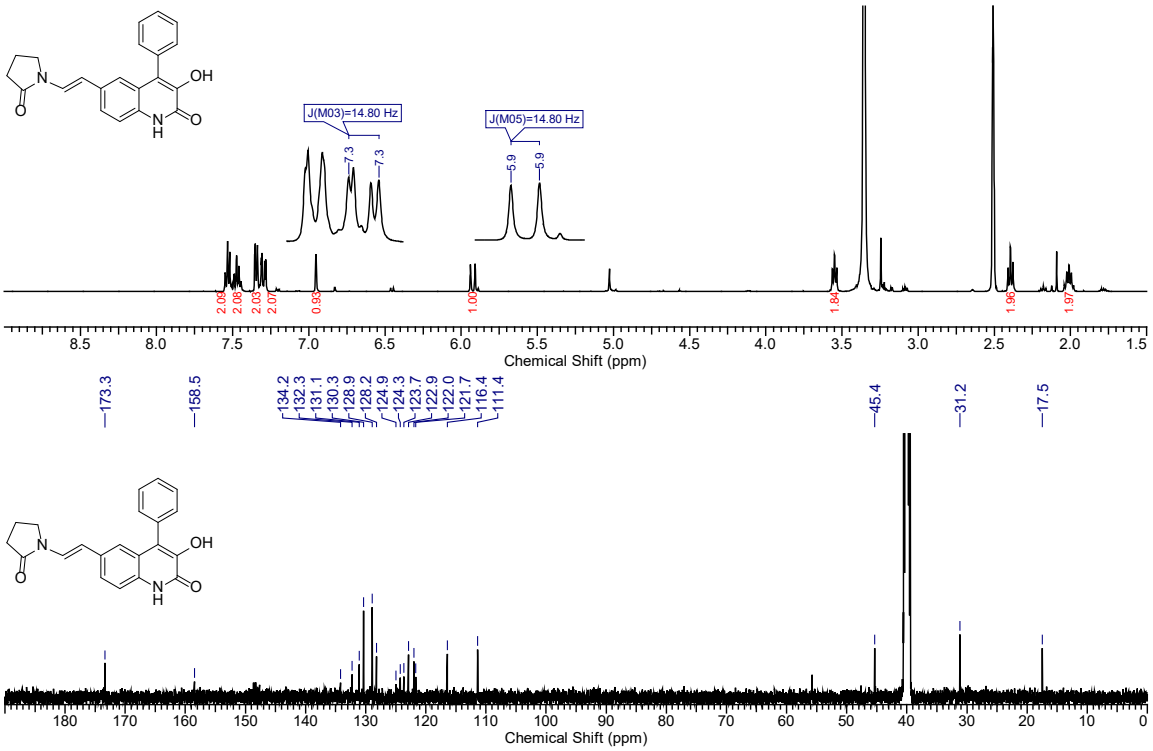

Figure S71. ^{1}H and ^{13}C NMR of **8c-X** in DMSO-d_6

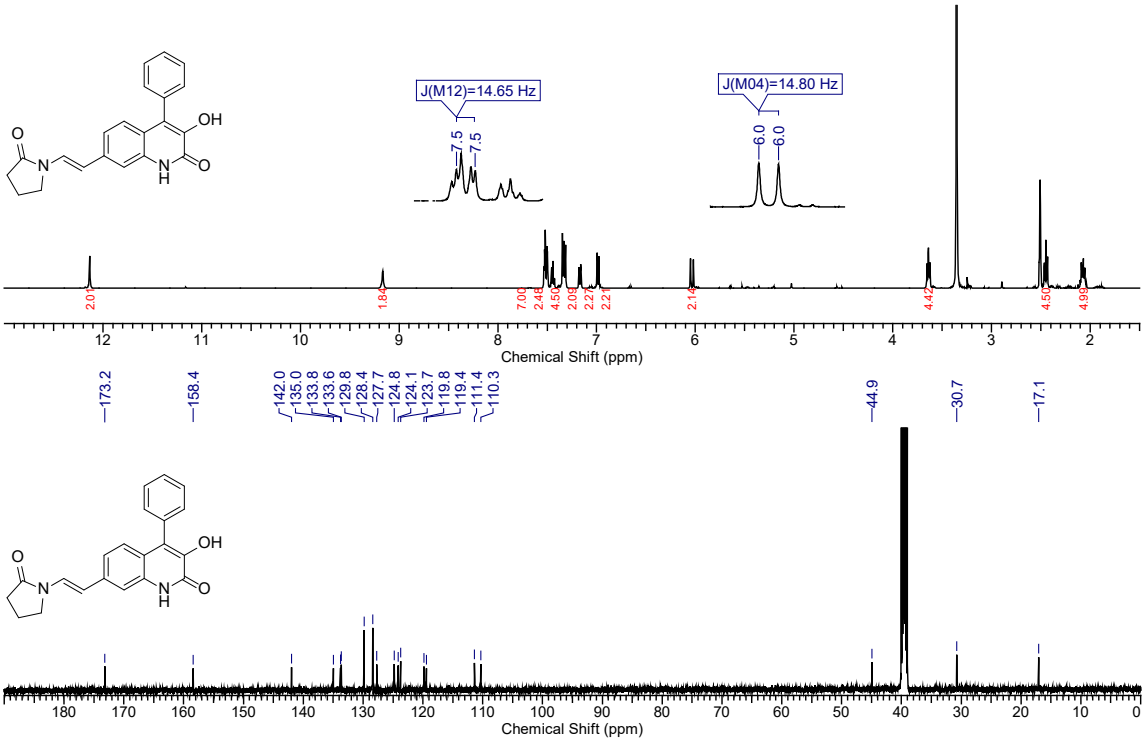

Figure S72. ^{1}H and ^{13}C NMR of **9d-X** in DMSO-d_6

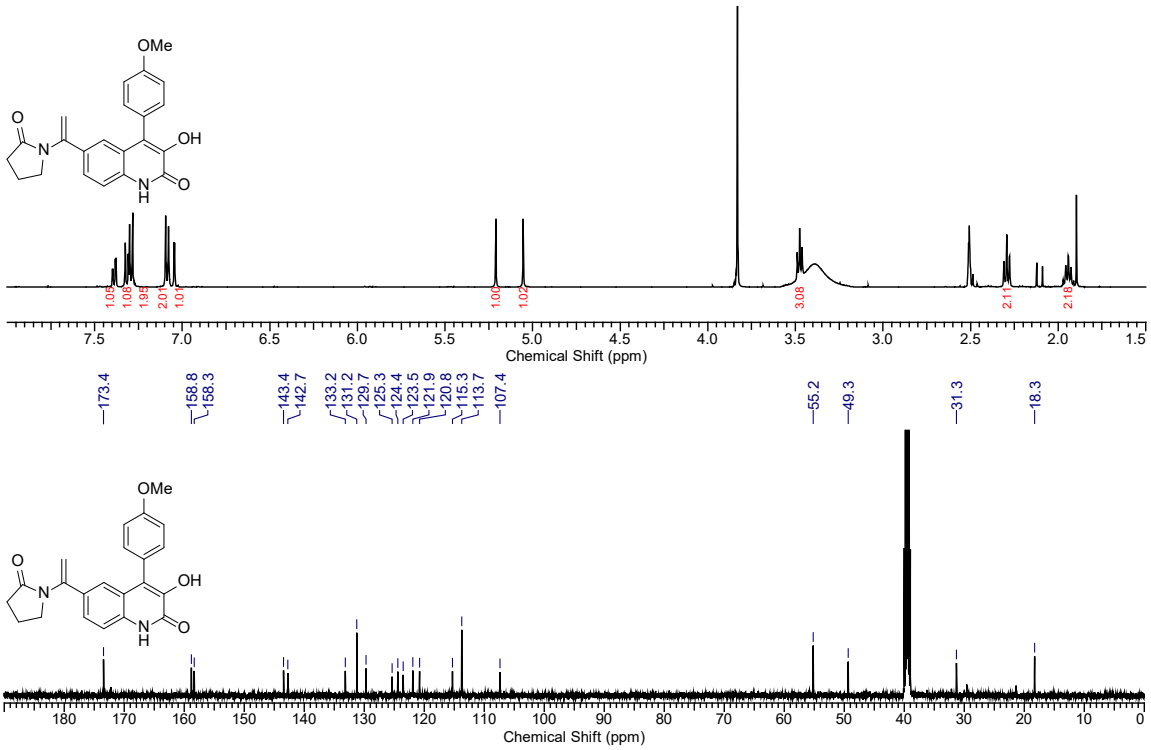

Figure S73. ^{1}H and ^{13}C NMR of **10a-X** in DMSO-d_6

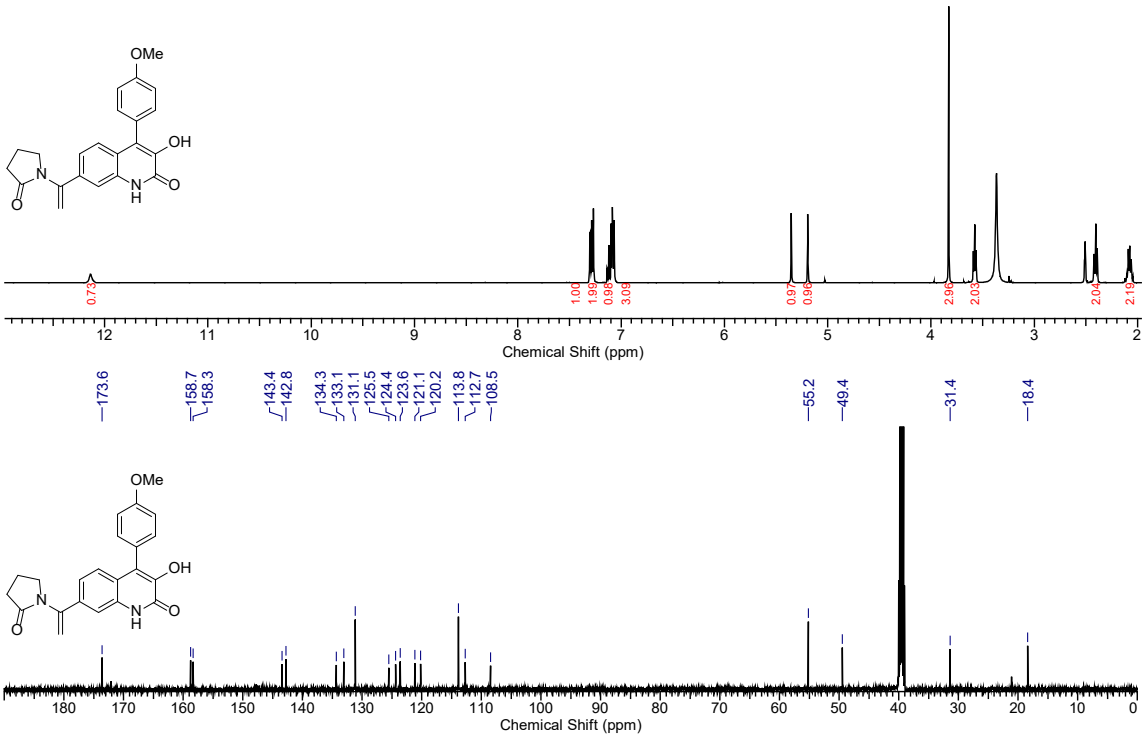

Figure S74. ^{1}H and ^{13}C NMR of **10b-X** in DMSO-d_6

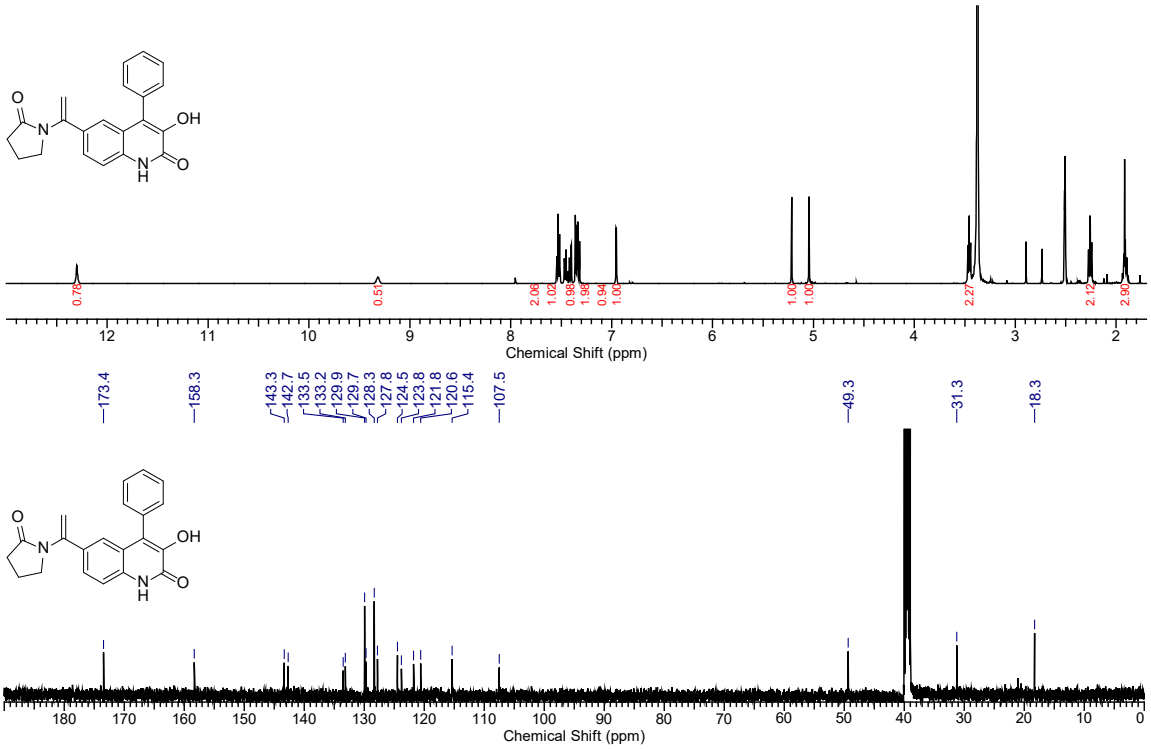

Figure S75. ^{1}H and ^{13}C NMR of **10c-X** in DMSO-d_6

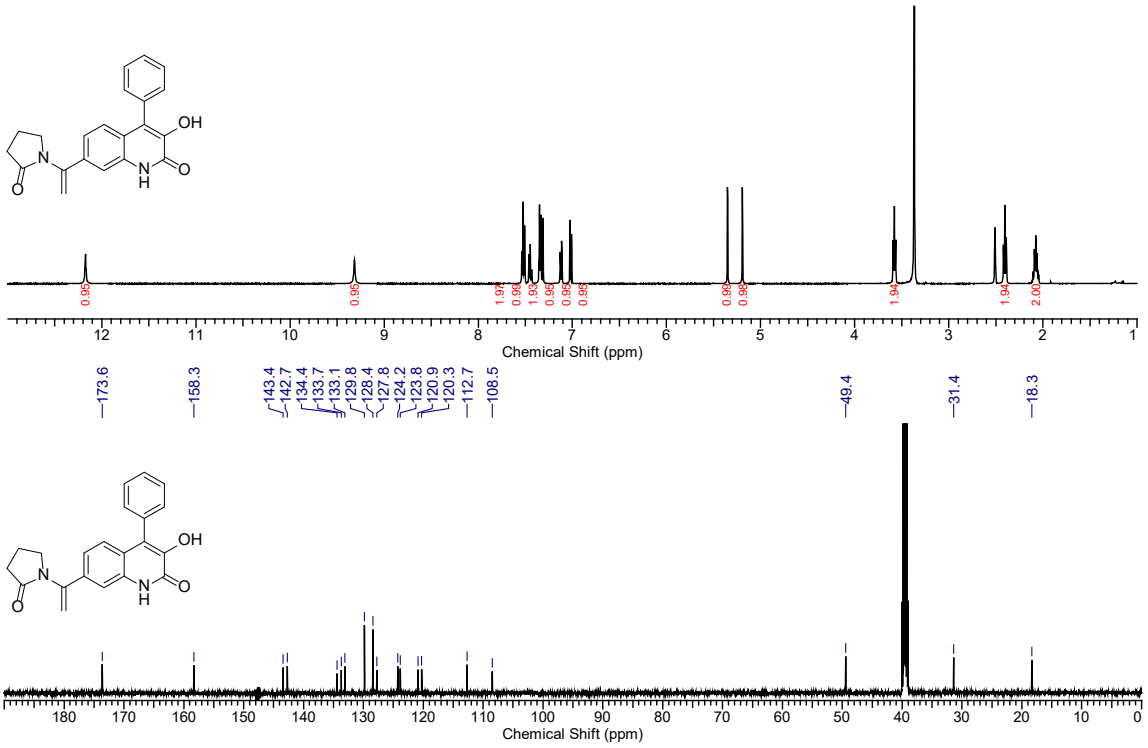

Figure S76. ^{1}H and ^{13}C NMR of **10d-X** in DMSO-d_6

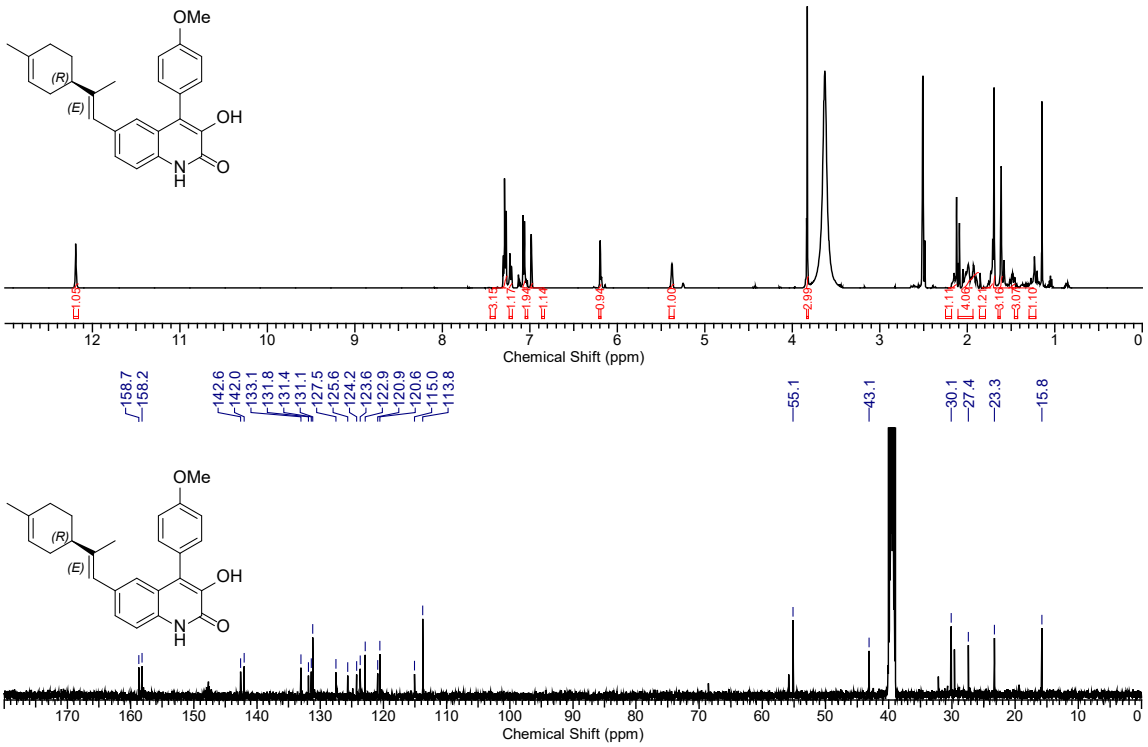

Figure S77. ^{1}H and ^{13}C NMR of **8a-XI** in DMSO-d_6

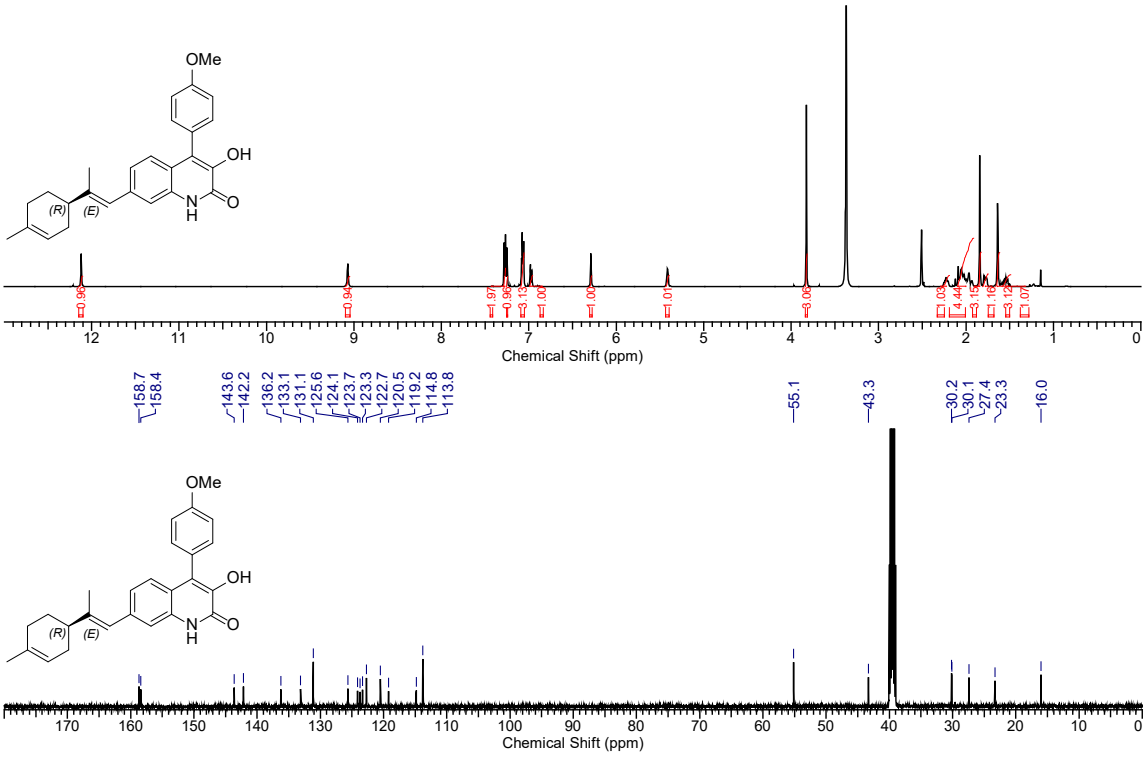

Figure S78. ^{1}H and ^{13}C NMR of **9b-XI** in DMSO-d_6

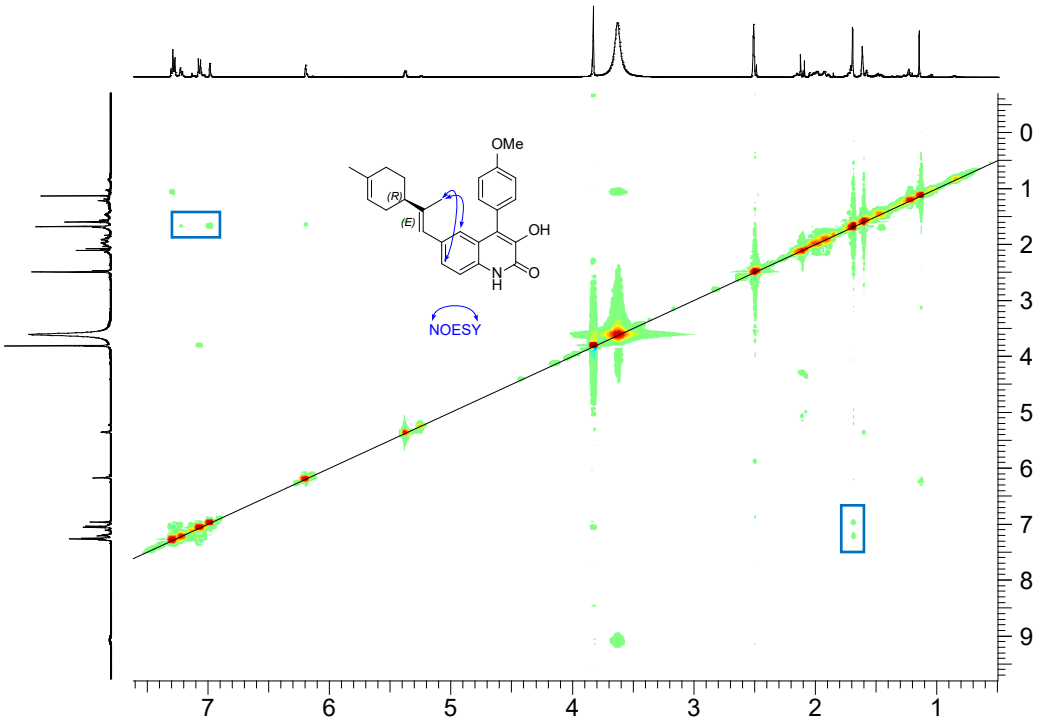

Figure S79. NOESY of **8a-XI** in DMSO-d_6

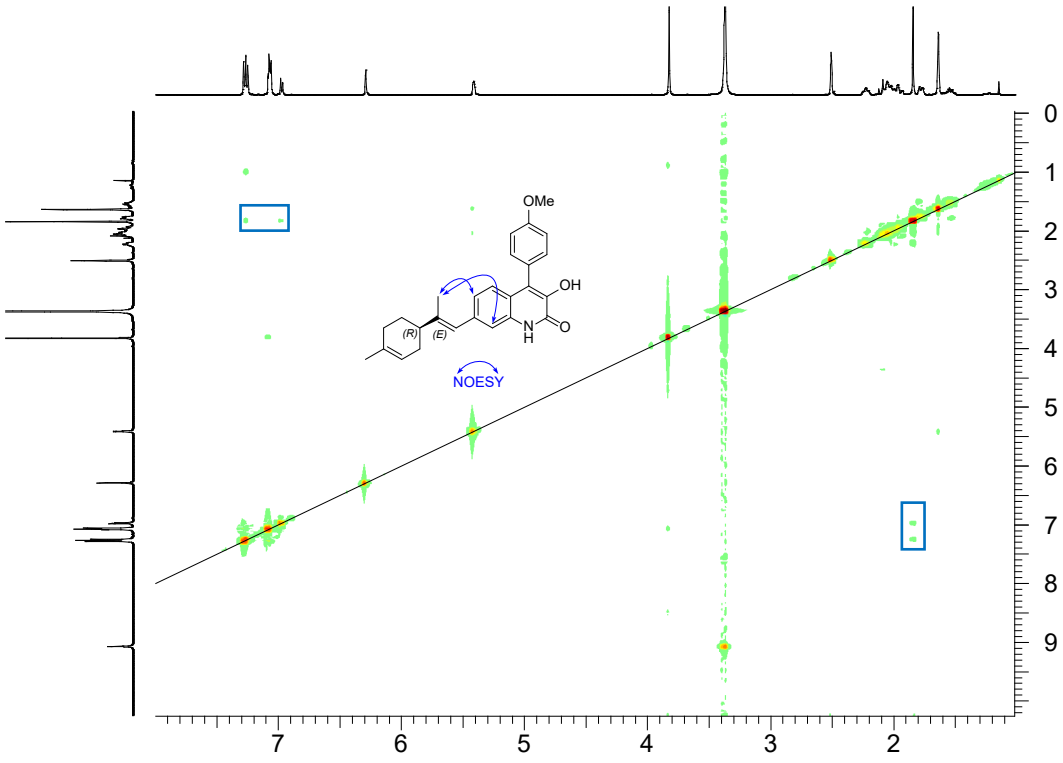

Figure S80. NOESY of **9b-XI** in DMSO-d_6

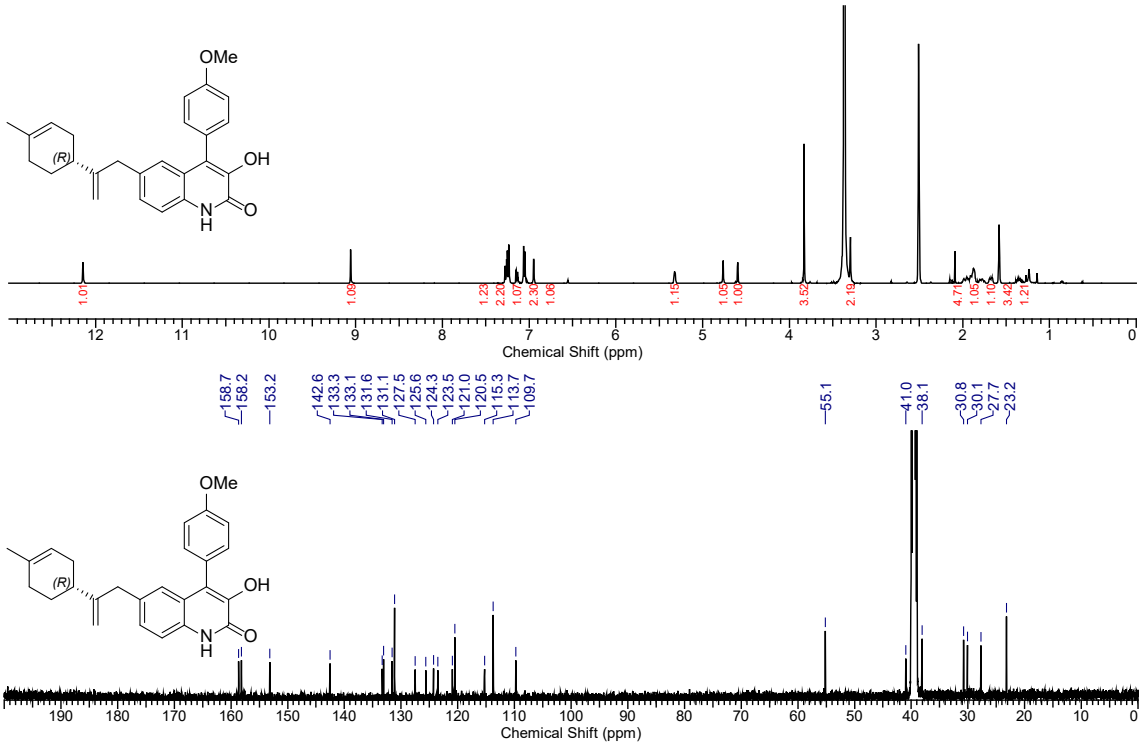

Figure S81. ^{1}H and ^{13}C NMR of **10a-XI** in DMSO-d_6

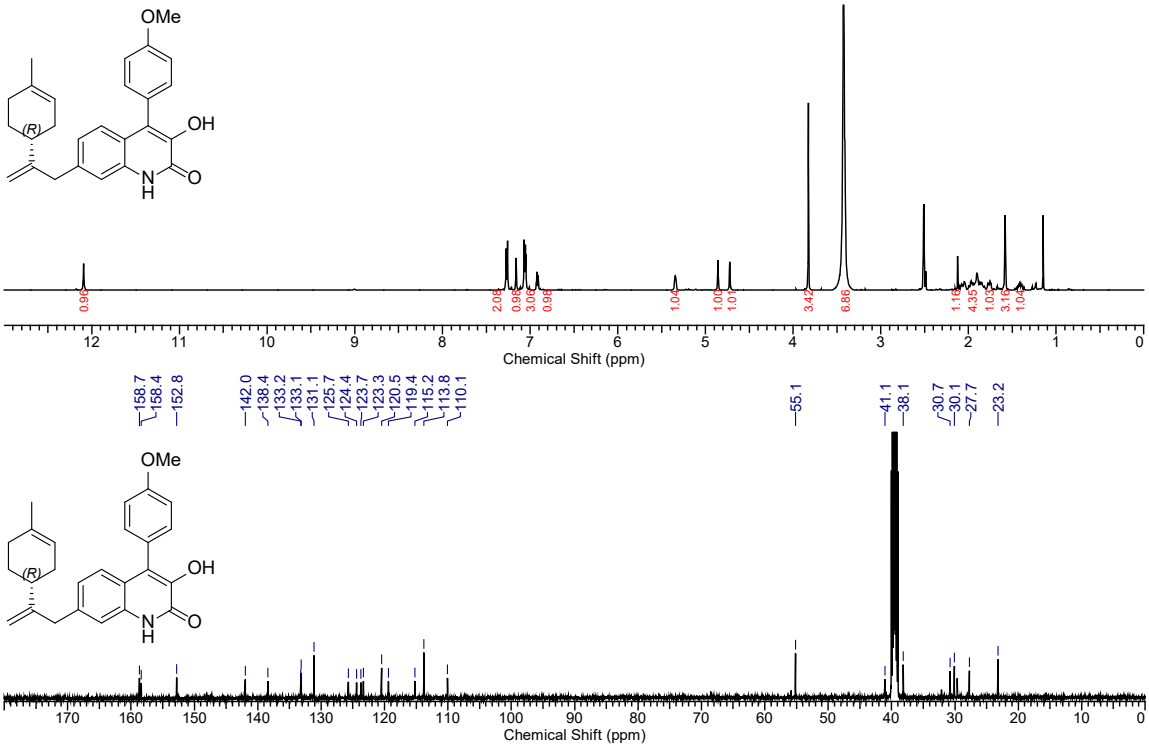

Figure S82. ^{1}H and ^{13}C NMR of **10b-XI** in DMSO-d_6

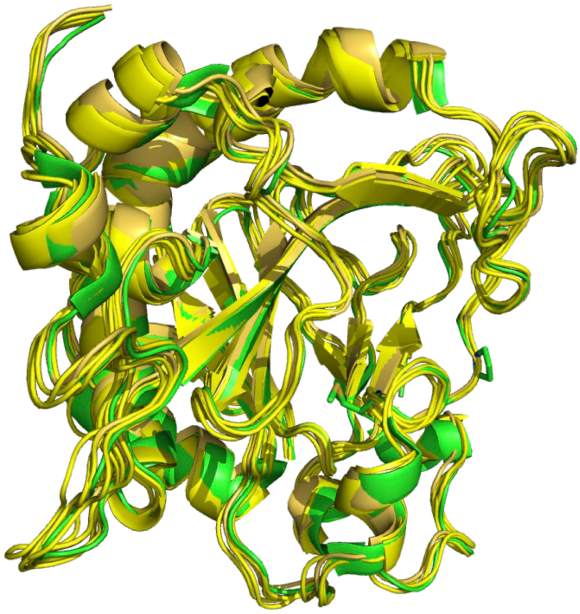

Figure S83. Structural overlay of the overall protein structure of the dehydrocyclopeptin (**1b**) bound AsqJ (obtained from a pdb file with PDB code: 6K0E, green) and the structures of the various substrate (**1a**, **1b**, **5a**-**5d**) bound AsqJ obtained from the MD simulations (yellow color).

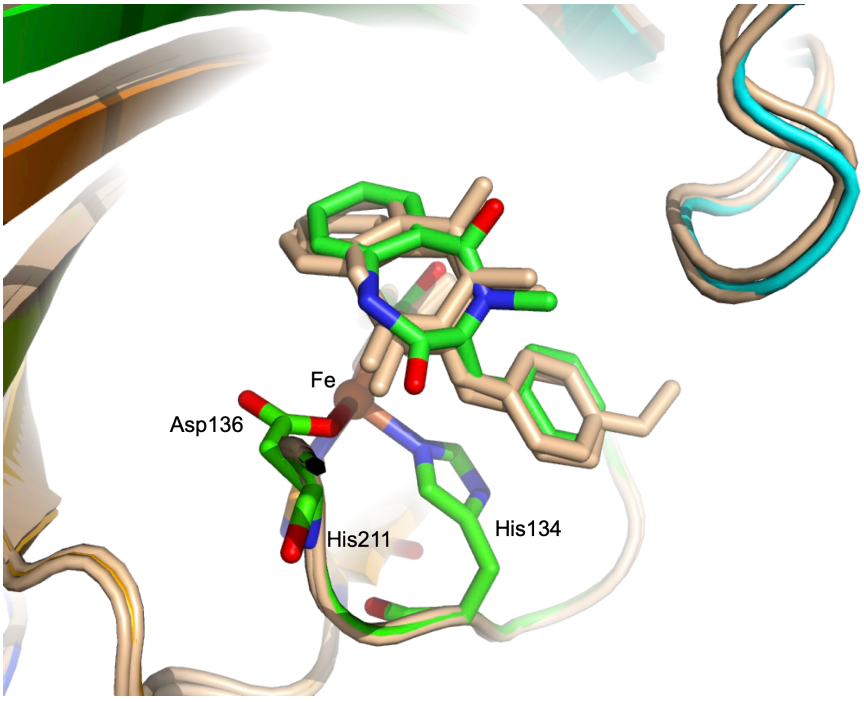

Figure S84. Structural overlay of the substrate positioning in the **1b**-bound AsqJ (PDB code 6K0E, green) and in the **1a**-bound and **1b**-bound AsqJ obtained from the MD simulations (wheat color).

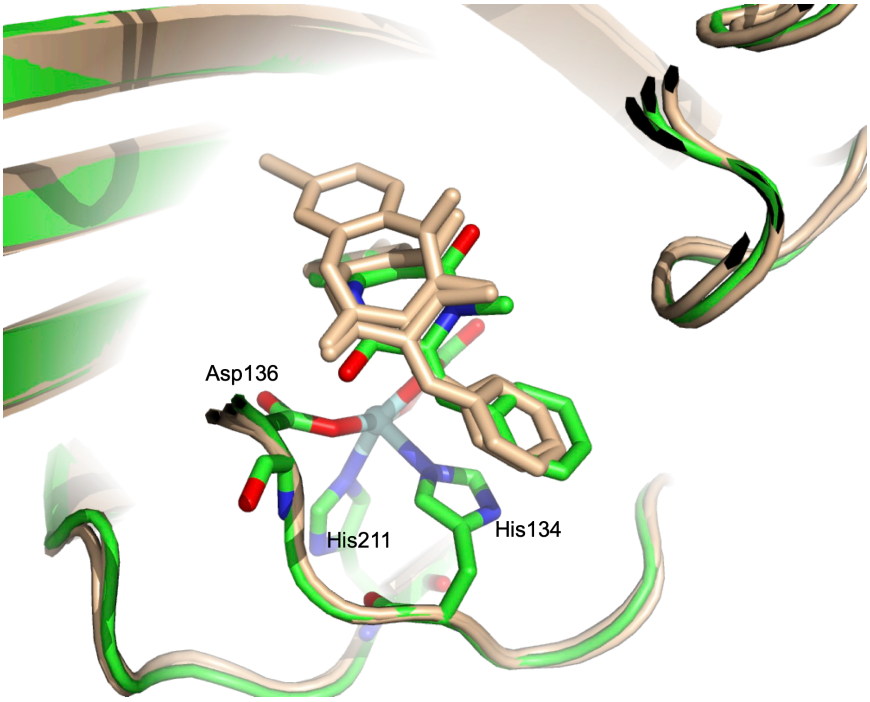

Figure S85. Structural overlay of the substrate positioning in the **1b**-bound (green color), **5c**-bound (wheat color), and **5d**-bound (wheat color) AsqJ obtained from the MD simulations.

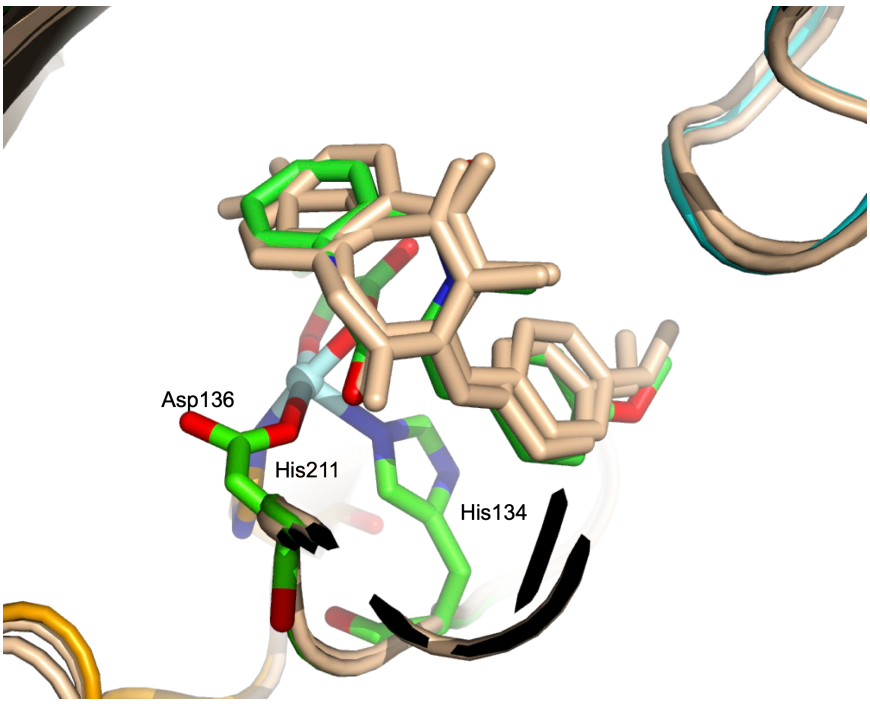

Figure 86. Structural overlay of the substrate positioning in the **1a**-bound (green color), **5a**-bound (wheat color), and **5b**-bound (wheat color) AsqJ obtained from the MD simulations.

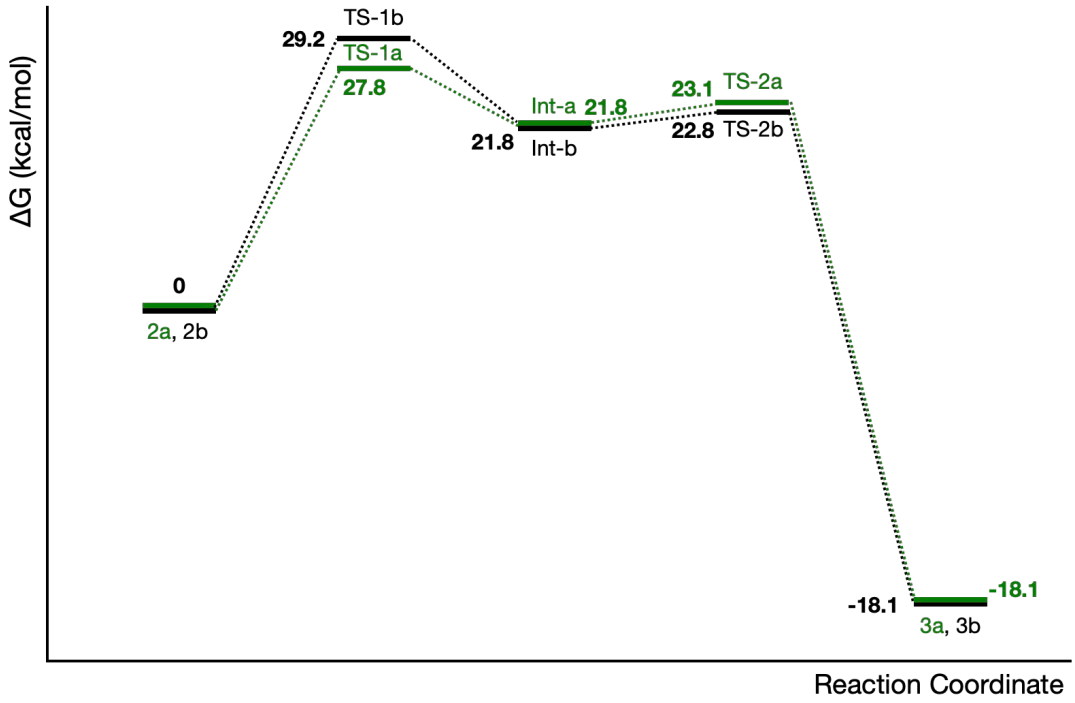

Figure S87. Reaction coordinate for the conversion of cyclopenin **2a** (green) and **2b** (black) to viridicatin (**3a**, **3b**) in water. The numerical values indicate the calculated free energy differences of various species.

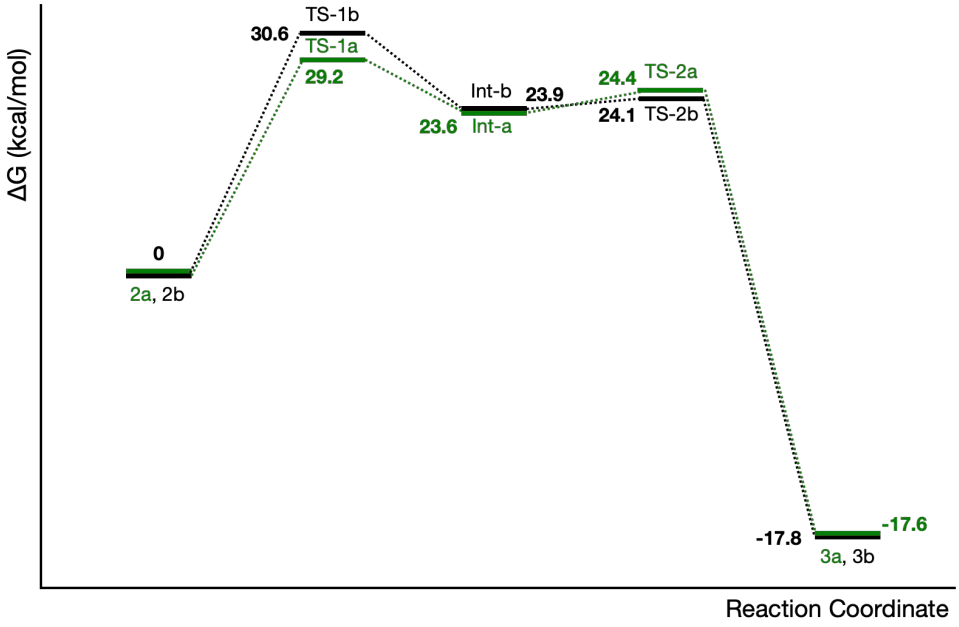

Figure S88. Reaction coordinate for the conversion of cyclopenin **2a** (green) and **2b** (black) to viridicatin (**3a**, **3b**) in dichloromethane. The numerical values indicate the calculated free energy differences of various species.

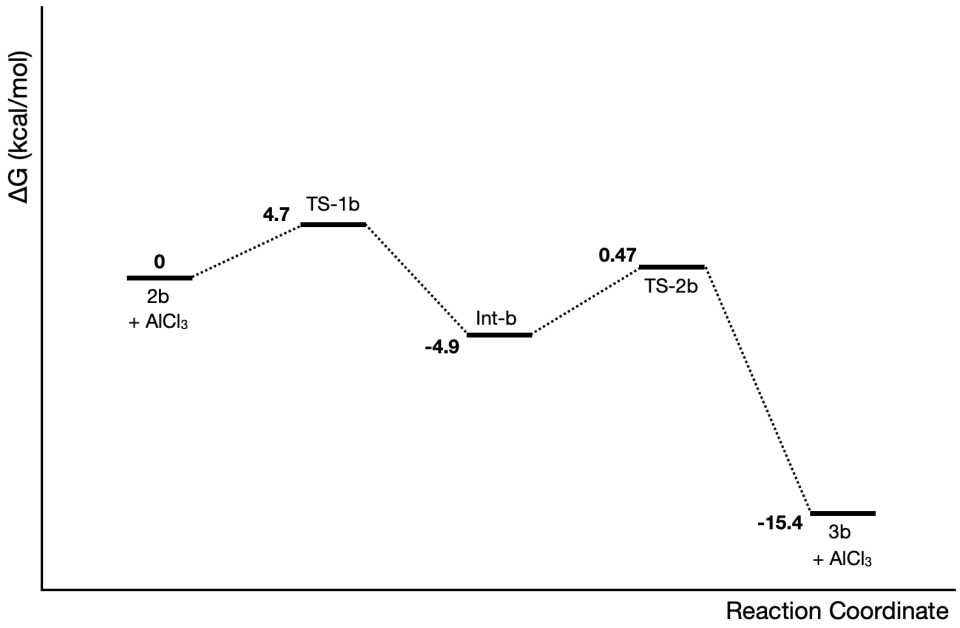

Figure S89. Reaction coordinate for the conversion of cyclopenin (**2b**) to viridicatin (**3b**) in dichloromethane with the presence of $AlCl_3$. The numerical values indicate the calculated free energy differences of various species.

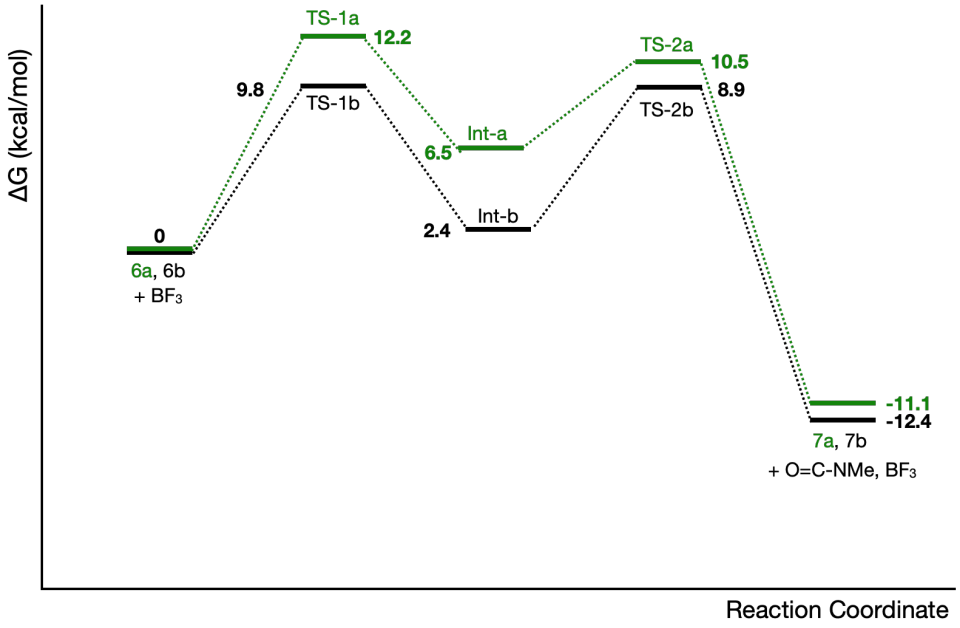

Figure S90. Reaction coordinate for the conversion of cyclopenin **6a** (green) and **6b** (black) to viridicatin (**7a**, **7b**) in dichloromethane with the presence of BF_3. The numerical values indicate the calculated free energy differences of various species.

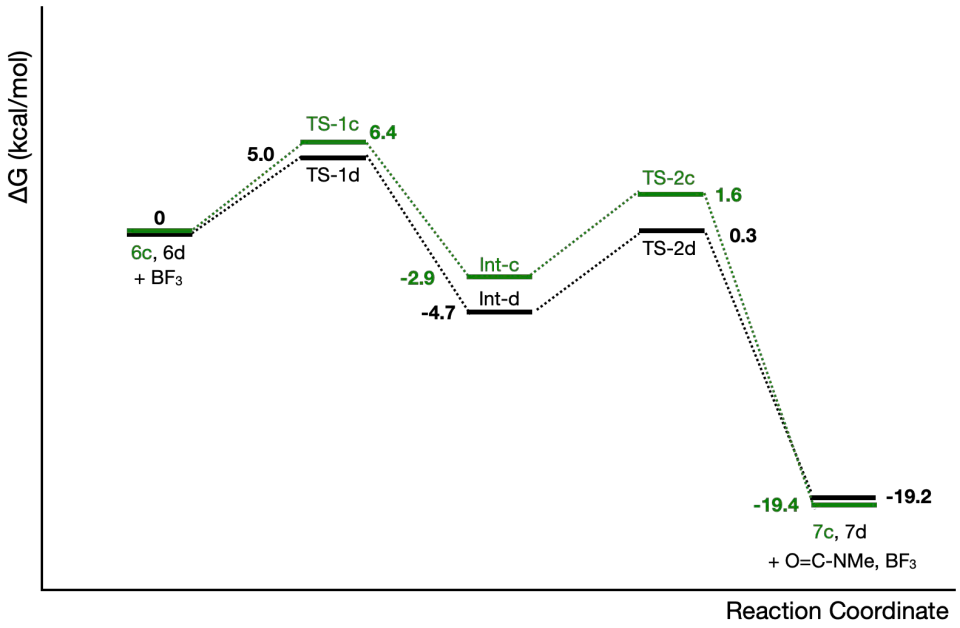

Figure S91. Reaction coordinate for the conversion of cyclopenin **6c** (green) and **6d** (black) to viridicatin (**7c**, **7d**) in dichloromethane with the presence of BF_3. The numerical values indicate the calculated free energy differences of various species.

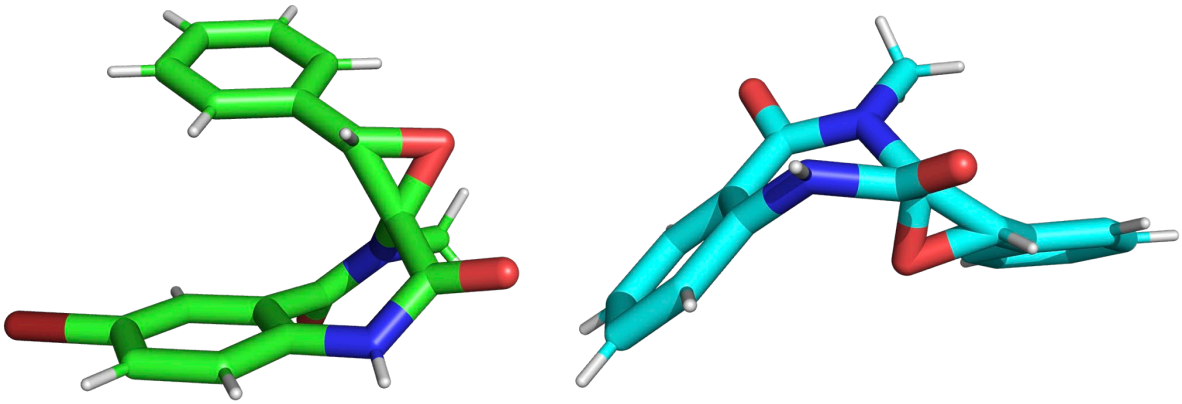

Figure S92. The crystal structures of **6c** obtained in solution (left) and **2b** obtained in AsqJ enzyme obtained from the protein crystal structure (right, PDB code: 6K0E).

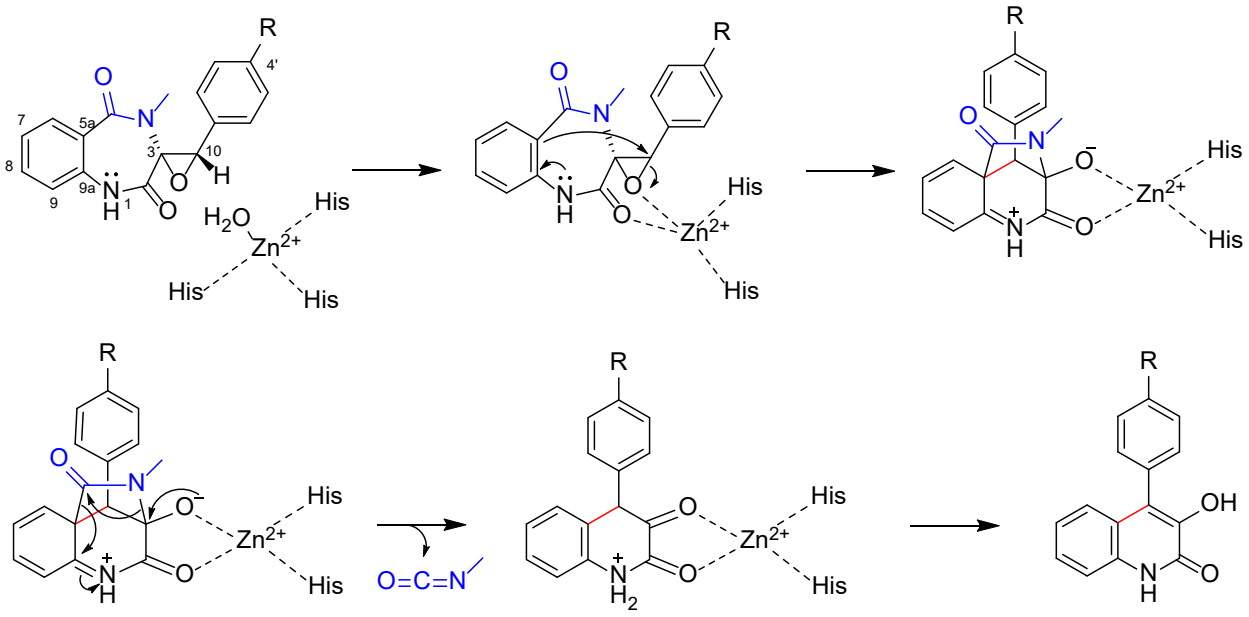

Figure S93. Proposed reaction mechanism of AsqI catalyzed rearrangement.[17]

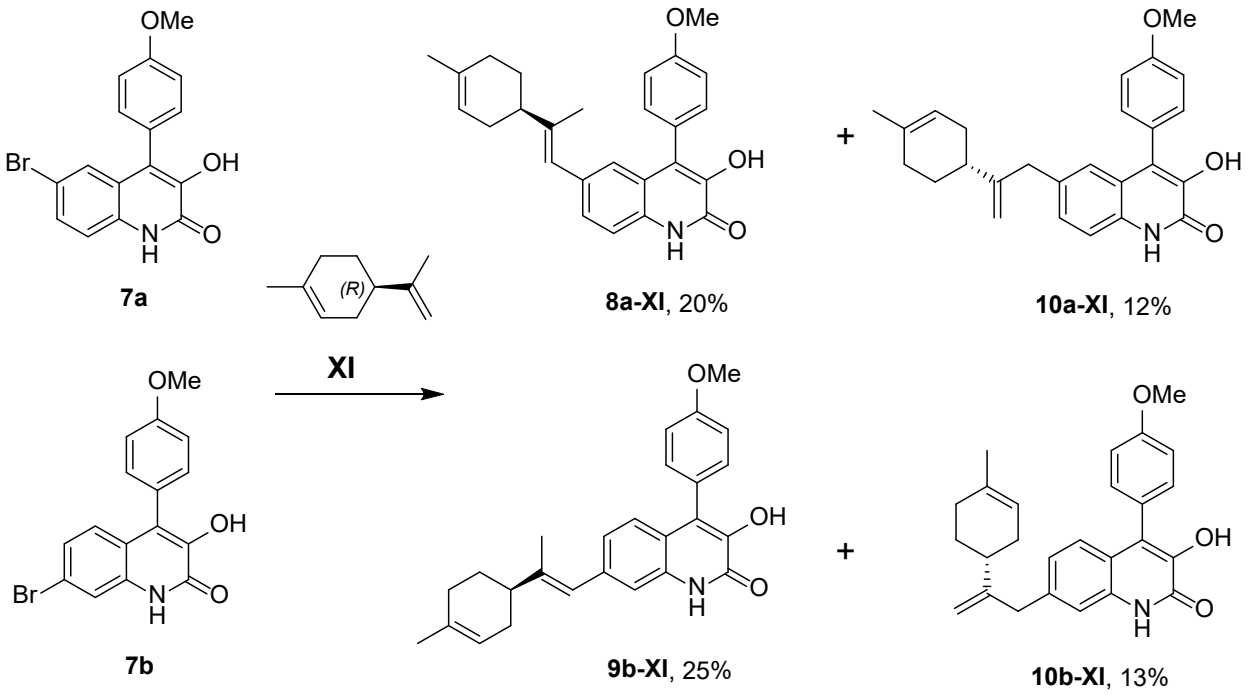

Figure S94 Limonene adduct analogues preparation

Table S1. Crystallographic data for 7-Br-cyclopenin (6c)

Identification code	rs031	
Chemical formula	$C_{17}H_{13}BrN_2O_3$	
Formula weight	373.20 g/mol	
Temperature	100(2) K	
Wavelength	0.71073 Å	
Crystal size	0.142 x 0.160 x 0.262 mm	
Crystal habit	colorless block	
Crystal system	orthorhombic	
Space group	$P2_12_12_1$	
Unit cell dimensions	a = 8.3786(4) Å	α = 90°
	b = 10.5626(5) Å	β = 90°
	c = 16.7996(6) Å	γ = 90°
Volume	1486.76(11) $Å^3$	
Z	4	
Density (calculated)	1.667 g/cm^3	
Absorption coefficient	2.782 mm^{-1}	
F(000)	752	
Diffractometer	Bruker D8 VENTURE	
Radiation source	Incoatec IμS 3.0 microfocus sealed tube (Mo Kα, λ = 0.71073 Å)	
Theta range for data collection	2.28 to 30.52°	
Index ranges	-11<=*h*<=11, -15<=*k*<=15, -24<=*l*<=22	
Reflections collected	63482	
Independent reflections	4530 [R(int) = 0.0436]	
Coverage of independent reflections	100.0%	
Absorption correction	Multi-Scan	
Max. and min. transmission	0.6930 and 0.5290	
Structure solution program	SHELXT 2014/5 (Sheldrick, 2014)	
Refinement method	Full-matrix least-squares on F^2	
Refinement program	SHELXL-2018/3 (Sheldrick, 2018)	
Data / restraints / parameters	4530 / 0 / 212	
Goodness-of-fit on F^2	1.034	
Δ/σ_{max}	0.004	
Final R indices	4370 data; I>2σ(I)	$R1^a$ = 0.0181, $wR2^b$ = 0.0420
	all data	R1 = 0.0196, wR2 = 0.0424
Absolute structure parameter	0.008(2)	
Largest diff. peak and hole	0.276 and -0.339 $eÅ^{-3}$	
R.M.S. deviation from mean	0.046 $eÅ^{-3}$	

Table S2. Steady-State enzymatic kinetics of AsqJ catalyzed epoxidation

	1a	**1b**	**5a**	**5b**	**5c**	**5d**
Km (mM)	0.084	0.051	0.29	0.52	0.34	0.60
kcat (s^{-1})	0.28	0.79	0.41	0.12	1.14	0.086
kcat/Km ($mM^{-1}s^{-1}$)	3.30	15.59	1.41	0.23	3.29	0.14

Table S3. DFT calculated free energies of various cyclopenin analogs in the two structural configurations.[a]

	Free energy (Hartree)	Free energy difference (kcal/mol)
2a (boat)	-1105.403473	
2a (chair)	-1105.400937	1.591347608
2b (boat)	-990.941232	
2b (chair)	-990.938503	1.712455687
6a (boat)	-3676.390485	
6a (chair)	-3676.387028	2.169277871
6b (boat)	-3676.389919	
6b (chair)	-3676.387223	1.691748088
6c (boat)	-3561.92776	
6c (chair)	-3561.925222	1.592602614
6d (boat)	-3561.927315	
6d (chair)	-3561.92493	1.496594655

[a] The free energy column lists the total free energies calculated by DFT in water modeled by the Polarized Continuum Model (PCM); the free energy differences are calculated by the expression: $\Delta G = G(\text{chair}) - G(\text{boat})$ for a given cyclopenin.

Reference

1. Yang, L.; Huang, Z.; Li, G.; Zhang, W.; Cao, R.; Wang, C.; Xiao, J.; Xue, D., Synthesis of Phenols: Organophotoredox/Nickel Dual Catalytic Hydroxylation of Aryl Halides with Water. *Angew. Chem. Int. Ed.* **2018,** *57* (7), 1968-72.
2. Chang, W.-c.; Li, J.; Lee, J. L.; Cronican, A. A.; Guo, Y., Mechanistic Investigation of a Non-Heme Iron Enzyme Catalyzed Epoxidation in (-)-4'-Methoxycyclopenin Biosynthesis. *J. Am. Chem. Soc.* **2016,** *138* (33), 10390-3.
3. Ishikawa, N.; Tanaka, H.; Koyama, F.; Noguchi, H.; Wang, C. C.; Hotta, K.; Watanabe, K., Non-heme dioxygenase catalyzes atypical oxidations of 6,7-bicyclic systems to form the 6,6-quinolone core of viridicatin-type fungal alkaloids. *Angew. Chem. Int. Ed.* **2014,** *53* (47), 12880-4.
4. M. J. Frisch, G. W. T., H. B. Schlegel, G. E. Scuseria, M. A. Robb, J. R. Cheeseman, G. Scalmani, V. Barone, G. A. Petersson, H. Nakatsuji, X. Li, M. Caricato, A. Marenich, J. Bloino, B. G. Janesko, R. Gomperts, B. Mennucci, H. P. Hratchian, J. V. Ortiz, A. F. Izmaylov, J. L. Sonnenberg, D. Williams-Young, F. Ding, F. Lipparini, F. Egidi, J. Goings, B. Peng, A. Petrone, T. Henderson, D. Ranasinghe, V. G. Zakrzewski, J. Gao, N. Rega, G. Zheng, W. Liang, M. Hada, M. Ehara, K. Toyota, R. Fukuda, J. Hasegawa, M. Ishida, T. Nakajima, Y. Honda, O. Kitao, H. Nakai, T. Vreven, K. Throssell, J. A. Montgomery, Jr., J. E. Peralta, F. Ogliaro, M. Bearpark, J. J. Heyd, E. Brothers, K. N. Kudin, V. N. Staroverov, T. Keith, R. Kobayashi, J. Normand, K. Raghavachari, A. Rendell, J. C. Burant, S. S. Iyengar, J. Tomasi, M. Cossi, J. M. Millam, M. Klene, C. Adamo, R. Cammi, J. W. Ochterski, R. L. Martin, K. Morokuma, O. Farkas, J. B. Foresman, and D. J. Fox, Gaussian, Inc., Wallingford CT, 2009.
5. Becke, A. D., Density-functional exchange-energy approximation with correct asymptotic behavior. *Phys. Rev. A Gen. Phys.* **1988,** *38* (6), 3098-100.
6. Lee, C.; Yang, W.; Parr, R. G., Development of the Colle-Salvetti correlation-energy formula into a functional of the electron density. *Phys. Rev. B Condens. Matter* **1988,** *37* (2), 785-9.
7. Miehlich, B.; Savin, A.; Stoll, H.; Preuss, H., Results Obtained with the Correlation-Energy Density Functionals of Becke and Lee, Yang and Parr. *Chem. Phys. Lett.* **1989,** *157* (3), 200-6.
8. Tomasi, J.; Mennucci, B.; Cammi, R., Quantum mechanical continuum solvation models. *Chem. Rev.* **2005,** *105* (8), 2999-3093.
9. Grimme, S.; Antony, J.; Ehrlich, S.; Krieg, H., A consistent and accurate ab initio parametrization of density functional dispersion correction (DFT-D) for the 94 elements H-Pu. *J. Chem. Phys.* **2010,** *132* (15), 154104.
10. Peng, C. Y.; Schlegel, H. B., Combining Synchronous Transit and Quasi-Newton Methods to Find Transition-States. *Isr. J. Chem.* **1993,** *33* (4), 449-54.
11. Peng, C. Y.; Ayala, P. Y.; Schlegel, H. B.; Frisch, M. J., Using redundant internal coordinates to optimize equilibrium geometries and transition states. *J. Comput. Chem.* **1996,** *17* (1), 49-56.
12. Fukui, K., The Path of Chemical-Reactions - the Irc Approach. *Accounts Chem. Res.* **1981,** *14* (12), 363-8.
13. Hratchian, H. P.; Schlegel, H. B., *Theory and Applications of Computational Chemistry: The First 40 Years*. Elsevier: Amsterdam, 2005.
14. Wang, J.; Wang, W.; Kollman, P. A.; Case, D. A., Automatic atom type and bond type perception in molecular mechanical calculations. *J. Mol. Graph. Model* **2006,** *25* (2), 247-60.
15. Wang, J.; Wolf, R. M.; Caldwell, J. W.; Kollman, P. A.; Case, D. A., Development and testing of a general amber force field. *J. Comput. Chem.* **2004,** *25* (9), 1157-74.
16. Sousa da Silva, A. W.; Vranken, W. F., ACPYPE - AnteChamber PYthon Parser interfacE. *BMC Res. Notes.* **2012,** *5*, 367.

17. Kishimoto, S.; Hara, K.; Hashimoto, H.; Hirayama, Y.; Champagne, P. A.; Houk, K. N.; Tang, Y.; Watanabe, K., Enzymatic one-step ring contraction for quinolone biosynthesis. *Nat. Commun.* **2018,** *9* (1), 2826.